

University of Nebraska - Lincoln

DigitalCommons@University of Nebraska - Lincoln

Student Research Projects, Dissertations, and
Theses - Chemistry Department

Chemistry, Department of

8-2010

Controlling Reductive Elimination From Novel I(III) Salts Using a SECURE Method

Joseph W. Graskemper

University of Nebraska at Lincoln, jgraskemper@huskers.unl.edu

Follow this and additional works at: <https://digitalcommons.unl.edu/chemistrydiss>



Part of the [Organic Chemistry Commons](#)

Graskemper, Joseph W., "Controlling Reductive Elimination From Novel I(III) Salts Using a SECURE Method" (2010). *Student Research Projects, Dissertations, and Theses - Chemistry Department*. 6.
<https://digitalcommons.unl.edu/chemistrydiss/6>

This Article is brought to you for free and open access by the Chemistry, Department of at DigitalCommons@University of Nebraska - Lincoln. It has been accepted for inclusion in Student Research Projects, Dissertations, and Theses - Chemistry Department by an authorized administrator of DigitalCommons@University of Nebraska - Lincoln.

CONTROLLING REDUCTIVE ELIMINATION
FROM NOVEL I(III) SALTS USING A SECURE METHOD

by

Joseph W. Graskemper

A THESIS

Presented to the Faculty of
The Graduate College in the University of Nebraska
In Partial Fulfillment of Requirements
For the Degree of Master of Science

Major: Chemistry

Under the Supervision of Professor Stephen G. DiMagno

Lincoln, Nebraska

August, 2010

CONTROLLING REDUCTIVE ELIMINATION
FROM NOVEL I(III) SALTS USING A SECURE METHOD

Joseph W. Graskemper, M.S.

University of Nebraska, 2010

Advisor: Stephen G. DiMagno

Positron Emission Tomography (PET) is a valuable clinical, research, and diagnostic technique for human and animal organ imaging. The current market for PET in the United States is \$500 million per year and is projected to be \$5.4 billion per year globally by 2015. To synthesize labeled radiotracers, we are most interested in using ^{18}F as the isotope of choice because it is a nearly ideal positron emitting radionuclide.

Electron-rich aromatic substrates can be particularly difficult to fluorinate. We show that reductive elimination of I(III) diaryliodonium salts provide increased fluorination of electron-rich aromatic substrates. Modest yields of fluorinated product were initially observed due to the lack of regioselectivity in the reductive elimination process. It seemed clear that a better directing group would be needed if extremely electron-rich rings are to be fluorinated in high chemical (or radiochemical) yields using diaryliodonium salts. The use of [2.2]paracyclophane as a directing ligand has been shown by computational and experimental data to provide an increase in steric demand above the plane of the aromatic ring; therefore, destabilizing a reductive elimination transition state. This effect is sufficiently large to provide stereoelectronic control of unidirectional reductive elimination (SECURE) for most nucleophiles; however, benzyne

chemistry was observed when fluorine and 2,2,2-trifluoroethoxide were used as nucleophiles.

To address the benzyne issue, we have shown that the choice of a judiciously substituted cyclophane substituent on I(III) can provide perfect regioselectivity for reductive elimination of iodocyclophanes and fluorination of electron-rich arenes. This work constitutes the first example of regiospecific fluorination of electron-rich aromatic rings using diaryliodonium fluorides. We believe this discovery paves the way for the synthesis of highly elaborated radiotracers from Ar_2IF salts.

Acknowledgements

First and foremost, I want to thank Dr. DiMagno for his enormous amount of support and dedication to my development as a chemist, for without his superb guidance this would have never been possible. I feel extremely lucky to have found such a wonderful advisor to work for, and I most certainly will look back at the times in lab with much enjoyment. I am also thankful to have been a teammate of Dr. DiMagno, or “Skywalker” on the basketball court, it was a good run. I would like to thank the members of the DiMagno group who I have had the pleasure of sharing the past couple years with: Kiel Neumann, Sara Hitchcock, Linlin Qin, Bijia Wang, Jason Kempinger, and Harsha Uppaluri. I am also thankful for having such a great friend in Kiel, we have had many great times (sometimes too great).

I am extremely thankful to my family (Mom, Dad, Dede, Gena, Paige) for all the unending love and support. I honestly do not know where I would be without you all. I would like to thank my dog, Dillinger, for getting me up every morning for the past six months and putting a smile on my face. Finally, to the person who was here by my side through the best and the worst, my incredible loving partner, Allie Salfity. You came out to Nebraska solely to support me in my venture for my degree; words cannot describe how thankful I am to have you in my life.

Table of Contents

ABSTRACT	ii
ACKNOWLEDGEMENTS	iv
TABLE OF CONTENTS	v
LIST OF TABLES	vii
LIST OF FIGURES	viii
LIST OF SCHEMES	ix
<u>CHAPTER ONE</u> – Introduction	11
1.1 Background.....	11
1.2 Fluorination via reductive elimination using diaryliodonium salts.....	16
1.3 References.....	23
<u>CHAPTER TWO</u> – The First I(III) Cyclophanes	24
2.1 Regiospecific reductive elimination from diaryliodonium salts.....	24
2.2 References.....	38
<u>CHAPTER THREE</u> - Regiospecific Fluorination of Electron-Rich Arenes	40
3.1 A solution to observed benzyne chemistry.....	40
3.2 Conclusion.....	42

3.3 References.....	44
<u>EXPERIMENTAL PROCEDURES</u>	45
<u>APPENDIX A</u> – Abbreviations.....	62
<u>APPENDIX B</u> – NMR Spectra.....	63

LIST OF TABLES

Table 1-1 List of commonly used positron emitters..... 11

Table 1-2 Observed yields of ArF from the decomposition of 1-8.....19

Table 2-1 Yields of reductive elimination products from the I(III)

salts shown in Scheme 2-4.....33

LIST OF FIGURES

Figure 1-1	Generation of ^{18}F	12
Figure 1-2	Examples of PET radiotracers.....	13
Figure 1-3	Structure of Kryptofix 222 KF.....	13
Figure 1-4	Iodine as a transition metal ion.....	16

LIST OF SCHEMES

Scheme 1-1 Pd-catalyzed aromatic fluorination utilizing tBuBrettPhos as the ligand...	15
Scheme 1-2 One-step methods to n.c.a. 1-bromo-4-[18F]fluorobenzene.....	17
Scheme 1-3 List of diaryliodonium fluorides made and studied.....	19
Scheme 1-4 Fluorination of drug candidates.....	21
Scheme 2-1 Examples of regioselectivities obtained in thermal decomposition reactions of unsymmetrical diaryliodonium salts.....	25
Scheme 2-2 Regiochemically controlled reductive elimination of an electron-rich, cyclophane-derived diaryliodonium salt.....	27
Scheme 2-3 Calculated TS structures and activation barriers for (2,5-dimethylphenyl) and [2.2]paracyclophan-4-yl iodonium salts.....	29
Scheme 2-4 Functionalization of diaryliodonium salts. (Reductively eliminated aryl iodides are omitted for clarity.).....	31
Scheme 2-5 Synthesis of 2-5.....	34
Scheme 2-6 Anisole functionalization by thermal decomposition of 2-5 in CD ₃ CN.....	35
Scheme 3-1 Observed products and proposed mechanistic benzyne pathway.....	40
Scheme 3-2 Synthesis of 3-1.....	41

Scheme 3-3 Reductive elimination from the iodonium fluoride of 3-1.....	42
--	----

CHAPTER ONE

Introduction

1.1 Background

Positron Emission Tomography (PET) is a valuable clinical, research, and diagnostic technique for human and animal organ imaging. The current market for PET in the United States is \$500 million per year and is projected to be \$5.4 billion per year globally by 2015.¹ The imaging process of PET begins when a labeled radioactive tracer is injected into a patient. The ^{18}F nucleus in the radioactive tracer undergoes radioactive decay ($p^+ \rightarrow n + B^+$) and emits a positron. This emitted positron collides with an electron in the environment resulting in an annihilation event. The destruction of matter results in the production of gamma radiation. The gamma radiation is then picked up by spatially addressable scintillation detectors surrounding the patient, and an image is then

Table 1-1 List of commonly used position emitters

Isotope	Half-life	Decay mode	$E_{\beta^+ \text{ avg.}}$ [keV]	Maximum (average) range in tissue [mm]	Maximum specific activity [GBq μmol^{-1}]
^{11}C	20.39 min	β^+ (99.8%) EC (0.24%)	385	3.8 (1)	3.4×10^5
^{13}N	9.965 min	β^+ (99.8%) EC (0.2%)	491	5 (1.5)	7.0×10^5
^{15}O	122.24 s	β^+ (99.9%) EC (0.01%)	735	7.6 (2.7)	3.4×10^6
^{18}F	109.77 min	β^+ (96.73%) EC (3.3%)	242	2.2 (0.3)	6.3×10^4
^{68}Ga	67.629 min	β^+ (89.1%) EC (11.0%)	740	13.6 (3.7)	1.0×10^5
^{124}I	4.1760 d	β^+ (22.8%) EC (11.0%), e^-	188	9.7 (3)	1.2×10^3

Table. Nuclear properties of commonly used positron emitters. (Data taken from Browne and Firestone 1986 and from Brookhaven National Laboratory internet data base, BNL 2003.)

reconstructed on a computer screen of a targeted area or organ.

Commonly used positron emitters include ^{11}C , ^{13}N , ^{15}O , ^{18}F , ^{68}Ga , and ^{124}I (Table 1-1). We are most interested in ^{18}F because it is a nearly ideal positron emitting radionuclide. Attractive characteristics of ^{18}F include: 1) It has a relatively long half life (109.77 min.), which allows ample time for the synthesis and transfer of radiotracers from a cyclotron facility to PET imaging centers. 2) The positron is emitted with relatively low kinetic energy (242 keV) and short range in tissue, and thus is captured proximal to the decay event. This leads to relatively high resolution (1 min.) 3) ^{18}F can be produced in large amounts in a single cyclotron run (>10 Ci). 4) Radiochemical yields for ^{18}F PET tracers can be extremely high.

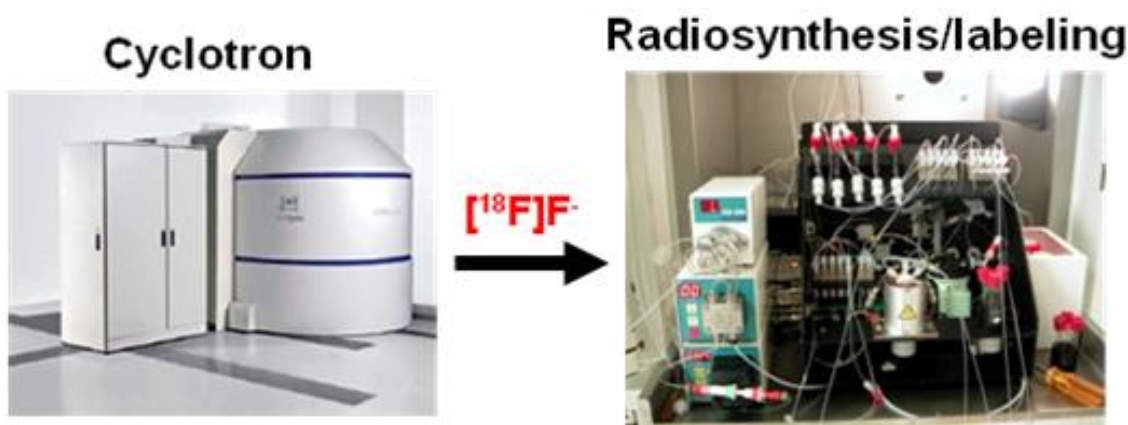


Figure 1-1 Generation of ^{18}F

^{18}F is generated in a particle accelerator (Figure 1-1). The most effective generation route of ^{18}F is through bombardment of H_2^{18}O with protons from the cyclotron. Once ^{18}F is generated, it is captured on an ion-exchange column, and liberated from the column with a salt solution, such as tetramethylammonium hydroxide (TMAOH), and a nucleophilic fluoride source tetramethylammonium fluoride (TMAF) is obtained. This TMA ^{18}F can now be introduced to a tracer of interest.

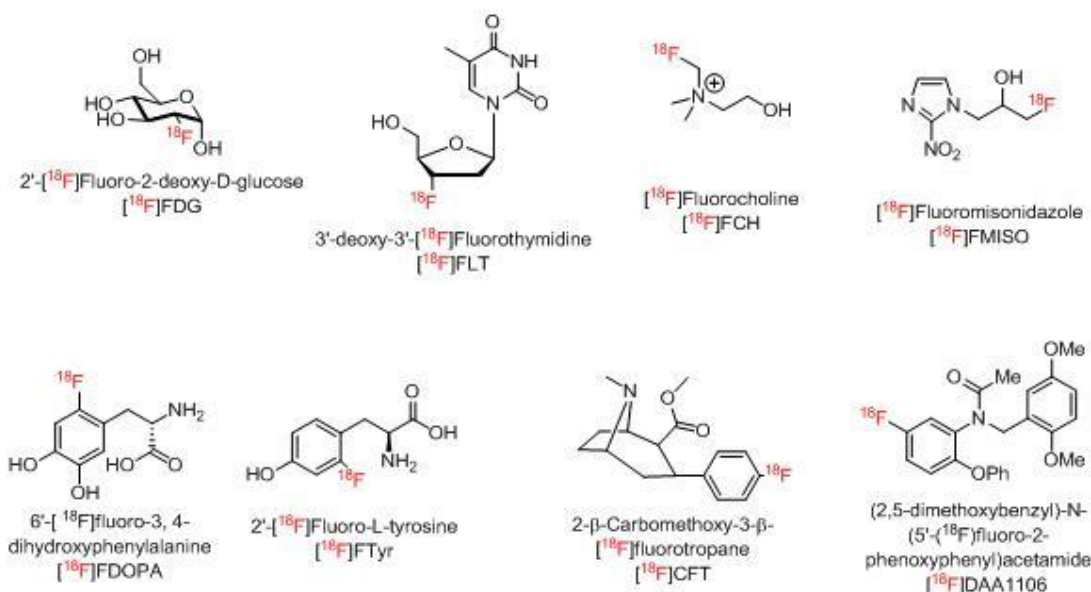


Figure 1-2 Examples of PET radiotracers

The most widely used ^{18}F PET radiotracer is 2-[^{18}F]Fluoro-2-deoxy-D-glucose ([^{18}F]FDG). It is widely used because of its ability to be produced in high yields and shorter reaction times. [^{18}F]FDG is synthesized by nucleophilic fluorination using mannose triflate as a precursor and Kryptofix 222 KF (Figure 1-3) or tetrabutylammonium salts (TBA). There are drawbacks to using [^{18}F]FDG as well. [^{18}F]FDG is rather widely distributed in the body, so identification of exceptionally metabolizing active tissues can be a problem. To address this issue, many different radiotracers need to be efficiently synthesized in order to target specific areas of interest throughout the body. A large number of these desired radiotracers require fluorination on an aromatic substrate (Figure 1-2).

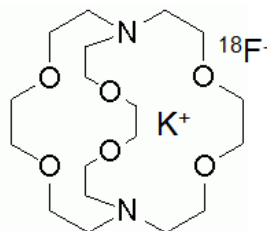
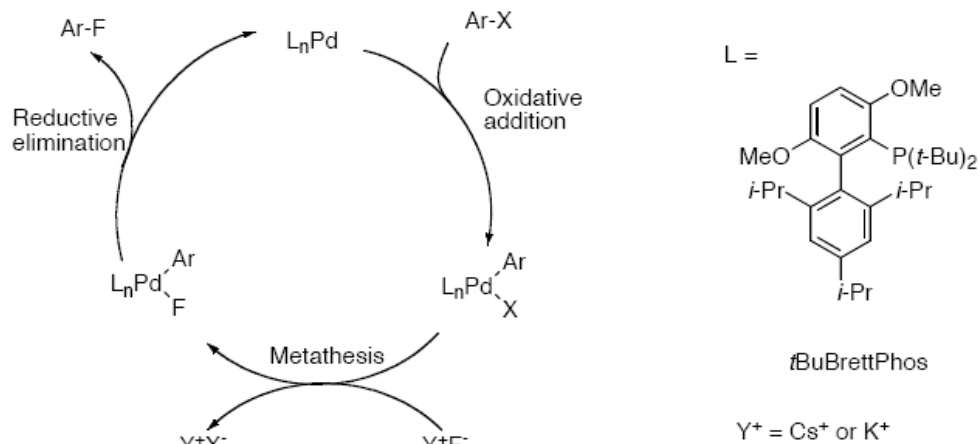


Figure 1-3 Structure of Kryptofix 222 KF

Two methods to prepare fluorinated aromatic radiotracers with ^{18}F include nucleophilic or electrophilic aromatic substitution. Nucleophilic aromatic fluorination is most commonly carried out with Kryptofix 222 KF or CsF. Nucleophilic fluoride, which has a moderate reactivity and high specific activity, is typically used for fluorination of electron-deficient arenes. Electrophilic fluorine is most commonly introduced through $[^{18}\text{F}]\text{F}_2$, or $[^{18}\text{F}]\text{AcOF}$. Electrophilic fluorine is highly reactive and carrier added (^{19}F present), which results in a low specific activity (amount of gamma radiation produced).

Electron-rich aromatic substrates can be particularly difficult to fluorinate. Nucleophilic fluorination of electron-rich arenes can only be accomplished by inclusion of an activating group that is subsequently removed; these multistep transformations are sometimes inefficient for PET chemistry. Direct fluorination of electron rich aromatic rings with $[^{18}\text{F}]\text{F}_2$ generally yields a mixture of regioisomers. Fluorodemetalation (usually fluorodestannylation) with $[^{18}\text{F}]\text{F}_2$ or $[^{18}\text{F}]\text{AcOF}$ can provide control of regiochemistry, however; metal toxicity is a concern and the fluorinated drug is still produced with relative low specific activity. Our goal is to develop a reliable, low-cost, easy-to-use system for on-demand radiolabeling, with the flexibility to develop new probes.



Scheme 1-1 Pd-catalyzed aromatic fluorination utilizing tBuBrettPhos as the ligand

Transition metal catalyzed fluorinations are one potential solution to fluorinate electron-rich aromatic substrates.² Recently, Buchwald and co-workers developed extremely hindered phosphine ligands that permit catalytic fluorination from fluoro-Pd(II) complexes for late stage incorporation of fluoride into electron-rich aromatic substrates (Scheme 1-1).² However, this approach is inefficient for PET applications for a number of reasons. The long reaction time (12 hours) and requirement for excess fluorinating agent (6 equiv. CsF) are clearly incompatible with the demands of radiotracer synthesis. In PET chemistry, the fluorinating agent is available in tiny amounts (10 ng / Curie). Regioisomers were identified as products during Buchwald's Pd-catalyzed fluorination of aryl triflates. Although no definitive explanation was given for the presence of regioisomers, the formation of benzyne was suspected to play a role in the formation of 3-fluoroanisole.

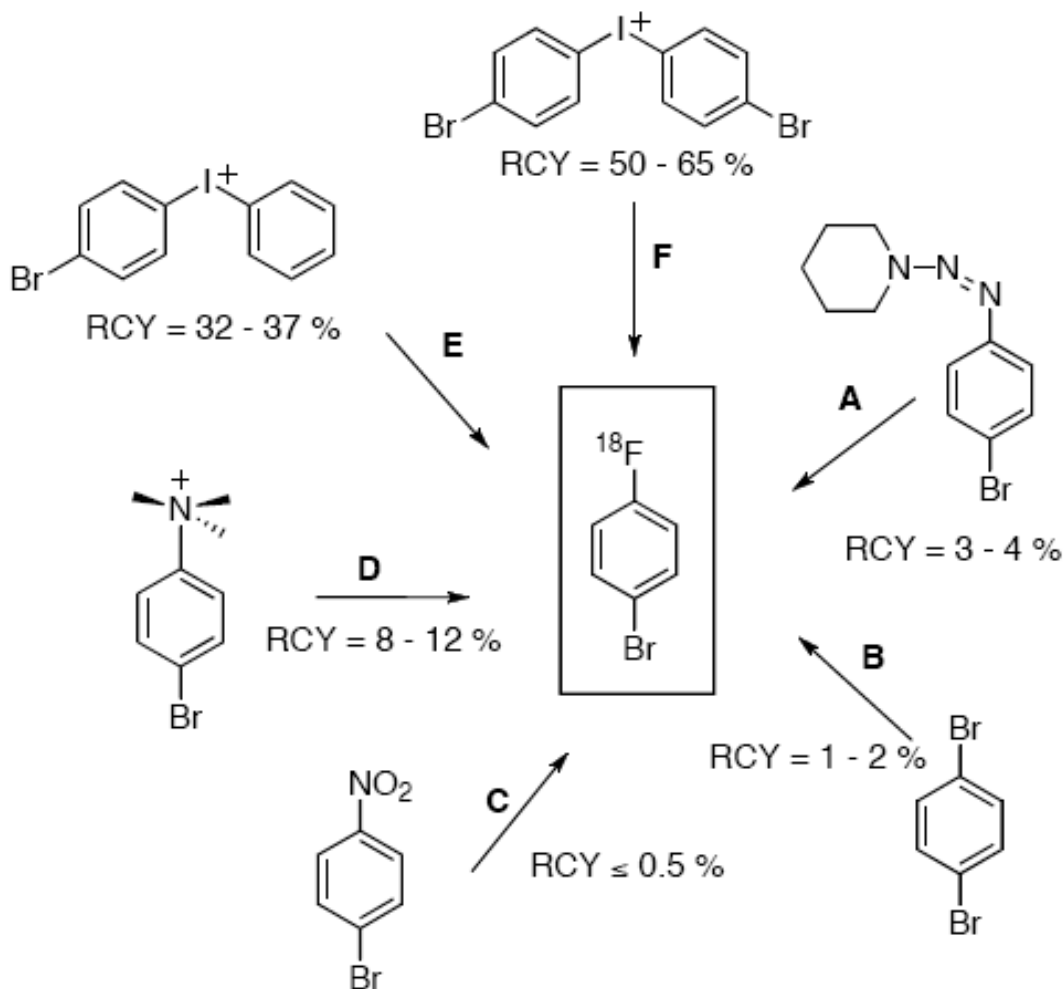
1.2 Fluorination via reductive elimination using diaryliodonium salts

While transition metal catalyzed fluorination appears to be a promising approach, given that the key step in the process for ^{18}F chemistry is a reductive elimination, we thought higher valent metal ions would show more promise. A difficulty with transition metals in high oxidation states is the potential for binding more than one anionic ligand. Since fluoride is generally extremely recalcitrant in reductive eliminations, we investigated stable aryl complexes that bound only one anion. It became clear that the conceptual framework used in the optimization of organometallic reactions is directly applicable to iodine chemistry: I(III) acts as a highly electronegative transition metal ion (Figure 1-4).



Figure 1-4 Iodine as a transition metal ion

There is a key difference in the reactivity of I(III) complexes and the late transition metal ions. While $\text{Ar}_2\text{M}(\text{X})_n$ complexes generally undergo reductive elimination of biaryls, Ar_2IX compounds form Ar-F and Ar-I upon reductive elimination. This different reactivity pattern is a direct consequence of the greater electronegativity of iodine and the tremendously increased stability of Ar-I(I) complexes compared to Ar-M complexes. This different reactivity manifold is a substantial advantage for I(III) chemistry.

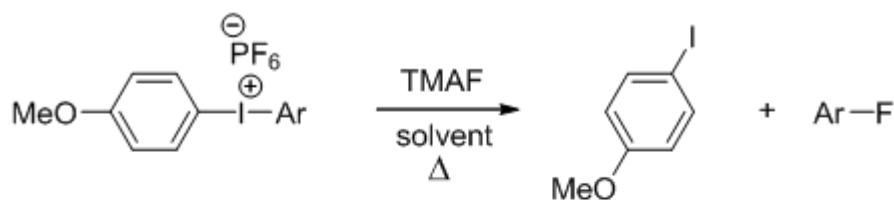


Scheme 1-2 One-step methods to n.c.a. 1-bromo-4-[^{18}F]fluorobenzene.³

Applications using iodine in diaryliodonium salts for fluorination of aromatic substrates has been known since the 1980's.⁴⁻⁶ This synthetic strategy was first introduced to ^{18}F PET radiotracers by Pike and co-workers in 1995.⁷ Prior to our work, the thermal decomposition reactions were performed exclusively in polar solvents, such as acetonitrile (CH_3CN). An example shown in Scheme 1-2 indicates that reductive elimination of diaryliodonium salts offers a highly competitive method to fluorinate unactivated aromatic compounds; The convenience of a one-step reaction to achieve a high radiochemical yield of product is an added bonus. Six different methods (Scheme 1-

2) to prepare 1-bromo-4-[^{18}F]fluorobenzene were compared by Ermert and co-workers.³ After comparison, it was concluded that the reductive elimination of the symmetrical diaryliodonium salts was the most efficient, with a radiochemical yields of up to 65 %. The unsymmetrical diaryliodonium salt reductive elimination resulted in lower yields of up to 37 %. This lower yield was attributed to the formation of [^{18}F]fluorobenzene (30 %). Although the symmetrical diaryliodonium salts offer the highest yields, it can be particularly difficult to synthesize the corresponding symmetrical salt of a desired radiotracer candidate if it is highly functionalized.

Studies have been performed in an effort to optimize fluorination of target compounds via reductive elimination of unsymmetrical diaryliodonium salts. Specifically, Woodcraft and co-workers⁸ and Suzuki and co-workers⁹ have achieved high radiochemical yields of multiple fluorinated aromatic substrates under nucleophilic conditions (Kryptofix 222 KF, Tetrabutylammonium fluoride (TBAF)) in polar solvents (CH_3CN , DMSO). A key conclusion from all fluorination is that the more electron-deficient ring is functionalized predominantly.¹⁰ The explanation for the observed regioselectivity is that negative charge builds on the attacked ring at the transition state, and this charge is best supported on the electron-poor ring.



- 1** Ar = 4-methoxyphenyl
2 Ar = 3,4-dimethoxyphenyl
3 Ar = 2-methoxyphenyl
4 Ar = 2-methyl-4,5-dimethoxyphenyl
5 Ar = 2,6-dimethoxyphenyl
6 Ar = Ph
7 Ar = m-CF₃Ph
8 Ar = m-CNPh

Scheme 1-3 List of diaryliodonium fluorides made and studied

Bijia Wang of the DiMagno group prepared a variety of diaryliodonium fluorides (Scheme 1-3). The reductive elimination of these diaryliodonium fluorides in acetonitrile was investigated, and the results of the thermal decomposition studies are included in Table 1-2.

Table 1-2 Observed yields of ArF from the decomposition of 1-8

#	1 eq. TMAPF ₆ present		No salt present	
	CD ₃ CN (ArF + 4FA)	C ₆ D ₆ (ArF + 4FA)	CD ₃ CN (ArF + 4FA)	C ₆ D ₆ (ArF + 4FA)
1	17 (-)	76 (-)	43 (-)	86 (-)
2	3 (2 + 1)	78 (59 + 19)	38 (30 + 8)	91 (77 + 14)
3	3 (2 + 1)	84 (59 + 25)	60 (40 + 20)	72 (49 + 23)
4	3 (2 + 1)	90 (76 + 14)	81 (49 + 32)	90 (78 + 12)
5	3 (1 + 2)	67 (28 + 39)	34 (7 + 27)	70 (32 + 38)
6	4 (3 + 1)	51 (41 + 10)	55 (40 + 15)	77 (57 + 20)
7	33 (33 + 0)	86 (86 + 0)	68 (68 + 0)	95 (85 + 10)
8	0	98 (93 + 5)	78 (78 + 0)	89 (89 + 0)

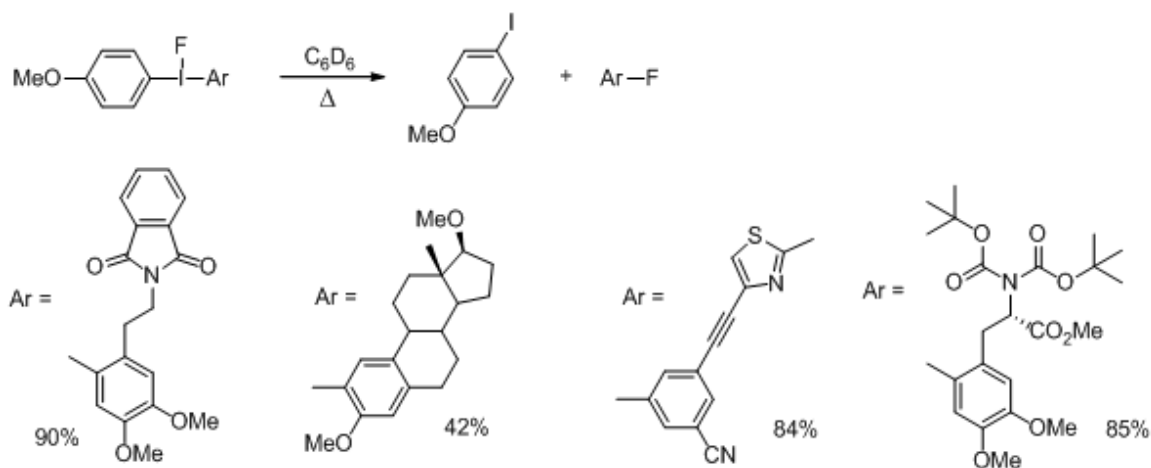
It was clear from this initial work that the use of polar solvents led to non-productive side reactions of these compounds. In the presence of fluoride, reduction of the I(III) salts to Aryl iodides was observed without generation of fluorinated arenes. Since fluoride is a strong donor for transition metal ions, it was suspected that disproportionation and subsequent redox reactions were the cause of this non-productive decomposition chemistry. To suppress these side reactions, the DiMagno group performed the thermal decomposition reactions in non-polar solvents; this change resulted in drastically improved yields of fluorinated arenes. After successfully optimizing solvent conditions, the effect of “spectator salts” such as tetramethylammonium hexafluorophosphate (TMAPF₆) was investigated by Kiel Neumann. He demonstrated (Table 1-1) that the presence of seemingly innocuous salts has a deleterious effect on the yield of fluorinated arenes isolated from the reaction. By filtering off the salt prior to the decomposition reaction, yields improved. It is worthwhile to note, as seen in previous studies, that fluorination of the more electron-deficient ring occurs selectively and that the reaction rates are faster for those salts bearing electron withdrawing substituents. Regioselectivity is not as high as is desired for some salts when the two rings are similarly electron-rich.

It is worth noting that diaryliodonium salt fluorination reactions can be scaled down for PET chemistry. Because the DiMagno group does not currently have access to ¹⁸F, we have developed a MS-based assay to detect nanogram amounts of product in the presence of a million fold excess of potential substrate, minimizing the conditions for radiotracer synthesis. This technique was sufficiently sensitive to detect and quantify

reproducible 500 femtograms of injected 4-fluoroanisole. This approach is also potentially useful for assessing $^{18}\text{F}/^{19}\text{F}$ ratios immediately after bombardment.

The impact of substrate and fluoride dilution was investigated because radiotracer synthesis is typically conducted in the fluoride concentration range of nM - μM . If only the pure bis(4-methoxyphenyl)iodonium fluoride is present, dilution greatly decreases yield of ArF. However, if a 20,000 fold excess of substrate (bis(4-methoxyphenyl)iodonium trifluoroacetate) is present, yields are reproducibly up to 80 % even if only 5 ng of fluoride is available.

Once the conditions for reductive elimination of diaryliodonium fluorides were optimized, the goal of the research was practical application of this new methodology to fluorinate a clinically-relevant radiotracer candidate (Scheme 1-4).



Scheme 1-4 Fluorination of drug candidates

Using our novel fluorination methodology and diaryliodonium salt precursors, ^{19}F -6-Fluorodopamine was prepared by Linlin Qin, ^{19}F -2-fluoroestradiol by ShriHarsha Uppaluri, 3-fluoro-5-[(2-methyl-1,3-thiazol-4-yl)ethynyl]benzonitrile (F-MTEB)¹¹ by Kiel Neumann, and ^{19}F -6-fluorodihydroxyphenylalanine (F-DOPA)¹² by Bijia Wang and Linlin Qin. Two Boc protecting groups were necessary in order to suppress the reducing

nature of the nitrogen and convenience of cleaving the protecting group. The yields for these fluorinated compounds were 90 %, 42 %, 84 %, and 85 %, respectively. Radiochemical yields for the F-MTEB were identical to chemical yields, fully surpassing previously established ^{18}F -MTEB radiochemical yield benchmarks (3 – 5 %)¹¹. The F-DOPA radiochemical yield was 30 % for n.c.a. methods, and is still climbing. Both the F-MTEB and F-DOPA reactions are complete within 50 minutes (including separation), which is also optimal for radiochemical tracer synthesis. The ^{19}F -2-fluoroestradiol suffered in yield due to the lack of regioselectivity in the reductive elimination process. These initial results of fluorination of drug candidates are very promising, but it seemed clear that a better directing group is needed if extremely electron-rich rings are to be fluorinated in high chemical (or radiochemical) yield using diaryliodonium salts.

1.3 References

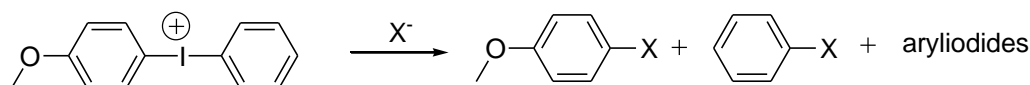
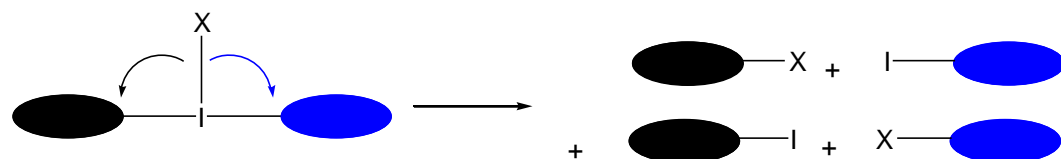
- [1] Global Industry Analyst “Radiopharmaceuticals – A US and European Market Report”
- [2] Watson, D. A.; Su, M.; Teverovskiy, G.; Zhang, Y.; Garcia-Fortanet, J.; Kinzel, T.; Buchwald, S. L. *Science* **2009**, 325 (5948), 1661-1664.
- [3] Ermert, J.; Hocke, C.; Ludwig, T.; Gail, R.; Coenen, H. H., *J. Labelled Compd. Radiopharm.* **2004**, 47 (7), 429-441.
- [4] Grushin, V. V.; Tolstaya, T. P.; Lisichkina, I. N., *Izv. Akad. Nauk SSSR, Ser. Khim.* **1983**, (9), 2165-8.
- [5] Van der Puy, M., *Journal of Fluorine Chemistry* **1982**, 21 (3), 385-92.
- [6] Grushin, V. V.; Kantor, M. M.; Tolstaya, T. P.; Shcherbina, T. M., *Izv. Akad. Nauk SSSR, Ser. Khim.* **1984**, (10), 2332-8.
- [7] Pike, V. W.; Aigbirhio, F. I., *J. Chem. Soc., Chem. Commun.* **1995**, (21), 2215-6.
- [8] Carroll, M. A.; Nairne, J.; Woodcraft, J. L.; *J. Labelled Compd. Radiopharm.*, 50, **2007**, 452-454
- [9] M.-R. Zhang, K. Kumata, K. Suzuki, *Tetrahedron Lett.*, 48, **2007**, 8632-8635
- [10] Yamada, Y.; Kashima, K.; Okawara, M., *Bull. Chem. Soc. Jpn.* **1974**, 47 (12), 3179-80.
- [11] Hamill, T. G.; Krause, S.; Ryan, C.; Bonnefous, C.; Govek, S.; Seiders, J.; Cosford, N.; Roppe, J.; Kamenecka, T.; Patel, S.; Gibson, R.; Danabria, S.; Riffel, K.; Eng, E.; King, C.; Green, M.; Burns, H. *Synapse* **2005**, 56, 205-216.
- [12] Garnett ES, Firna G, Nahmias C. *Nature*. **1983**, 305, 137-138.

CHAPTER TWO

The First I(III) Cyclophanes

2.1 Regiospecific Reductive Elimination from Diaryliodonium Salts

Diaryliodonium salts are useful precursors for arylation of diverse carbon and heteroatom nucleophiles.^[1-4] In practice, poor regioselectivity for reductive elimination narrows the synthetic scope of diaryliodonium salts (Scheme 2-1). Efficient conversion is best obtained when two identical aryl substituents are on I(III), however, the preparation of symmetrical diaryliodonium salts can be problematic and uneconomical.^[11] For relatively complex aromatic molecules, the tandem synthesis and protection of the oxidized (I(III)) and reduced (organometallic) coupling partners necessary to prepare the symmetrical diaryliodonium salt is often a significant challenge, and purification of the functionalized product from the reductively eliminated aryl iodide can prove difficult.

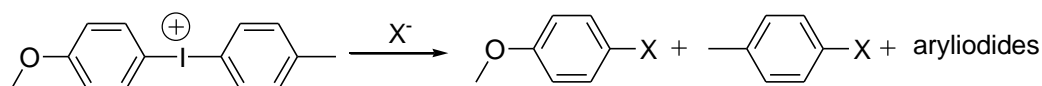


X = Br, 0.1 M in chloroform, 55 °C

1 : 9

X = diethyl methylmalonate,
0.25 M in DMF, with NaH, RT

7 : 93 combined yield: 86%

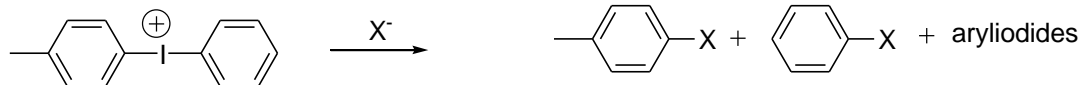


X = Br, 10 mM in DMF, 100 °C 10 h

27.1 : 72.9

X = diethyl methylmalonate,
0.25 M in DMF, with NaH, 0 °C

1 : 9 combined yield: 82%



X = Br, 10 mM in DMF, 100 °C 10 h

26.8 : 73.2

X = N₃, 0.25 M in Dioxane/water, 80 °C 2 h

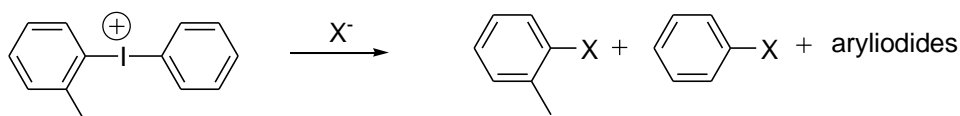
24 : 65

X = SCN, 0.25 M in Dioxane/water, 100 °C 24 h

30 : 69

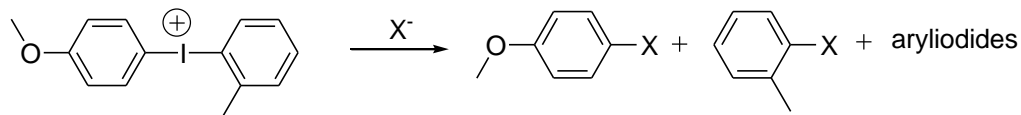
X = diethyl methylmalonate,
0.25 M in DMF, with NaH, RT

25 : 75 combined yield: 91%



X = Br, 12.5 mM in DMF, 100 °C 5 h

86.7 : 13.3



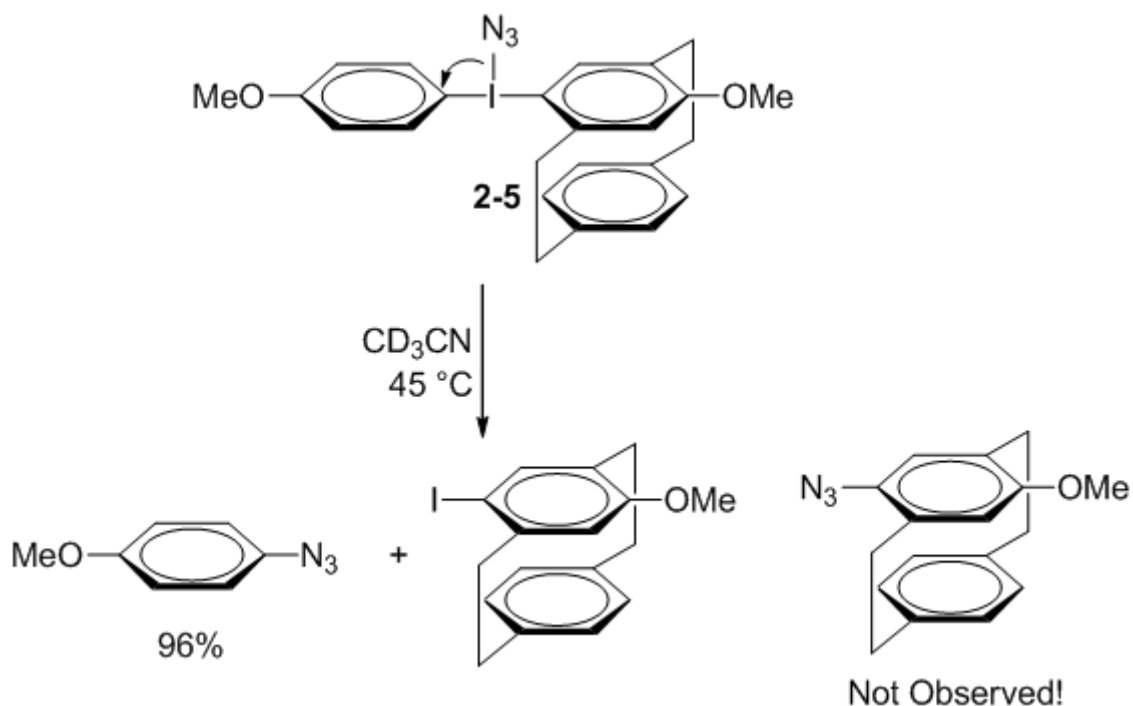
X = F, 80 mM in acetonitrile,
85 °C 40 min

only product yield: 11%

Scheme 2-1 Examples of regioselectivities obtained in thermal decomposition reactions of unsymmetrical diaryliodonium salts.^[5-10]

In the thermal decomposition of unsymmetrical diaryliodonium salts, the identity of the aryl iodide reductively eliminated is typically dictated by electronic effects; the electron-rich aryl iodide and the functionalized electron-poor aromatic compound are formed predominantly (Scheme 2-1). Selectively functionalized electron-rich aromatic rings are often the desired target compounds, but extremely electron-rich diaryliodonium salts are prone to side reactions involving redox and inner-sphere electron transfer, thus there is a limit to using electronic control to achieve regioselectivity.

We sought a universal “locked” aryl substituent that would result in StereoElectronic Control of Unidirectional Reductive Elimination (*SECURE*) from diaryliodonium salts. Since electronic effects cannot be used exclusively to achieve this end, steric and/or stereoelectronic effects must be exploited to gain regiocontrol of reductive elimination. Here we show that the use of cyclophane-derived iodonium salts permits regiospecific reductive elimination (Scheme 2-2).

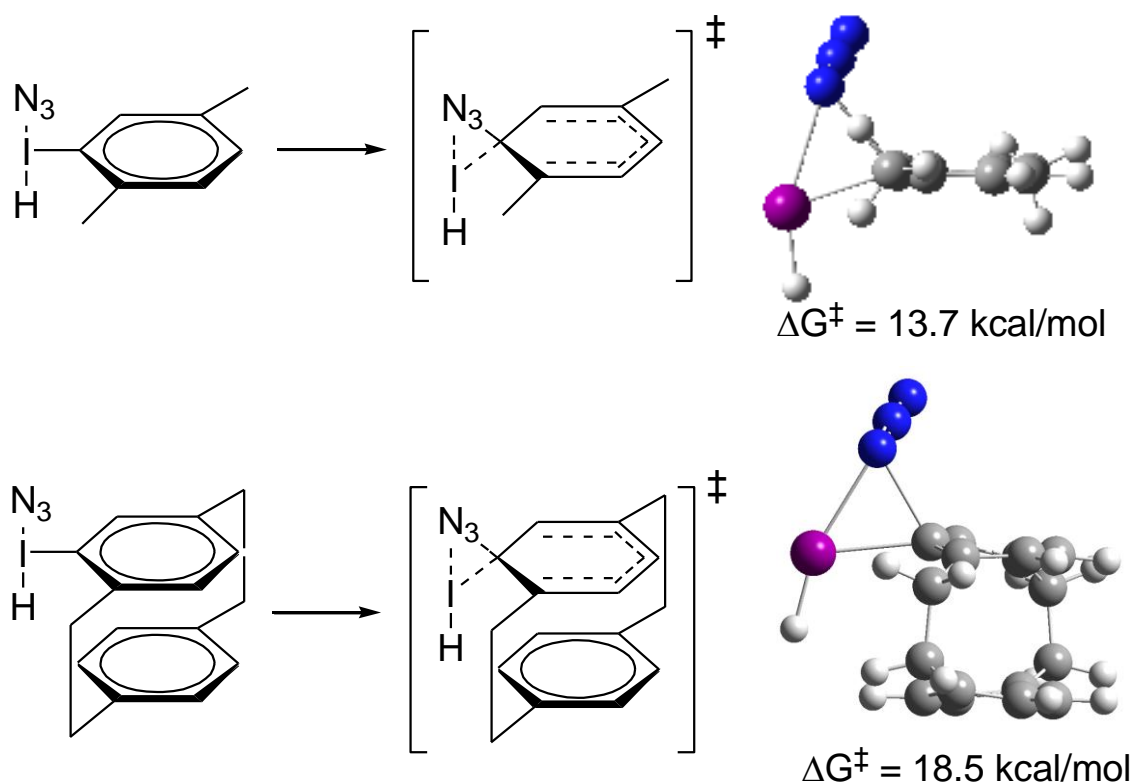


Scheme 2-2 Regiochemically controlled reductive elimination of an electron-rich, cyclophane-derived diaryliodonium salt

The impact of steric effects upon reductive elimination in diaryliodonium salts has been investigated in some detail. Aryl methyl substituents ortho to the I(III) center offer a modest acceleration in elimination rates, so that there is a slight preference for the more highly substituted product to be functionalized (Scheme 2-2).^[7, 12] Two potential origins of this “ortho effect” are: 1) the more sterically demanding aromatic ring prefers an equatorial position syn to the nucleophile, and 2) the ortho-substituted aromatic is more likely to prefer a conformation in which the π -system is more likely to align with the incoming nucleophile.^[13-15] In an exception to this rule, Ochiai and coworkers have shown that for binaphthyl aryl iodonium salts, ortho-substitution coupled with sterically demanding enolate nucleophiles results in alkylation of the less hindered ring, though only a small number of electronically similar aryl rings were investigated.^[16] Selective

functionalization of the more electron-rich aromatic ring in an unsymmetrical diaryliodonium salt remains an unsolved problem.

Our approach was to design an aryl ligand on iodine that would generate a highly strained reductive elimination transition state. If the mechanistic assumption of a concerted reductive elimination process is adopted, selective destabilization of this transition state requires significant steric congestion above and/or below the aromatic ring and little steric congestion in the plane of the ring. Thus, “strapped” or “capped” aromatic compounds were the initial leads for investigating *SECURE* methodology. [2.2]Paracyclophane^[17, 18] is a particularly attractive potential iodine(III) ligand because of its commercial availability, its efficient and established functionalization chemistry,^[19] its severe out of plane steric congestion, and the potential to exploit the planar chiral ligand in stereoselective reactions;^[20] however, compounds in which an I(III) center is bonded directly to [2.2]paracyclophane have not been reported to date.

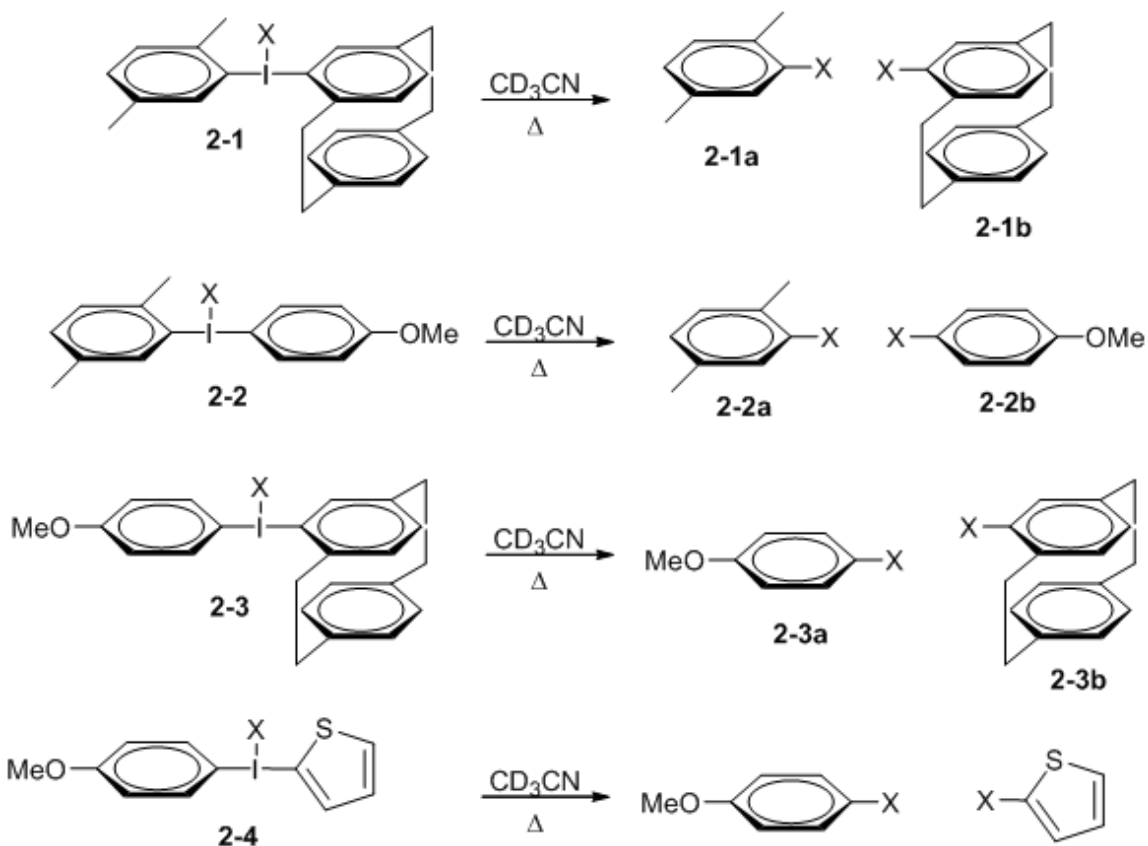


Scheme 2-3 Calculated TS structures and activation barriers for (2,5-dimethylphenyl) and [2.2]paracyclophan-4-yl iodonium salts.

The results of an initial computational study (B3LYP/DGDZVP, ZPE corrected) are shown in Scheme 2-3. We selected azide transfer in diaryliodonium salts for our test reaction since diaryliodonium azides are known to undergo reductive elimination at or near room temperature,^[9, 21] and because the small azide nucleophile has a relatively modest steric demand. Ground and transition state energies were calculated for a highly simplified model of azide substitution, loss of HI from the HIN_3Ar complexes of *p*-xylene and [2.2]paracyclophane. Inspection of Scheme 2-3 shows that movement from the ground state to the transition state geometries for azide substitution is accompanied by ipso carbon rehybridization and deflection of the HI group out of the plane. For the xylyl derivative the C4-C1-I angle is 161.9°. However, in the [2.2]paracyclophan-4-yl transition state structure the significant steric demand of the

second ring in the planar chiral ligand inhibits out of plane movement of the iodine atom (C4-C1-I angle is 167.2°). This structural difference is associated with an energetic penalty; the calculated free energy of activation for reductive elimination of HI from the *p*-xylene salt is 13.7 kcal/mol, while the barrier for the cyclophane derivative is 4.8 kcal/mol higher. Armed with an “in silico” justification for the *SECURE* concept, we sought its empirical validation.

To compare the directing effects of the electronically similar *p*-xylyl and [2.2]paracyclophan-4-yl groups experimentally, we synthesized the appropriate unsymmetrical diaryliodonium salts **1**. 4-Bromo-[2.2]paracyclophane^[19, 22] was lithiated (t-BuLi, Et₂O, -78 °C) and transmetalated with anhydrous zinc chloride. Following removal of the ether solvent, the organozinc chloride reagent was treated with 2,5-dimethyl(diacetoxyiodo)benzene in acetonitrile at -40 °C. After isolation and ion exchange to the hexafluorophosphate salt, compound **1** was formed in 18% yield. (Though organolithium,^[23, 24] organoboron,^[25] organosilicon,^[26] and organotin^[27] compounds have been used for diaryliodonium salt synthesis, to our knowledge this is the first example of the preparation of a diaryliodonium salt from an arylzinc chloride. The unusual reaction conditions used here were required because 4-trialkylstannyl[2.2]paracyclophanes do not transfer the cyclophane moiety cleanly in transmetalation reactions.^[28] A likely explanation for the poor reactivity of the stannane is that the transition state for cyclophane transfer is highly congested and resembles that shown in Scheme 2-3.)



Scheme 2-4 Functionalization of diaryliodonium salts. (Reductively eliminated aryl iodides are omitted for clarity.)

The hexafluorophosphate salt of **2-1** is particularly convenient because a wide range of nucleophiles may be introduced via their tetraalkylammonium or sodium salts. Accordingly, when compound **2-1** was treated with TBAN_3 and heated at 45 °C in CD_3CN (0.04 M), conversion of the diaryliodonium azide was complete within a few hours. In support of the initial hypothesis, the azidoxylene is formed exclusively in excellent yield, and no azidocyclophane is observed at the detection limit of ^1H NMR spectroscopy. This unidirectional elimination is also observed with thiocyanate, phenoxide, thiophenoxide, trifluoroethoxide, and acetate (Table 1). The observed

selectivity (> 99:1) corresponds to a difference in the free energies of activation ($\Delta\Delta G^\ddagger$) of at least 2.8 kcal/mol. Thus, the validity of the computational model is confirmed.

To provide context for the *SECURE* results, arene functionalization by various nucleophiles (X) in compound **2-2** was investigated. The regioselectivity observed during the reductive elimination of cyclophanyl-substituted diaryliodonium salts mirrors that of 4-methoxyphenyl derivatives (Table 2-1). The 4-methoxyphenyl moiety is the most effective, commonly employed directing group in diaryliodonium chemistry^[10, 29, 30], however perfect regioselectivity for arene functionalization is not observed with this directing group. For the redox active thiophenoxide and phenoxide nucleophiles, some loss of regiocontrol is evident and functionalized anisoles are formed.

To test the relative directing group abilities of 4-methoxyphenyl and [2.2]paracyclophan-4-yl substituents, we prepared the unsymmetrical I(III) derivative **2-3** from 4-methoxy(diacetoxyiodo)benzene (38% yield) and examined its thermal decomposition chemistry. More vigorous reaction conditions (80 °C, CD₃CN) were necessary to promote speedy carbon-heteroatom bond formation with acetate and thiocyanate from **2-3** in comparison to **2-1** or **2-2**. As can be seen from inspection of Table 2-1, the directing group ability of the [2.2]paracyclophane ligand is comparable or slightly superior to that of the 4-methoxyphenyl substituent on I(III).

The 2-thienyl substituent has been reported to deliver high regioselectivities for the radiofluorination of various electron-rich arenes,^[31] We synthesized **4** to examine the relative directing group abilities of the 2-thienyl and 4-methoxyphenyl substituents under stoichiometric conditions. Inspection of the data in Table 2-1 indicates that, for the nucleophiles examined here, the 2-thienyl moiety's directing group ability is roughly

comparable to the 4-methoxyphenyl and [2.2]paracyclophane ligands on I(III). In all cases significant amounts of the 4-iodoanisole are generated during the thermal decomposition reactions of **2-4**, even when 2-functionalized thiophenes are not observed. These data support Carroll's assessment^[32] and the original observations by Yamada and Okawara^[33] that the directing group ability of the 2-thienyl and 4-methoxyphenyl substituents are similar.

Table 2-1 Yields^a of reductive elimination products from the I(III) salts shown in Scheme 2-4.

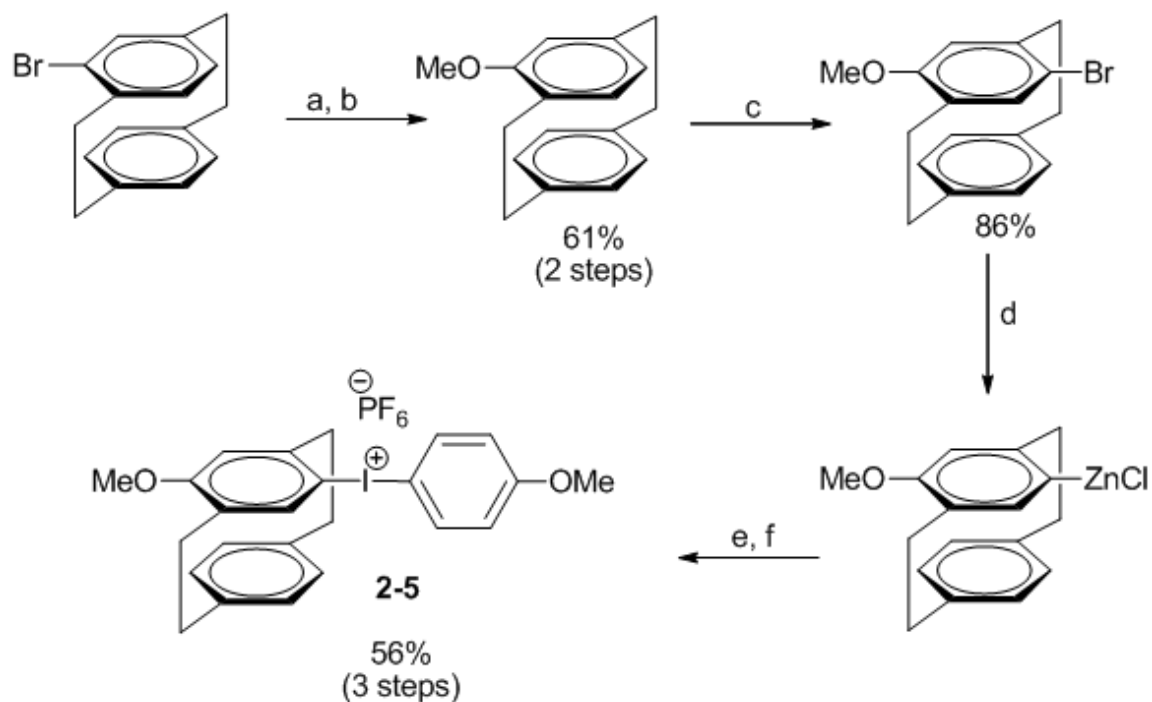
X	2-1		2-2		2-3		2-4	
	2-1a	2-1b	2-2a	2-2b	2-3a	2-3b	2-4a	2-4b
N ₃	99<	0	99<	0	86	14	66	0 ^b
OAc	85	0	99<	0	68	31	18	0 ^b
OPh	87	0	96	4	51	40	69	23
OCH ₂ CF ₃	82	0	80	0	19	39	17	43
SCN	99<	0	99<	0	81	18	43	0 ^b
SPh	98	0	95	5	43	52	30	40

^aAll yields were determined by ¹H NMR spectroscopy and confirmed by GC-MS.

^bDecomposition of the functionalized thiophene was observed.

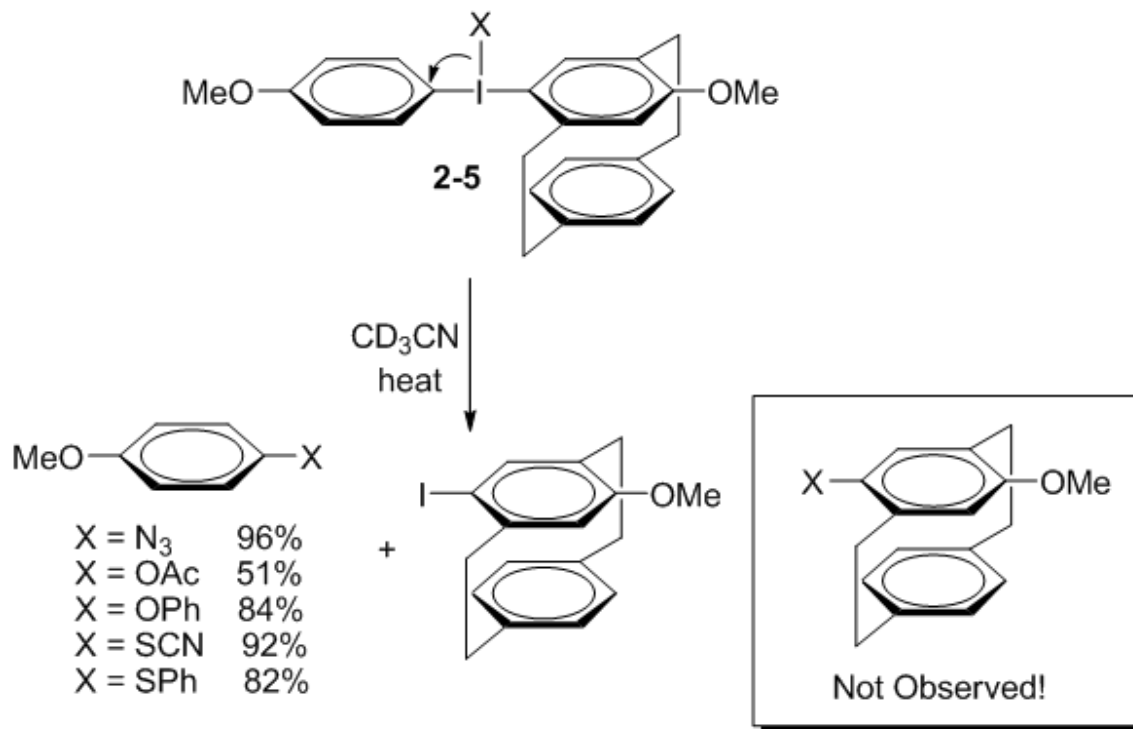
Though the data in Table 1 are limited, it appears that for oxygen or sulphur nucleophiles the directing group ability of the cyclophane ligand diminishes as nucleophile basicity and the driving force for functionalizing the more electron-poor ring increase. Such a trend is consistent with Hammond's postulate and a concerted, reductive elimination mechanism in which less steric strain is developed at the cyclophane ipso carbon atom as the reaction becomes more exergonic.

The kinetics of aryl azide formation from N_3 salts of **2-1**, **2-2** and **2-3** were investigated to probe the relative steric and electronic contributions to the observed regioselectivity. The observed rate constants for xylyl azide formation (CD_3CN , 45 °C) were $4.2 \times 10^{-4} \text{ s}^{-1}$, $5.5 \times 10^{-5} \text{ s}^{-1}$, and $3.3 \times 10^{-6} \text{ s}^{-1}$, corresponding to free energies of activation of 21.7, 22.9, and 24.6 kcal/mol for the reactions of **2-1**, **2-2** and **2-3**, respectively. The fact that the rate constant for formation of azidoxylene is greater for **1** than **2-2** indicates that 4-iodo-[2.2]paracyclophane is a significantly better leaving group than 4-iodoanisole. Since leaving group ability is correlated with the electron density on iodine in the aryl iodide being reductively eliminated, these kinetic data show experimentally that the [2.2]paracyclophane ligand is a significantly more electron-poor aryl substituent than 4-methoxyphenyl and that steric destabilization of the transition state is responsible for the enhanced directing group ability of the [2.2]paracyclophane ligand.



Scheme 2-5 Synthesis of 2-5. (a. 1. *t*-BuLi, Et₂O, -78 °C, 2. B(OMe)₃, 3. H₂O₂, NaOH, H₂O; b. K₂CO₃, CH₃I, CH₃CN, 80 °C; c. NBS, CH₂Cl₂; d. 1. *t*-BuLi, Et₂O, -78 °C, 2. ZnCl₂; e. 1. 4-MeOC₆H₄I(OAc)₂, CH₃CN, -40 °C, f. NaPF₆, H₂O.)

These initial results validated the *SECURE* concept, but perfect regiochemical control was still not available for functionalizing very electron-rich rings. To address this issue we prepared compound **2-5**, which features an electron donating methoxy substituent para to the I(III) center (Scheme 2-5). The methoxy substituent enhances the solubility of the cyclophane organozinc chloride reagent, leading to improved yield in the I(III) transfer reaction.



Scheme 2-6 Anisole functionalization by thermal decomposition of 2-5 in CD₃CN

We were gratified to find that **2-5** provides excellent regiochemical control for arene functionalization across the range of nucleophiles investigated here. Only anisole substitution was observed after the thermal decomposition of the azide, acetate, phenoxide, thiocyanate, and thiophenoxide salts (Scheme 2-6). However, a mixture of cyclophane- (30%) and anisole-substituted (60%) products was obtained from the reductive elimination of the 2,2,2-trifluoroethoxide salt of **2-5**. The reason for the breakdown in regioselectivity is clear from the product analysis, which shows roughly equal amounts of 3- and 4-(2,2,2-trifluoroethoxy)anisole, as well as roughly equal amounts of the two CF₃CH₂O-substituted cyclophane regioisomers. This lack of selectivity and distribution of regioisomers is consistent with a change in mechanism to one involving benzyne intermediates. For this basic nucleophile, the strategy of raising

the transition state energy for reductive elimination of the aryl iodide enables the benzyne reaction manifold to be competitive.

In summary, computational and experimental data show that an increase in steric demand above the plane of the aromatic ring destabilizes a reductive elimination transition state. This effect is sufficiently large to provide stereoelectronic control of unidirectional reductive elimination (*SECURE*); a number of examples are provided to show that the intrinsic electronic bias in reductive elimination reactions of I(III) compounds can be overcome. Significantly, even 4-methoxyphenyl groups can be functionalized regiospecifically. Moreover, since the approach is a general one, it is anticipated that *SECURE* will be useful for controlling reductive elimination from a variety of high valent main group and transition metal ions.

2.2 References

- [1] E. A. Merritt, B. Olofsson, *Angew. Chem., Int. Ed.* **2009**, 48, 9052.
- [2] V. V. Zhdankin, P. J. Stang, *Chem. Rev.* **2008**, 108, 5299.
- [3] T. Wirth, *Angew. Chem., Int. Ed.* **2005**, 44, 3656.
- [4] T. Wirth, in *Top. Curr. Chem., Vol. 224*, Springer, Berlin, **2003**.
- [5] M. Fujita, E. Mishima, T. Okuyama, *J. Phys. Org. Chem.* **2007**, 20, 241.
- [6] C. H. Oh, J. S. Kim, H. H. Jung, *J. Org. Chem.* **1999**, 64, 1338.
- [7] Y. Yamada, M. Okawara, *Bull. Chem. Soc. Jap.* **1972**, 45, 1860.
- [8] Y. Yamada, K. Kashima, M. Okawara, *Bull. Chem. Soc. Jpn.* **1974**, 47, 3179.
- [9] J. J. Lubinkowski, M. Gomez, J. L. Calderon, W. E. McEwen, *J. Org. Chem.* **1978**, 43, 2432.
- [10] A. Shah, V. W. Pike, D. A. Widdowson, *J. Chem. Soc., Perkin Trans. 1* **1998**, 2043.
- [11] L. Cai, S. Lu, V. W. Pike, *Eur. J. Org. Chem.* **2008**, 2853.
- [12] K. M. Lancer, G. H. Wiegand, *J. Org. Chem.* **1976**, 41, 3360.
- [13] V. V. Grushin, *Acc. Chem. Res.* **1992**, 25, 529.
- [14] V. V. Grushin, I. I. Demkina, T. P. Tolstaya, *J. Chem. Soc., Perkin Trans. 2* **1992**, 505.
- [15] M. A. Carroll, S. Martin-Santamaria, V. W. Pike, H. S. Rzepa, D. A. Widdowson, *J. Chem. Soc., Perkin Trans. 2* **1999**, 2707.
- [16] M. Ochiai, Y. Kitagawa, N. Takayama, Y. Takaoka, M. Shiro, *J. Am. Chem. Soc.* **1999**, 121, 9233.
- [17] D. J. Cram, H. Steinberg, *J. Am. Chem. Soc.* **1951**, 73, 5691.

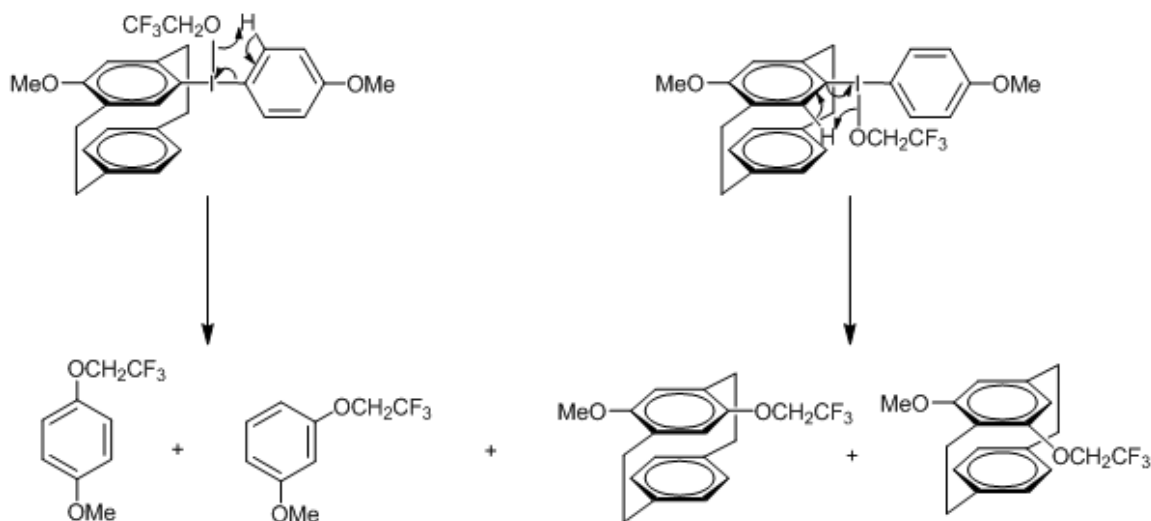
- [18] C. J. Brown, A. C. Farthing, *Nature (London, U. K.)* **1949**, *164*, 915.
- [19] H. J. Reich, D. J. Cram, *J. Amer. Chem. Soc.* **1969**, *91*, 3534.
- [20] S. E. Gibson, J. D. Knight, *Org. Biomol. Chem.* **2003**, *1*, 1256.
- [21] V. V. Grushin, M. M. Kantor, T. P. Tolstaya, T. M. Shcherbina, *Izv. Akad. Nauk SSSR, Ser. Khim.* **1984**, 2332.
- [22] H. J. Reich, D. J. Cram, *J. Amer. Chem. Soc.* **1968**, *90*, 1365.
- [23] F. M. Beringer, R. A. Nathan, *J. Org. Chem.* **1970**, *35*, 2095.
- [24] F. M. Beringer, L. L. Chang, *J. Org. Chem.* **1972**, *37*, 1516.
- [25] M. A. Carroll, V. W. Pike, D. A. Widdowson, *Tetrahedron Lett.* **2000**, *41*, 5393.
- [26] G. F. Koser, R. H. Wettach, C. S. Smith, *J. Org. Chem.* **1980**, *45*, 1543.
- [27] V. W. Pike, F. Butt, A. Shah, D. A. Widdowson, *J. Chem. Soc., Perkin Trans. I* **1999**, 245.
- [28] V. A. Nikanorov, V. I. Rozenberg, V. G. Kharitonov, E. V. Yatsenko, V. V. Mikul'shina, N. A. Bumagin, I. P. Beletskaya, V. N. Guryshchev, V. V. Yur'ev, O. A. Reutov, *Metalloorg. Khim.* **1991**, *4*, 689.
- [29] M. A. Carroll, J. Nairne, J. L. Woodcraft, *J. Labelled Compd. Radiopharm.* **2007**, *50*, 452.
- [30] M.-R. Zhang, K. Kumata, K. Suzuki, *Tetrahedron Lett.* **2007**, *48*, 8632.
- [31] T. L. Ross, J. Ermert, C. Hocke, H. H. Coenen, *J. Am. Chem. Soc.* **2007**, *129*, 8018.
- [32] M. A. Carroll, C. Jones, S.-L. Tang, *J. Labelled Compd. Radiopharm.* **2007**, *50*, 450.
- [33] Y. Yamada, M. Okawara, *Bull. Chem. Soc. Jap.* **1972**, *45*, 2515.
- [34] A. R. Katritzky, J. K. Gallos, H. D. Durst, *Magn. Reson. Chem.* **1989**, *27*, 815.
- [35] G. Cerioni, G. Uccheddu, *Tetrahedron Lett.* **2004**, *45*, 505.

CHAPTER THREE

Regiospecific Fluorination of Electron-Rich Arenes

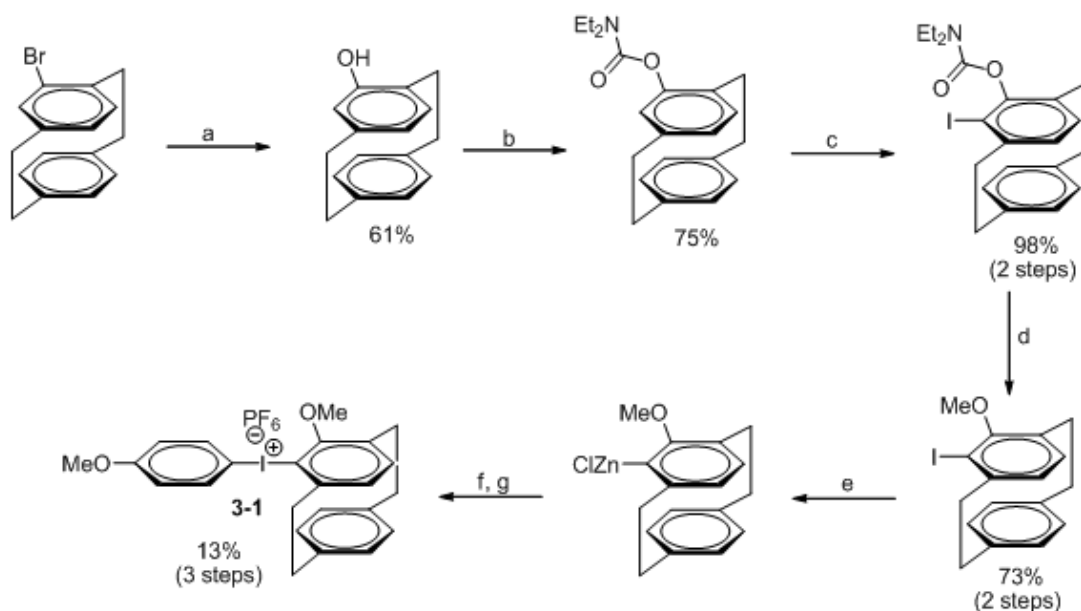
3.1 A solution to observed benzyne chemistry

As stated in 2.1, a mixture of products (cyclophane- (30 %) and anisole-substituted (60 %)) were obtained from reductive elimination of the 2,2,2-trifluoroethoxide salt. This suspected benzyne chemistry was also observed when fluorine was used as the nucleophile. The proposed mechanism that resulted in formation of these products is shown in Scheme 3-1.



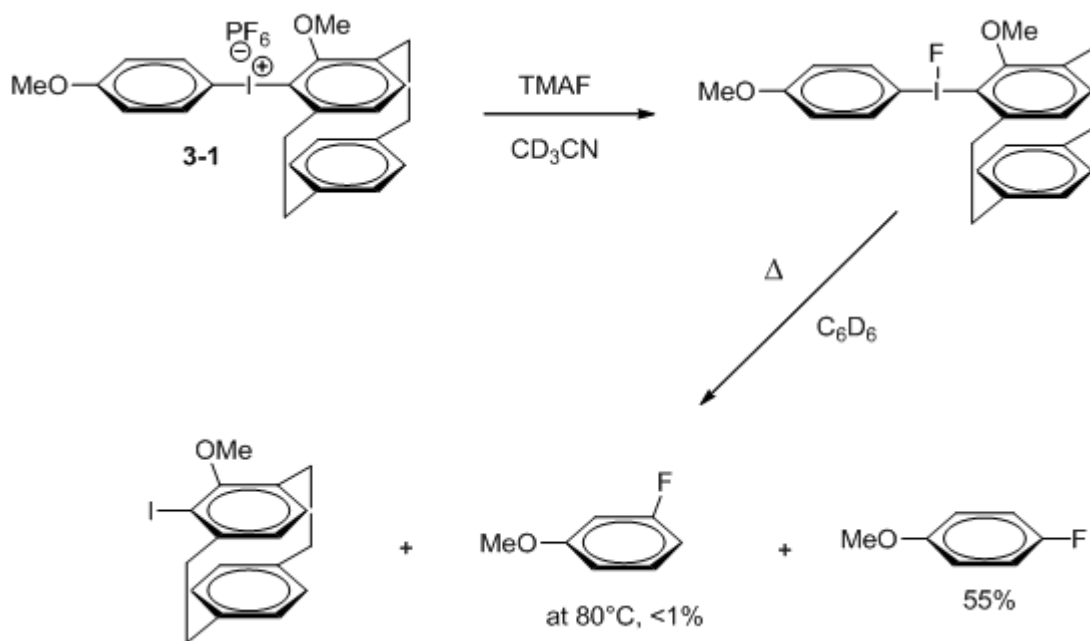
Scheme 3-1 Observed products and proposed mechanistic benzyne pathway

We suspected that a cyclophane substituent ortho to the I(III) center would shut down benzyne chemistry on the cyclophane and restore regiospecificity for fluorination. Toward this end, we developed a synthesis of compound **3-1** shown in Scheme 3-2.



Scheme 3-2 Synthesis of 3-1

Our original approach to obtaining **3-1** was through ortho-lithiation of 4-methoxy[2.2]paracyclophane and subsequent transmetalation with zinc chloride. Direct ortho-lithiation of methoxy cyclophane was not successful, even with $t\text{-BuLi}$ or with $n\text{-BuLi}$ / tetramethylethyldiamine (TMEDA) mixtures. We suspect that the steric congestion of the cyclophane ring system makes ortho-activation difficult. Thus, we installed a better ortho directing group (carbamate) and planned a more indirect synthesis (Scheme 3-2). This synthesis relied heavily on the work of Hopf¹, Lectka², and Snieckus³ who showed that efficient lithiation was possible with the carbamated directing group. By synthesizing O-(4-[2.2]paracyclopentyl) diethylcarbamate, we were able to obtain the corresponding 4-methoxy-5-iodo[2.2]paracyclophane in 73% yield over four steps. Following our previous synthetic strategy for introducing the iodoaniso moiety into **2-3**, **2-4**, and **2-5**, we were able to obtain **3-1** in 13% yield.



Scheme 3-3 Reductive elimination from the iodonium fluoride of **3-1.**

Reductive elimination reactions with the iodonium fluoride of **3-1** were studied (Scheme 3-3). The results demonstrated that by blocking the ortho position with a methoxy group, benzyne chemistry was completely shut down on the cyclophane ring. Using NMR and GC analysis, the 4-fluoroanisole was the major product, and was obtained in 55 % yield. To our surprise, evidence for benzyne chemistry on the anisole ring was almost absent; less than a 1% yield of 3-fluoroanisole was present when the thermal decomposition reaction was conducted at 80°C (Scheme 3-3).

3.2 Conclusion

We have shown that the choice of a judiciously substituted cyclophane substituent on I(III) can provide perfect regioselectivity for reductive elimination of iodocyclophanes and fluorination of electron-rich arenes. This work constitutes the first example of regiospecific fluorination of electron-rich aromatic rings using diaryliodonium fluorides.

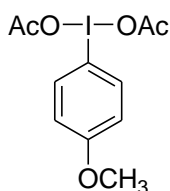
We believe this discovery paves the way for the synthesis of highly elaborated radiotracers from Ar_2IF salts.

3.3 References

- 1) Barrett, D.G.; Hopf, H. *Liebigs. Ann.* **1995**, 449-451.
- 2) Wack, H.; France, S.; Hafez, A.; Drury, W.; Weatherwax, A.; Lectka, T. *J. Org. Chem.* **2004**, 69, 4531.
- 3) Sibi, M. P.; Snieckus, V. *J. Org. Chem.* **1983**, 48, 1935.

Experimental Procedures

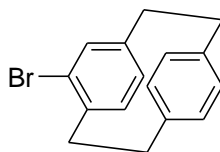
Bis(acetyloxy)-(4-methoxyphenyl)- λ_3 -iodane; (1-(diacetoxyiodo)-4-methoxybenzene)



4-Iodoanisole (2.34 g, 10 mmol) was dissolved in 90 mL of glacial acetic acid and the stirred solution was warmed to 40 °C. Sodium perborate tetrahydrate (13.6 g, 110 mmol) was added in portions over the course of one hour. After the addition was complete, the temperature of the reaction mixture was maintained at 40 °C for 8 h before it was allowed to cool to room temperature. Half of the acetic acid (~ 45 mL) was removed by distillation at reduced pressure. The remaining solution was treated with 100 mL of deionized water and the aqueous layer was extracted (3 × 40 mL) with dichloromethane. The combined organic fractions were dried over sodium sulfate, and the solvent was removed by rotary evaporation to give 2.25 g (64%) of 1-(diacetoxyiodo)-4-methoxybenzene, **1**. This compound was dried in vacuo and used without further purification. ¹H NMR (CD₃CN, 400 MHz, 25 °C): δ 8.055 (d, J = 9.1 Hz, 2H, H2/H6), 7.053 (d, J = 9.1 Hz, 2H, H3/H5), 3.861 (s, 3H, OMe), 1.905 (s, 6H, (OCOCH₃)₂); ¹³C NMR (CD₃CN, 100 MHz, 25 °C) δ 177.73 (CO), 163.73 (C4), 138.75

(C2/C6), 118.00, (C3/C5), 111.97 (C1), 56.85 (OMe), 20.76 ((OCOCH₃)₂); HRMS: (HRFAB) calcd. for C₁₄H₁₃NO₄I [M – 2OAc+3-NBA]⁺ 385.9889 found 385.9885. (lit. ^{2,3} ¹³C NMR (CDCl₃, 50 MHz, 20 °C) δ 162.0 (C4), 137.0 (C2/C6), 116.5 (C3/C5), 111.4 (C1).); ¹³C NMR (CDCl₃, 75 MHz, 25 °C) δ 176.31 (CO), 111.64 (C1), 20.36 ((OCOCH₃)₂).)

4-Bromo-[2.2]paracyclophane

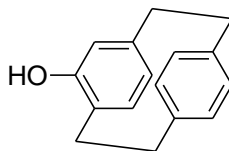


N-Bromosuccinimide (890.1 mg, 5.0 mmol) and trifluoroacetic acid (570 mg, 0.385 mL, 5.0 mmol) were dissolved in 40 mL of dichloromethane and added to a CH₂Cl₂ solution (80 mL) of [2.2]paracyclophane (1.0297 g, 4.9 mmol). The resulting mixture was covered from light and stirred for 4 hours at room temperature. The solution was transferred to a separatory funnel and washed (3 x 50 mL) with 2 M aqueous sodium bicarbonate solution followed by a single deionized water wash. The organic layer was separated, dried over Na₂SO₄, and the solvent was evaporated to give a nearly colorless solid (1.061 g, 75%) that was sufficiently pure to carry forward in the synthesis. ¹H NMR (CDCl₃, 400 MHz, 25 °C): δ 7.18 (dd, J = 7.8, 1.9 Hz, 1 H), 6.45-6.61 (m, 6 H), 3.45-3.52 (m, 1 H), 2.80-3.26 (m, 7 H); ¹³C NMR (CDCl₃, 100 MHz, 25 °C) δ 141.61, 139.33,

139.11, 137.25, 135.05, 133.31, 133.02, 132.91, 132.25, 131.46, 128.69, 126.97, 35.85, 35.48, 34.82, 33.47.

Cram, D. J.; Day, A. C. *J. Am. Chem. Soc.* **1966**, *31*, 1227-32.

4-Hydroxy[2.2]paracyclophane

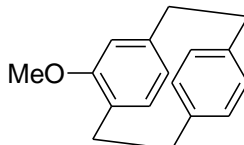


In a 50 mL Schlenk tube under nitrogen, a stirred, cold (-78 °C) solution of 4-bromo[2.2]paracyclophane (4.0 mmol, 1.14 g) in 50 mL of anhydrous diethyl ether was treated with t-BuLi (1.7 M in pentane, 2.5 equiv., added dropwise). The resulting mixture was stirred at -78 °C for 20 minutes and held subsequently at 0 °C for 20 min. To this heterogeneous yellow mixture trimethyl borate (831.29 mg, 8.0 mmol) was added dropwise and the mixture was stirred for 1 hour at room temperature. During this period the solution became homogeneous and dark yellow. Aqueous NaOH (0.5 M, 2 mL) and H₂O₂ (30%, 1.5 mL) were added. There was a slight exotherm and gas was evolved. The resulting mixture was allowed to stir overnight at room temperature. Additional aqueous NaOH solution (0.5 M, 5 mL) was added and the pH of the solution was adjusted to neutral using saturated sodium bicarbonate solution and 1 M HCl. The mixture was extracted (3 x 20 mL) with diethyl ether. The combined ether extracts were washed with 0.5 M sodium bisulfite, separated, and dried over Na₂SO₄. Removal of the solvent by

rotary evaporation gave a light brown solid (844.1 mg, 94.1%). ^1H NMR (CDCl_3 , 400 MHz, 25 °C): δ 7.01 (dd, $J = 7.8, 1.9$ Hz, 1 H), 6.56 (dd, $J = 7.8, 1.9$ Hz, 1 H), 6.46 (dd, $J = 7.8, 1.9$ Hz, 1 H), 6.38-6.42 (m, 2 H), 6.27 (dd, $J = 7.7, 1.6$ Hz, 1 H), 5.55 (d, $J = 1.6$ Hz, 1 H), 3.29-3.39 (m, 1 H), 2.87-3.16 (m, 6 H), 2.62-2.73 (m, 1 H). ^{13}C NMR (CDCl_3 , 100 MHz, 25 °C): δ 153.7, 142.0, 139.6, 138.8, 135.5, 133.0, 132.8, 131.9, 127.9, 125.4, 125.0, 122.6, 35.3, 34.8, 33.8, 31.1.

Krohn, K.; Rieger, H.; Hopf, H.; Barrett, D.; Jones, P. G.; Döring, D. *Chem. Ber.* **1990**, *123* 1729.

4-Methoxy[2.2]paracyclophane

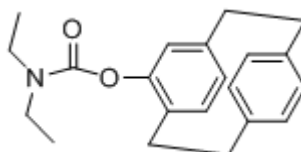


In a 100 mL glass tube sealed with a Teflon screw cap closure, potassium carbonate (1.66 g, 12 mmol) and 4-hydroxy[2.2]paracyclophane (869.6 mg, 3.87 mmol) were heated to 80 °C in 60 mL of acetonitrile for 30 minutes. Iodomethane (1.7 g, 12 mmol) was added to the mixture, the storage tube was sealed, and the stirred solution was heated at 80 °C for 3 days. The solvent was removed by rotary evaporation and the remaining solid was treated with ethyl acetate and water and transferred to a separatory funnel. The aqueous layer was neutralized with 0.1 M HCl solution, the mixture was shaken, and the organic layer was separated and dried over Na_2SO_4 . Rotary evaporation of solvent yielded a nearly colorless solid. The somewhat insoluble material was

dissolved in hot hexanes and purified via column chromatography (silica gel, hexanes, R_f = 0.28) to afford a colorless solid (602.4 mg, 65.4%). ^1H NMR (CDCl_3 , 400 MHz, 25 °C): δ 6.76 (dd, J = 7.8, 1.8 Hz, 1 H), 6.38 – 6.55 (m, 4 H), 6.28 (dd, J = 7.5, 1.4 Hz, 1 H), 5.67 (d, J = 1.3, 1 H), 3.71 (s, 3 H), 3.42 – 3.48 (m, 1 H), 2.99 – 3.13 (m, 6 H), 2.59 – 2.66 (m, 1 H). ^{13}C NMR (CDCl_3 , 100 MHz, 25 °C): δ 157.6, 142.1, 140.3, 138.8, 135.0, 133.7, 133.1, 131.5, 128.4, 127.5, 124.4, 116.7, 54.3, 35.5, 35.4, 34.1, 31.7.

Cram, D. J.; Day, A. C. *J. Org. Chem.* **1966**, *31*, 1227-32.

O-(4-[2.2]paracyclophanyl) diethylcarbamate

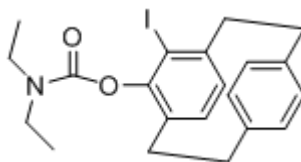


In a 250 mL Schlenk flask, a solution of 4-hydroxy[2.2]paracyclophane (2.88 mmol, 644.9 mg) in 50 mL of anhydrous toluene was treated with 4-(dimethylamino)pyridine (DMAP) (5.76 mmol, 703.7 mg) and diethylcarbamoyl chloride (5.76 mmol, 0.73 mL). The resulting mixture was stirred at reflux for 7 hours, while the progress of the reaction was monitored by TLC (silica gel, dichloromethane). The reaction was cooled to room temperature, hydrolyzed with 50 mL of deionized water, and extracted (3 x 35 mL) with dichloromethane. The combined organic extracts were dried over Na_2SO_4 . The solvent was removed by rotary evaporation, and the raw product was purified by column chromatography (silica gel, dichloromethane) to afford a white

crystalline solid (698.9 mg, 75%). ^1H NMR (CDCl_3 , 400 MHz, 25 °C): δ 6.85 (dd, J = 7.8, 1.3 Hz, 1 H), 6.41-6.57 (m, 5 H), 6.12 (d, J = 1.3 Hz, 1 H), 3.66 (q, br, 2 H), 3.40 (q, br, 2 H), 3.25 (m, 1 H), 3.05, (m, 6 H), 2.73 (m, 1 H), 1.42 (t, br, 3 H), 1.22 (t, br, 3 H) ^{13}C NMR (CDCl_3 , 100 MHz, 25 °C): δ 153.7, 149.5, 141.3, 139.5, 139.3, 135.1, 133.4, 133.0, 132.2, 131.1, 129.5, 129.4, 128.6, 42.2, 41.9, 35.3, 34.9, 34.6, 31.7, 14.5, 13.5.

Barrett, D.G.; Hopf, H. *Liebigs. Ann.* **1995**, 449-451.

O-[4-(5-iodo-[2.2]paracyclophanyl)] diethylcarbamate

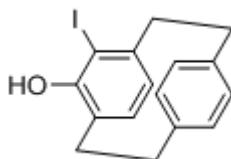


In a 250 mL Schlenk tube, a solution of O-(4-[2.2]paracyclophanyl) diethylcarbamate (2.16 mmol, 698.9 mg) in 55 mL of anhydrous tetrahydrofuran (THF) was treated with tetramethylethyldiamine (TMEDA) (2.6 mmol, 0.39 mL) and cooled to -78 °C. The resulting mixture was treated with sec-butyllithium (1.4 M in cyclohexane, 2.92 mmol, drop wise) and stirred at -78 °C for 2 h. The reaction mixture became clear yellow. After 2 h, a solution of diiodoethane (6.48 mmol, 1.83 g) in anhydrous THF was added drop wise to the reaction mixture. The resulting mixture was then allowed to slowly warm to room temperature overnight. After 15 h, the solution had turned dark purple. The THF was removed in vacuo and the residue dissolved in 55 mL of Et_2O and

55 mL of aqueous 5% sodium thiosulfate. The organic layer was washed again with an additional 55 mL of aqueous 5% sodium thiosulfate. The aqueous phase was extracted with Et₂O (3 x 20 mL). The organic layers were combined, washed with 20 mL 1 M HCl, and dried over Na₂SO₄. The solvent was evaporated to afford an off-white crystalline solid (949.2 mg, 98%). ¹H NMR (CDCl₃, 400 MHz, 25 °C): δ 7.14 (d, J = 8.0 Hz, 1 H), 6.67 (d, J = 7.3 Hz, 1 H), 6.52 – 6.60 (m, 3 H), 6.45 (d, J = 7.8 Hz, 1 H), 3.77 – 3.85 (m, 1 H), 3.52 – 3.61 (m, 1 H), 3.35 – 3.47 (m, 3H), 2.97 – 3.21 (m, 6 H), 2.78 – 2.86 (m, 1 H), 1.50 (t, J = 7.1 Hz, 3 H), 1.23 (t, J = 7.1 Hz, 3 H). ¹³C NMR (CDCl₃, 100 MHz, 25 °C): δ 152.6, 149.1, 145.3, 139.1, 138.6, 134.4, 133.3, 132.9, 132.9, 130.6, 128.9, 128.6, 103.6, 42.4, 42.1, 39.2, 34.5, 33.0, 31.8, 14.7, 13.4.

Wack, H.; France, S.; Hafez, A.; Drury, W.; Weatherwax, A.; Lectka, T. *J. Org. Chem.* **2004**, *69*, 4531.

4-Hydroxy-5-iodo-[2.2]paracyclophane

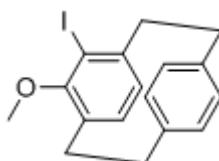


In a 50 mL round bottom flask, O-[4-(5-iodo-[2.2]paracyclophanyl)] diethylcarbamate (930.8 mg, 2.07 mmol) and potassium hydroxide (2.90 g, 51.75 mmol) were suspended in 15 mL of ethylene glycol. Hydrazine (331.7 mg, 10.35 mmol) was added and the mixture was heated at reflux for 2 h. During the reflux period, the mixture became homogenous. The solution was cooled to room temperature, transferred to a separatory funnel, acidified to pH 1 with 1 M HCl, and diluted with deionized water. The

aqueous phase was extracted with Et₂O (4 x 40 mL). The organic layers were combined, dried over Na₂SO₄, and solvent was removed in vacuo to afford an off-white solid (550.2 mg, 78%). ¹H NMR (CDCl₃, 400 MHz, 25 °C): δ 7.04 (dd, J = 7.8, 1.5 Hz, 1 H), 6.78 (dd, J = 7.8, 1.5 Hz, 1 H), 6.47 – 6.57 (m, 3 H), 6.27 (d, J = 7.6 Hz, 1H), 5.12 (s, 1 H), 3.38 – 3.44 (m, 1 H), 3.25 – 3.33 (m, 1 H), 2.96 – 3.15 (m, 5 H), 2.69 – 2.76 (m, 1 H). ¹³C NMR (CDCl₃, 100 MHz, 25 °C): δ 152.3, 144.5, 139.7, 137.7, 134.9, 133.1, 133.0, 128.1, 127.3, 126.2, 125.6, 99.5, 39.3, 34.0, 32.9, 31.5.

Wack, H.; France, S.; Hafez, A.; Drury, W.; Weatherwax, A.; Lectka, T. *J. Org. Chem.* **2004**, *69*, 4531.

4-Methoxy-5-iodo-[2.2]paracyclophane

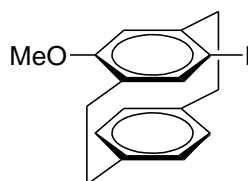


In a 100 mL glass tube sealed with a Teflon screw cap closure, potassium carbonate (992.3 mg, 7.18 mmol) and 4-hydroxy-5-iodo[2.2]paracyclophane (548.3 mg, 1.56 mmol) were heated to 70 °C in 15 mL of acetone for 30 minutes. Iodomethane (553.6 mg, 3.90 mmol) was added to the mixture, the tube was sealed, and the stirred solution was heated at 70 °C for 1 day. The mixture was transferred to a round bottom flask, the solvent was removed by rotary evaporation and the remaining solid was treated with 15 mL of deionized water and 15 mL of dichloromethane, and transferred to a separatory funnel. The aqueous layer was extracted with dichloromethane (3 x 30 mL).

The organic layers were combined, dried over Na₂SO₄, and the solvent was removed in vacuo to yield a nearly colorless oil. This somewhat insoluble material was dissolved in hot hexanes, loaded onto a silica gel column, and eluted with 10% EtOAc/hexanes) to afford an almost colorless product (416.7 mg, 73%) ¹H NMR (CDCl₃, 400 MHz, 25 °C): δ 7.09 (d, J = 7.9 Hz, 1 H), 6.70 (d, J = 7.9 Hz, 1 H), 6.53 (d, J = 7.7 Hz, 1 H), 6.52 (s, 2 H), 6.35 (d, J = 7.7 Hz, 1 H), 3.64 (s, 3 H), 3.38 – 3.43 (m, 1 H), 3.26 – 3.33 (m, 1 H), 3.08 – 3.19 (m, 2 H), 2.92 – 3.03 (m, 3 H), 2.74 – 2.81 (m, 1 H). ¹³C NMR (CDCl₃, 100 MHz, 25 °C): δ 157.7, 145.6, 139.4, 138.4, 135.2, 132.8, 132.7, 131.8, 129.4, 128.9, 128.7, 103.5, 60.9, 39.2, 34.5, 33.0, 31.2.

Wack, H.; France, S.; Hafez, A.; Drury, W.; Weatherwax, A.; Lectka, T. *J. Org. Chem.* **2004**, *69*, 4531.

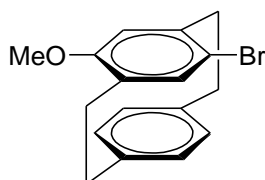
4-Methoxy-7-iodo[2.2]paracyclophane



In a 100 mL round bottom flask, a solution of 4-methoxy[2.2]paracyclophane (0.8 mmol, 192.3 mg) in CH₂Cl₂ (25 mL) of CH₂Cl₂ was treated with a solution of N-iodosuccinimide (0.648 mmol, 145.2 mg) and trifluoroacetic acid (0.648 mmol, 75.3 mg) in 25 mL of dichloromethane. The resulting mixture was stirred for 5 minutes and the

dark purple color of iodine developed. The solution was transferred to a separatory funnel and washed (3 x 50 mL) with 2 M aqueous sodium bicarbonate solution followed by a single deionized water wash. The organic layer was separated, dried over Na_2SO_4 , and the solvent was evaporated to give an off-white solid (295.0 mg, 99%). ^1H NMR (CDCl_3 , 400 MHz, 25 °C): δ 7.13 (dd, J = 7.9, 1.8 Hz, 1 H), 6.75 (dd, J = 7.9, 1.8 Hz, 1 H), 6.71 (s, 1 H), 6.46 (dd, J = 7.9, 1.8, 1 H), 6.40 (dd, J = 7.8, 1.8 Hz, 1 H), 5.69 (s, 1 H), 3.68 (s, 3 H), 2.82-3.37 (m, 7 H), 2.43-2.53 (m, 1H). ^{13}C NMR (CDCl_3 , 100 MHz, 25 °C): δ 157.9, 144.7, 143.9, 139.9, 138.5, 132.9, 131.5, 129.9, 129.6, 128.9, 117.7, 91.9, 54.3, 39.3, 33.6, 33.2, 31.1.

4-Methoxy-7-bromo[2.2]paracyclophane

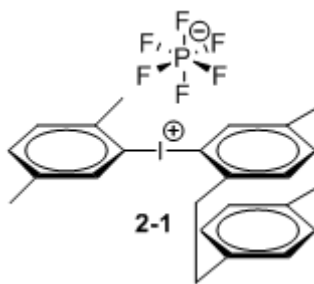


N-Bromosuccinimide (279.4 mg, 1.57 mmol) and trifluoroacetic acid (179.0 mg, 0.12 mL, 1.57 mmol) were dissolved in 15 mL of CH_2Cl_2 and added to a solution of 4-methoxy[2.2]paracyclophane (349.7 g, 1.47 mmol) in 30 mL CH_2Cl_2 . The resulting mixture was covered from light and stirred for 30 minutes at room temperature. The solution was transferred to a separatory funnel and washed (3 x 50 mL) with 2 M aqueous sodium bicarbonate solution followed by a single deionized water wash. The organic

layer was separated, dried over Na_2SO_4 , and the solvent was evaporated to give light brown solid (400.6 mg, 86%). ^1H NMR (CDCl_3 , 400 MHz, 25 °C): δ 7.10 (dd, $J = 7.8$, 1.8 Hz, 1 H), 6.76 (dd, $J = 7.9$, 1.9 Hz, 1 H), 6.41 - 6.46 (m, 3 H), 5.69 (s, 1 H), 3.71 (s, 3 H), 3.34 - 3.45 (m, 2 H), 3.18 - 3.25 (m, 1 H), 2.98 - 3.10 (m, 3 H), 2.71 - 2.78 (m, 1 H), 2.46 - 2.54 (m, 1 H); ^{13}C NMR (CDCl_3 , 100 MHz, 25 °C) δ 157.15, 140.81, 139.95, 138.76, 138.65, 133.19, 133.16, 131.83, 130.00, 129.19, 118.54, 117.26, 54.69, 35.89, 33.82, 33.51, 31.29.

Rozenberg, V.; Zhuravsky, R.; Sergeeva, E. *Chirality* **2006**, 18, 95-102.

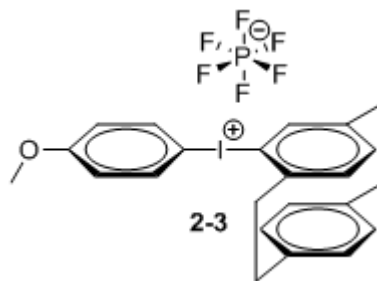
[(2.2]Paracyclophan-4-yl)(2',5'-dimethylphenyl)iodonium hexafluorophosphate, 2-1



In a 50 mL Schlenk tube under nitrogen, a stirred solution of 4-bromocyclophane (1 mmol, 282 mg) in 10 mL of anhydrous diethyl ether was cooled to -78 °C. A solution of *t*-BuLi (1.7 M in pentane, 2.3 equiv.) was added dropwise and the resulting mixture was stirred at -78 °C for 20 minutes and then warmed to 0 °C and allowed to stir for an additional 20 min. The reaction mixture was cooled again to -78 °C before a solution of zinc chloride (200 mg, 1.5 mmol) in ether (10 mL) was added dropwise by cannula. After the addition, the reaction mixture was allowed to warm to room temperature over the

course of one hour before the solvents were removed in vacuo. The remaining solid was dissolved in anhydrous CH_3CN and the solution was cooled to $-40\text{ }^\circ\text{C}$ and added dropwise to precooled ($-40\text{ }^\circ\text{C}$) suspension of bis(acetyloxy)-(2,5-dimethylphenyl)- λ_3 -iodane (350 mg, 1 mmol) in 10 mL of acetonitrile. The mixture was allowed to warm to room temperature over 30 minutes before the solvent was removed in vacuo. The resulting solid was washed with hexanes and then dissolved in aqueous acetonitrile. Addition of an aqueous NaPF_6 solution precipitated the product, which was extracted from the aqueous mixture with CH_2Cl_2 . The organic layer was evaporated, dissolved in a minimal amount of CH_2Cl_2 , precipitated with hexanes, filtered and dried in vacuo to yield **1** (105 mg, 18 % yield). ^1H NMR (CD_3CN , 400 MHz, $25\text{ }^\circ\text{C}$): δ 7.93 (s, 1H), 7.41 (s, 2H), 7.29 (d, $J = 1.3\text{ Hz}$, 1H), 6.84 (dd, $J_1 = 7.8\text{ Hz}$, $J_2 = 1.3\text{ Hz}$, 1H), 6.78 (d, $J = 7.8\text{ Hz}$, 1H), 6.66 (s, 2H), 6.53 (d, $J = 7.9\text{ Hz}$, 1H), 6.51 (d, $J = 7.9\text{ Hz}$, 1H), 3.04-3.41 (m, 8H), 2.50 (s, 3H), 2.33 (s, 3H); ^{13}C NMR (CD_3CN , 100 MHz, $25\text{ }^\circ\text{C}$) δ 146.5, 143.6, 141.9, 141.1, 140.2, 139.9, 139.5, 138.2, 137.7, 135.6, 134.7, 134.5, 134.1, 133.9, 133.1, 132.5, 120.6, 118.8, 100.8, 38.9, 35.8, 35.5, 35.4, 25.3, 20.6; HRMS: (HRFAB) calcd. for $\text{C}_{24}\text{H}_{24}\text{I} [\text{M}]^+$ 439.0923, found 439.0907.

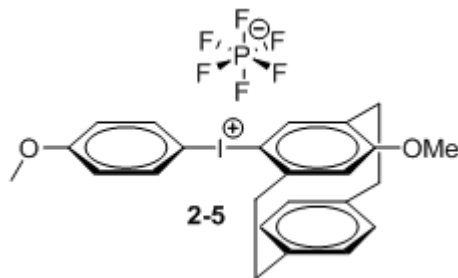
([2.2]Paracyclophan-4-yl)(4'-methoxyphenyl)iodonium hexafluorophosphate, 2-3



In a 50 mL Schlenk tube under nitrogen, a stirred solution of bromocyclophane (1 mmol, 282 mg) in 10 mL of anhydrous diethyl ether was cooled to $-78\text{ }^{\circ}\text{C}$. A solution of *t*-BuLi (1.7 M in pentane, 2.3 equiv.) was added dropwise and the resulting mixture was stirred at $-78\text{ }^{\circ}\text{C}$ for 20 minutes and then warmed to $0\text{ }^{\circ}\text{C}$ and allowed to stir for an additional 20 min. The reaction mixture was cooled again to $-78\text{ }^{\circ}\text{C}$ before a solution of zinc chloride (200 mg, 1.5 mmol) in ether (10 mL) was added dropwise by cannula. After the addition, the reaction mixture was allowed to warm to room temperature over the course of one hour before the solvents were removed in vacuo. The remaining solid was dissolved in anhydrous CH_3CN and the solution was cooled to $-40\text{ }^{\circ}\text{C}$ and added dropwise to precooled ($-40\text{ }^{\circ}\text{C}$) suspension of bis(acetyloxy)-(4-methoxyphenyl)- λ_3 -iodane (352 mg, 1 mmol) in 10 mL of acetonitrile. The mixture was allowed to warm to room temperature over 30 minutes before the solvent was removed in vacuo. The resulting solid was washed with hexanes and then dissolved in aqueous acetonitrile. Addition of an aqueous NaPF_6 solution precipitated the product, which was extracted from the aqueous mixture with CH_2Cl_2 . The organic layer was evaporated, dissolved in a minimal amount of CH_2Cl_2 , precipitated with hexanes, filtered and dried in vacuo to yield **2** (225 mg, 38.4 % yield). ^1H NMR (CD_3CN , 400 MHz, $25\text{ }^{\circ}\text{C}$): δ 8.00 (d, $J = 9.1\text{ Hz}$, 2H), 7.27 (s, 1H), 7.08 (d, $J = 9.1\text{ Hz}$, 2H), 6.83 (d, $J = 7.7\text{ Hz}$, 1H), 6.76 (d, $J = 7.7\text{ Hz}$,

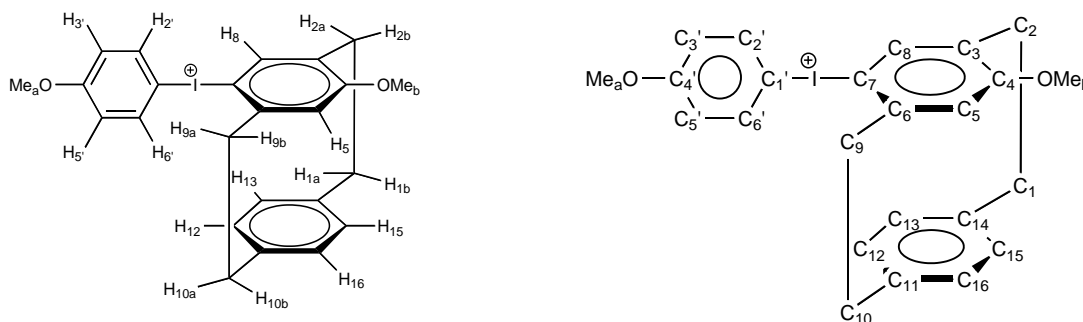
1H), 6.65 (s (broad), 2H), 6.38 (d, $J = 7.9$ Hz, 1H), 6.31 (d, $J = 7.9$ Hz, 1H), 3.84 (s, 3H), 3.04-3.35 (m, 8H); ^{13}C NMR (CD_3CN , 100 MHz, 25 °C) δ 164.1, 143.2, 140.9, 139.8, 139.4, 139.2, 138.8, 137.6, 134.3, 134.2, 133.7, 132.4, 120.9, 119.4, 100.8, 56.7, 38.4, 35.6, 35.4, 35.3; HRMS: (HRFAB) calcd. for $\text{C}_{23}\text{H}_{22}\text{OI}$ $[\text{M}]^+$ 441.07098, found 441.0712.

**(7-Methoxy[2.2]paracyclophanyl)(4'-methoxyphenyl)iodonium
hexafluorophosphate, 2-5**



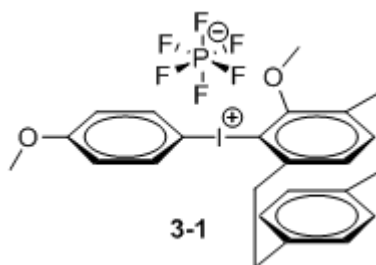
In a 100 mL Schlenk tube, 4-methoxy-7-bromo[2.2]paracyclophane (1.26 mmol, 400.6 mg) was dissolved in 25 mL of distilled ether and cooled to -78 °C. To the cooled solution, 1.7M t-butyl lithium (3.16 mmol, 1.85 mL) was added dropwise and the stirred solution was held at -78 °C for 1 hour. A solution of anhydrous zinc chloride (1.51 mmol, 206.1 mg) in 10 mL of diethyl ether was added dropwise to the cooled solution. The mixture was allowed to warm to room temperature, and the solvent was removed under reduced pressure. The residual solid (organozinc chloride reagent and lithium salts) was taken up in anhydrous acetonitrile and cooled to -40 °C before a solution of 4-methoxyphenyl iodonium diacetate (1.89 mmol, 665.5 mg) in acetonitrile (10 mL) was added in a dropwise fashion. After 1 hour at -40 °C, the mixture was warmed to room temperature and the solvent was removed under reduced pressure. Deionized water and

sodium hexafluorophosphate (410 mg) were added, followed by 50 mL of dichloromethane. The mixture was transferred to a separatory funnel and the organic phase was separated. The solvent was removed by rotary evaporation and the remaining solid was dissolved in 5 mL of dichloromethane and dripped into 150 mL hexanes. The precipitate was aged for one hour, collected by gravity filtration, and dried in vacuo to yield a colorless salt (55.6 %, 431.7 mg).



(C4'), 146.4 (C6), 140.5 (C8), 139.9 (C11), 137.9 (C14), 137.4 (C2', C6'), 133.2 (C13), 132.4 (C3), 131.4 (C12), 131.3 (C16), 128.8 (C15), 119.8 (C5), 118.2 (C3', C5'), 107.4 (C7), 101.1 (C1'), 55.8 (Me_a), 54.9 (Me_b), 37.2 (C9), 34.5 (C10), 32.9 (C1), 30.7 (C2). ¹⁹F NMR (CD₃CN, 400 MHz, 25 °C): δ -72.7 (d, J = 706.7 Hz, 6F). HRMS: (HRFAB) calcd. for C₂₄H₂₄IO₂ [M]⁺ 471.08210 (100%), 472.08454 (26%); found 471.08221 (100%), 472.08561 (23%).

**(5-(4-Methoxy[2.2]paracyclophanyl))(4'-methoxyphenyl)iodonium
hexafluorophosphate, 3-1**



In a 100 mL Schlenk tube, 4-methoxy-5-iodo-[2.2]paracyclophane (1.14 mmol, 416.7 mg) was dissolved in 25 mL of distilled ether and cooled to -78 °C. To this stirred solution, 1.7 M t-butyl lithium (2.85 mmol, 1.68 mL) was added dropwise and the solution was held at -78 °C for 1 hour. A solution of anhydrous zinc chloride (1.37 mmol, 190.0 mg) in 10 mL of diethyl ether was added dropwise to the cold solution over the course of 1 h. The mixture was allowed to warm to room temperature, and the solvent was removed under reduced pressure. The residual solid (comprising organozinc chloride reagent and lithium salts) was taken up in anhydrous acetonitrile and cooled to -40 °C before a solution of 4-methoxyphenyl iodonium diacetate (1.89 mmol, 665.5 mg) in

acetonitrile (10 mL) was added in a dropwise fashion. After 1 hour at -40 °C, the mixture was allowed to warm to room temperature and the solvent was removed under reduced pressure. Deionized water and sodium hexafluorophosphate (470 mg) were added, followed by 50 mL of dichloromethane. The mixture was transferred to a separatory funnel and the organic phase was separated. The solvent was removed by rotary evaporation and the remaining solid was dissolved in 5 mL of dichloromethane and dripped into 150 mL hexanes. The precipitate was aged for one hour, collected by gravity filtration, and dried in vacuo to yield a colorless salt (13.0 %, 91.0 mg). ^1H NMR (CD_3CN , 400 MHz, 25 °C): δ 7.99 (d, 9.3 Hz, 2H), 7.07 (d, 9.2 Hz, 2H), 6.84 (d, 7.8 Hz, 1H), 6.59- 6.69 (m, 4H), 6.11 (d, 7.9 Hz, 1H), 3.88 (s, 3H), 3.84 (s, 3H), 3.32 – 3.38 (m, 1H), 3.06 – 3.26 (m, 6H), 2.93 – 3.00 (m, 1H). ^{13}C NMR (CD_3CN , 400 MHz, 25 °C): δ 163.4, 156.9, 144.9, 142.3, 140.0, 138.3, 138.2, 133.7, 133.3, 133.2, 131.8, 130.4, 129.2, 118.3, 99.3, 62.5, 55.8, 36.9, 33.8, 33.7, 31.9. ^{19}F NMR (CD_3CN , 400 MHz, 25 °C): δ -72.8 (d, J = 706.9 Hz, 6F). HRMS: (HRFAB) calcd. for $\text{C}_{24}\text{H}_{24}\text{IO}_2$ $[\text{M}]^+$ 471.0821, found 471.0806.

Appendix A

Common abbreviations used in this thesis

PET	Positron Emission Tomography
TMAOH	Tetramethylammonium hydroxide
TMAF	Tetramethylammonium fluoride
[¹⁸ F]FDG	2-[¹⁸ F]Fluoro-2-deoxy-D-glucose
CsF	Cesium fluoride
K2.2.2KF	Kryptofix 2.2.2. KF
CH ₃ CN	Acetonitrile
C ₆ H ₆	Benzene
TMAPF ₆	Tetramethylammonium hexafluorophosphate
F-MTEB	3-Fluoro-5-[(2-methyl-1,3-thiazol-4-yl)ethynyl]benzonitrile
F-DOPA	6-fluorodihydroxyphenylalanine
TMEDA	Tetramethylethyl diamine
t-BuLi	t-Butyl Lithium
n-BuLi	n-Butyl Lithium

Appendix B

NMR Spectra

Contents of Appendix B

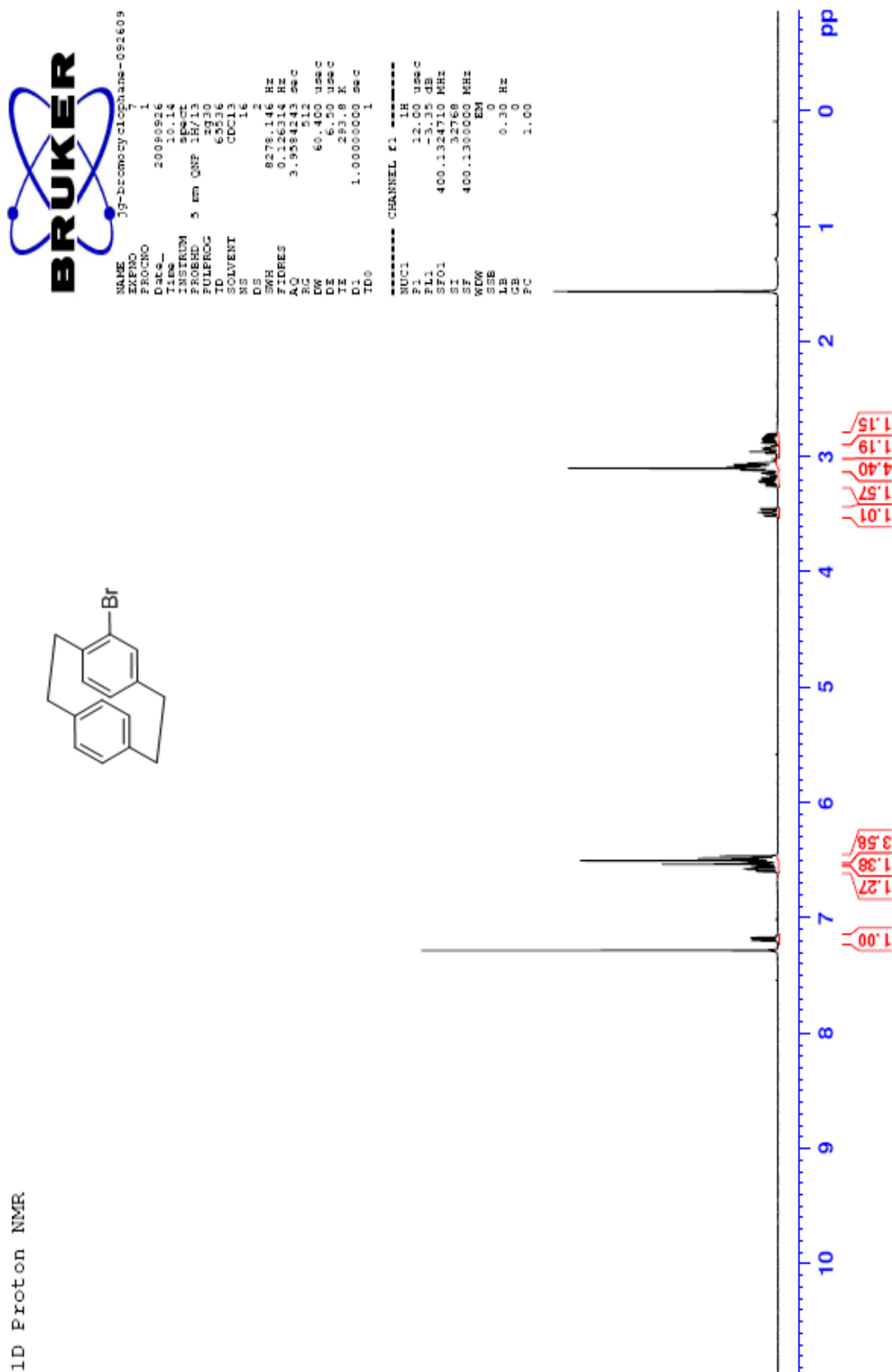
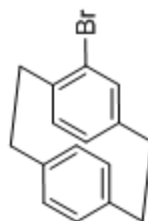
NMR Spectra

1. ^1H of 4-Bromo[2.2]paracyclophane in CDCl_3
2. ^{13}C of 4-Bromo[2.2]paracyclophane in CDCl_3
3. ^1H of 4-Hydroxy[2.2]paracyclophane in CDCl_3
4. ^{13}C of 4-Hydroxy[2.2]paracyclophane in CDCl_3
5. ^1H of 4-Methoxy[2.2]paracyclophane in CDCl_3
6. ^{13}C of 4-Methoxy[2.2]paracyclophane in CDCl_3
7. ^1H of 4-Methoxy-7-iodo[2.2]paracyclophane in CDCl_3
8. ^{13}C of 4-Methoxy-7-iodo[2.2]paracyclophane in CDCl_3
9. ^1H of 4-Methoxy-7-bromo[2.2]paracyclophane in CDCl_3
10. ^{13}C of 4-Methoxy-7-bromo[2.2]paracyclophane in CDCl_3
11. ^1H , ^{13}C HSQC of 4-Methoxy-7-bromo[2.2]paracyclophane in CDCl_3
12. ^1H , ^{13}C HSQC of 4-Methoxy-7-bromo[2.2]paracyclophane (aliphatic) in CDCl_3
13. ^1H , ^{13}C HSQC of 4-Methoxy-7-bromo[2.2]paracyclophane (aromatic) in CDCl_3
14. ^1H and ^{13}C NMR spectra of ([2.2]Paracyclophan-4-yl)(2',5'-dimethylphenyl)iodonium hexafluorophosphate, 2-1 in CD_3CN

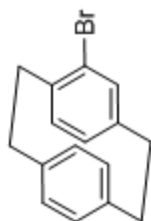
15. ^1H and ^{13}C NMR spectra of ([2.2]Paracyclophan-4-yl)(4'-methoxyphenyl)iodonium hexafluorophosphate, 2-3 in CD_3CN
16. ^1H , ^{13}C HMQC spectrum of ([2.2]Paracyclophan-4-yl)(4'-methoxyphenyl)iodonium hexafluorophosphate, 2-3 in CD_3CN
17. ^1H and ^{13}C NMR spectra of (7-Methoxy[2.2]paracyclophanyl)(4'-methoxyphenyl)iodonium hexafluorophosphate, 2-5 in CD_3CN
18. ^1H , ^{13}C HSQC spectrum of (7-Methoxy[2.2]paracyclophanyl)(4'-methoxyphenyl)iodonium hexafluorophosphate, 2-5 in CD_3CN
19. ^1H , ^{13}C HSQC spectrum of (7-Methoxy[2.2]paracyclophanyl)(4'-methoxyphenyl)iodonium hexafluorophosphate, 2-5 in CD_3CN (aliphatic)
20. ^1H , ^{13}C HSQC spectrum of (7-Methoxy[2.2]paracyclophanyl)(4'-methoxyphenyl)iodonium hexafluorophosphate, 2-5 in CD_3CN (aromatic)
21. ^1H , ^{13}C HSQC-HMBC spectrum of (7-Methoxy[2.2]paracyclophanyl)(4'-methoxyphenyl)iodonium hexafluorophosphate, 2-5 in CD_3CN
22. ^1H - ^1H COSY spectrum of (7-Methoxy[2.2]paracyclophanyl)(4'-methoxyphenyl)iodonium hexafluorophosphate, 2-5 in CD_3CN
23. ^1H - ^1H NOESY spectrum of (7-Methoxy[2.2]paracyclophanyl)(4'-methoxyphenyl)iodonium hexafluorophosphate, 2-5 in CD_3CN (full)
24. ^1H - ^1H NOESY spectrum of (7-Methoxy[2.2]paracyclophanyl)(4'-methoxyphenyl)iodonium hexafluorophosphate, 2-5 in CD_3CN (aliphatic-aliphatic)

25. ^1H - ^1H NOESY spectrum of (7-Methoxy[2.2]paracyclophanyl)(4'-methoxyphenyl)iodonium hexafluorophosphate, 2-5 in CD_3CN (aliphatic-aromatic)
26. ^1H - ^1H NOESY spectrum of (7-Methoxy[2.2]paracyclophanyl)(4'-methoxyphenyl)iodonium hexafluorophosphate, 2-5 in CD_3CN (aromatic-aromatic)
27. ^1H of O-(4-[2.2]paracyclophanyl) Diethylcarbamate in CDCl_3
28. ^{13}C of O-(4-[2.2]paracyclophanyl) Diethylcarbamate in CDCl_3
29. ^1H of O-[4-(5-Iodo-[2.2]paracyclophanyl)] Diethylcarbamate in CDCl_3
30. ^{13}C of O-[4-(5-Iodo-[2.2]paracyclophanyl)] Diethylcarbamate in CDCl_3
31. ^1H of 4-Hydroxy-5-iodo-[2.2]paracyclophane in CDCl_3
32. ^{13}C of 4-Hydroxy-5-iodo-[2.2]paracyclophane in CDCl_3
33. ^1H of 4-Methoxy-5-iodo-[2.2]paracyclophane in CDCl_3
34. ^{13}C of 4-Methoxy-5-iodo-[2.2]paracyclophane in CDCl_3
35. ^1H of (4-Methoxy[2.2]paracyclophanyl)(4'-methoxyphenyl)iodonium hexafluorophosphate, 3-1 in CD_3CN
36. ^{13}C of (4-Methoxy[2.2]paracyclophanyl)(4'-methoxyphenyl)iodonium hexafluorophosphate, 3-1 in CD_3CN
37. ^1H - ^1H COSY spectrum of (4-Methoxy[2.2]paracyclophanyl)(4'-methoxyphenyl)iodonium hexafluorophosphate, 3-1 in CD_3CN

1D Proton NMR



13C



141.61
139.33
139.11
137.25
135.05
133.31
133.02
132.91
132.25
131.46
128.69
126.97

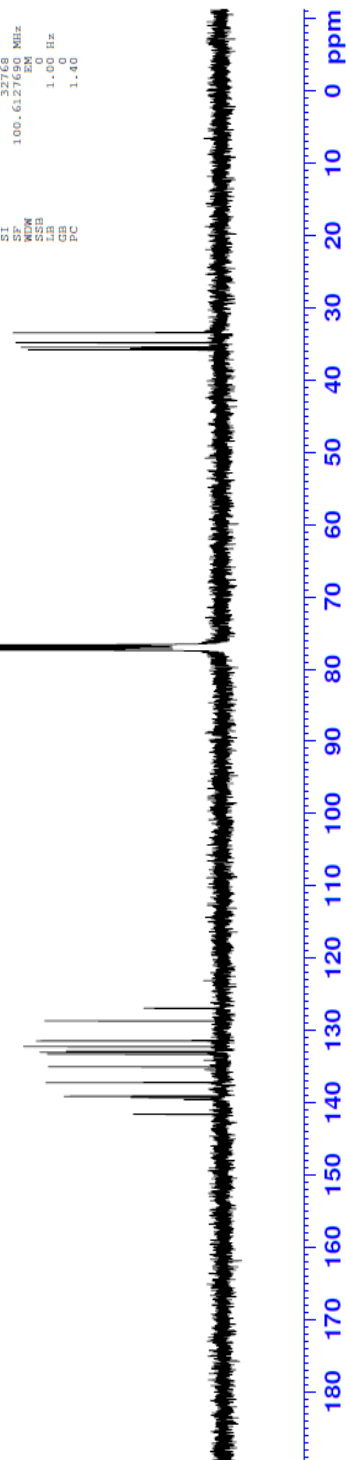
35.85
35.48
34.82
34.02
33.47



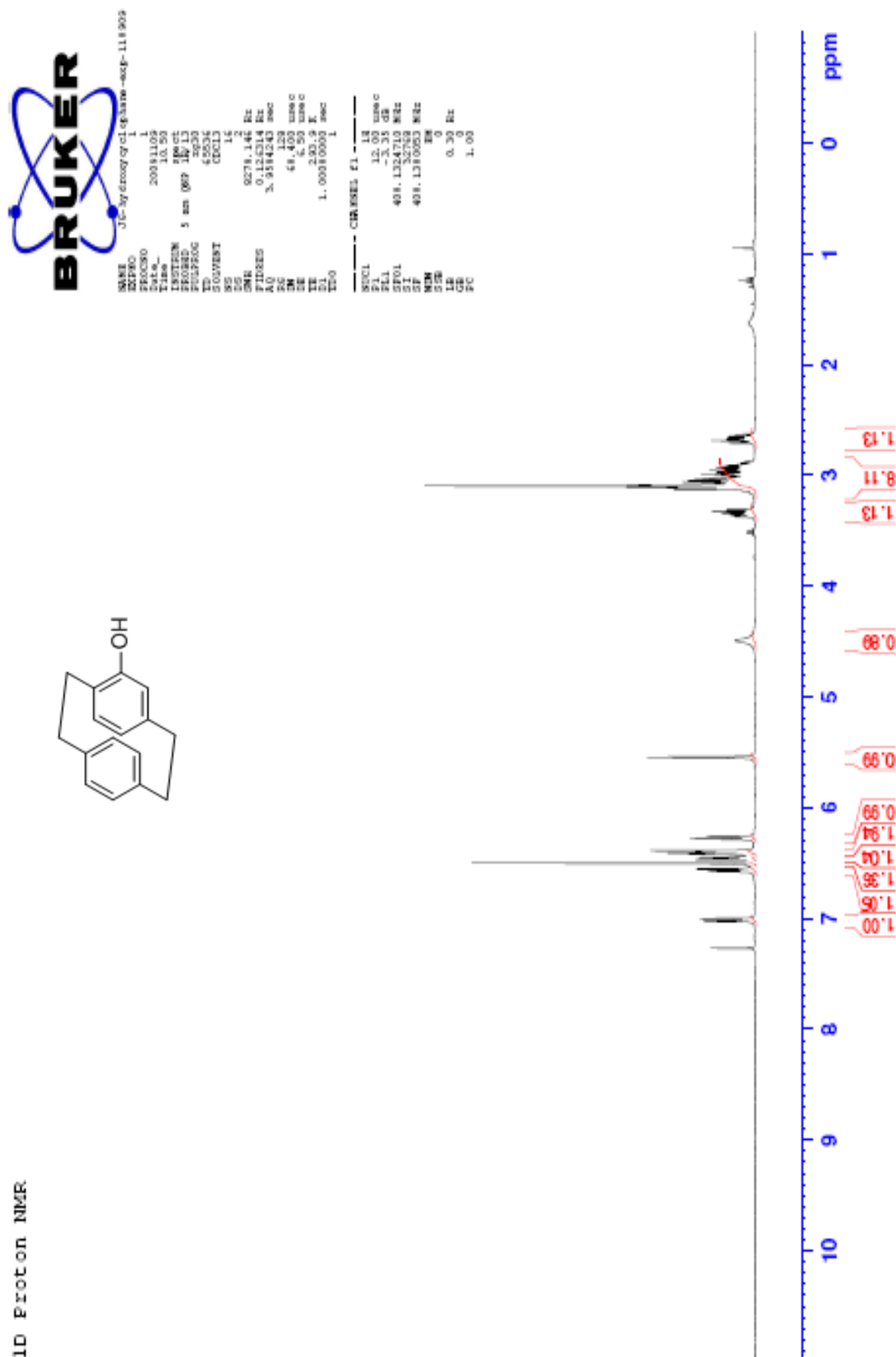
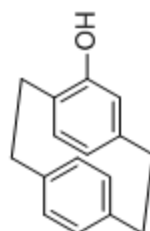
Current Data Parameters
NAME JG-bromocyclophane-13C-110509-1
EXPNO 1
PROCNO 1

F2 - Acquisition Parameters
Time 2001.13.37
INSTRUM spect
PROBHD 5 mm QNP
PULPROG zgpg30
TD 65536
SOLVENT CDCl3
DS 864
SWH 23980.814 Hz
FIDRES 0.263154 Hz
AQ 1.366756 sec
RG 812.7
DM 20.850 usec
DE 6.00 usec
TE 295.3 K
D1 2.0000000 sec
D11 1.11 sec
TD0 0.0300000 sec

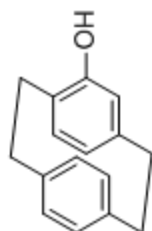
===== CHANNEL f1 =====
NUC1 13C
P1 10.00 usec
PL1 0.00 dB
SFO1 100.6228298 MHz
===== CHANNEL f2 =====
NUC2 1H
P2 wait115
PL2 70.00 usec
PL3 3.35 dB
PL13 11.97 dB
SFO2 400.1316005 MHz
F2 - Processing parameters
SI 32768
SF 100.6127690 MHz
WDW EM
SSB 0
LB 1.00 Hz
GB 0
PC 1.40



1D Proton NMR



13C



153.67
142.01
139.63
138.84
135.46
133.04
132.77
131.86
127.95
125.44
125.04
122.57

35.31
34.82
33.84
31.10



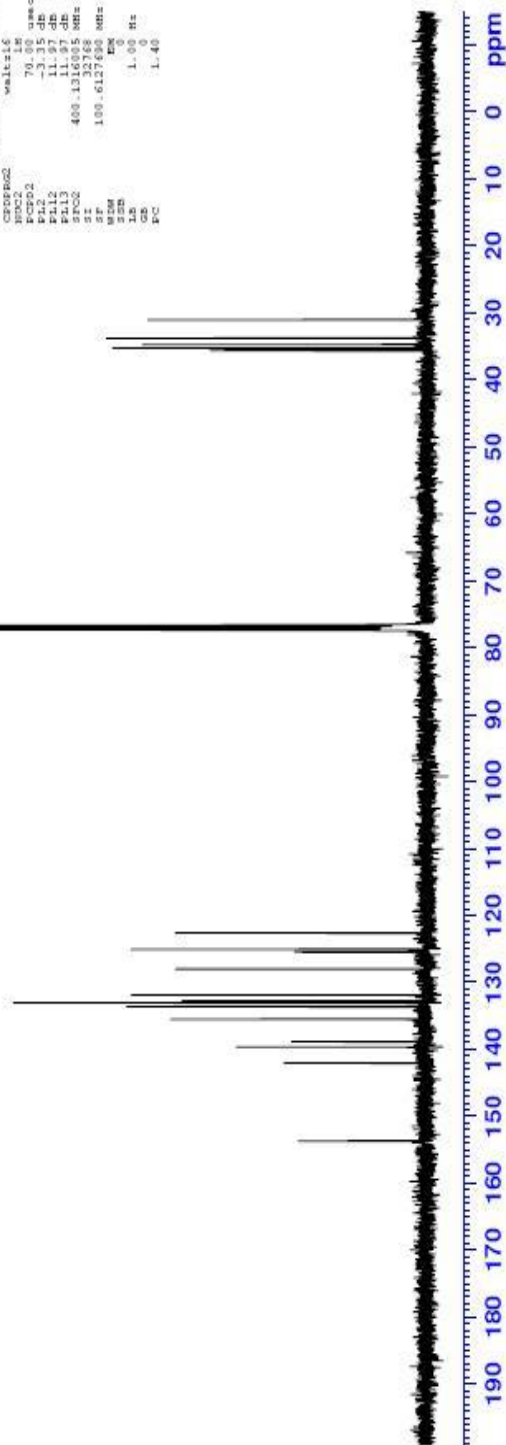
NAME 3,5-bis(hydroxy)phenylamine-13C-110909
PROCNO 1
Date_ 20031101
Time_ 11:18
INSTRUM spect
PROBHD 5 mm QNP 1H/13
PULPROG zgpg30
TD 65536
SOLVENT CDCl3
DS 4
SS 4
SMH 23080.814 Hz
F2FREQ 101.626126 MHz
AQ 0.363972 sec
RG 812.7
DW 20.950 usec
DE 0.50 usec
TE 300.2 K
D1 2.0000000 sec
D11 0.0300000 sec
D12 0.0300000 sec
D13 0.0300000 sec

===== CHANNEL F1 =====
NUC1 13C
P1 12.00 usec
PL1 0.50 dB
SFO1 100.626126 MHz

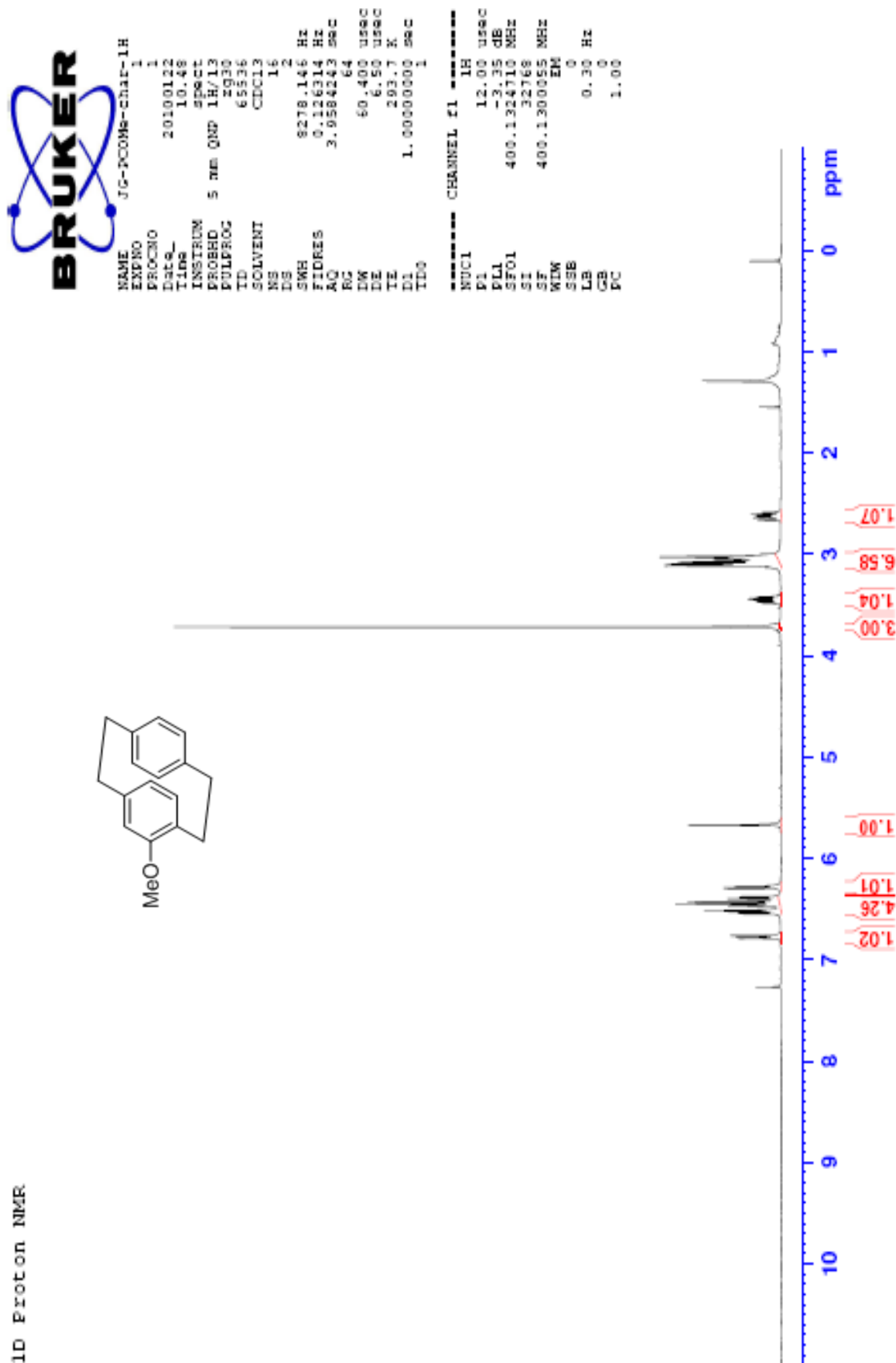
===== CHANNEL F2 =====
NUC2 1H
P2 7.00 usec
PL2 -2.15 dB
SFO2 400.146055 MHz

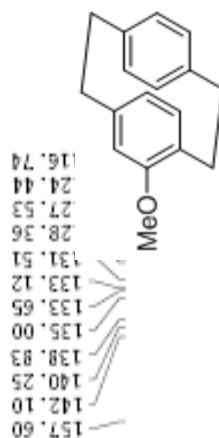
===== WALTZ16 =====
NUC3 13C
P3 12.00 usec
PL3 0.50 dB
SFO3 100.626126 MHz
NUC4 1H
P4 7.00 usec
PL4 -2.15 dB
SFO4 400.146055 MHz

===== PC =====
PC 1.40



1D Proton NMR



¹³C

157.60
142.10
140.25
138.83
135.00
133.65
133.12
131.51
28.36
27.53
24.44
16.74

54.25
35.50
35.42
34.09
31.67



NAME JG-PCOMs-char-13C
 PROCNO 1
 Date_ 20100122
 Time 12.08

INSTRUM spect
 PROBRD 5 mm QNP 1H/13
 PULPROG zgpg30

ID 65536
 SOLVENT CDCl3

NS 512
 DS 4

SWH 23080.814 Hz
 FIDRES 0.365318 Hz
 AQ 1.3664756 sec

RG 812.7
 DW 20.850 usec
 DE 6.50 usec

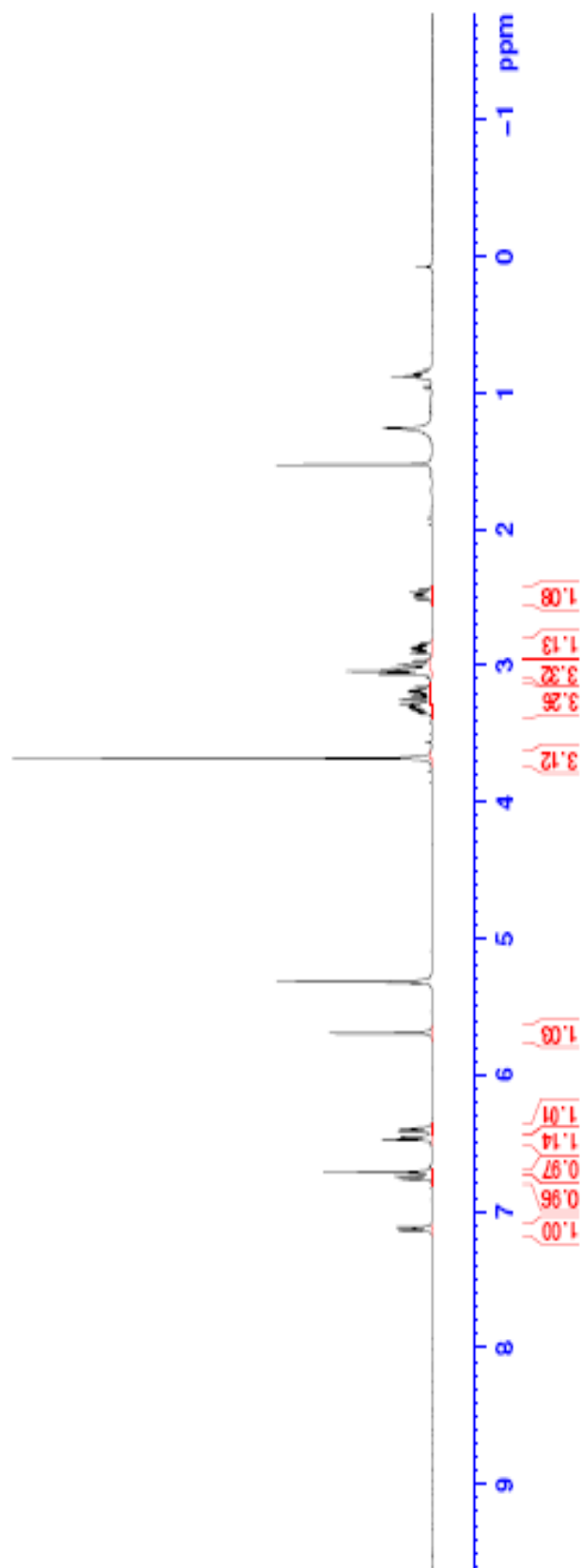
TE 294.1 K
 D1 2.00000000 sec
 D11 0.03000000 sec

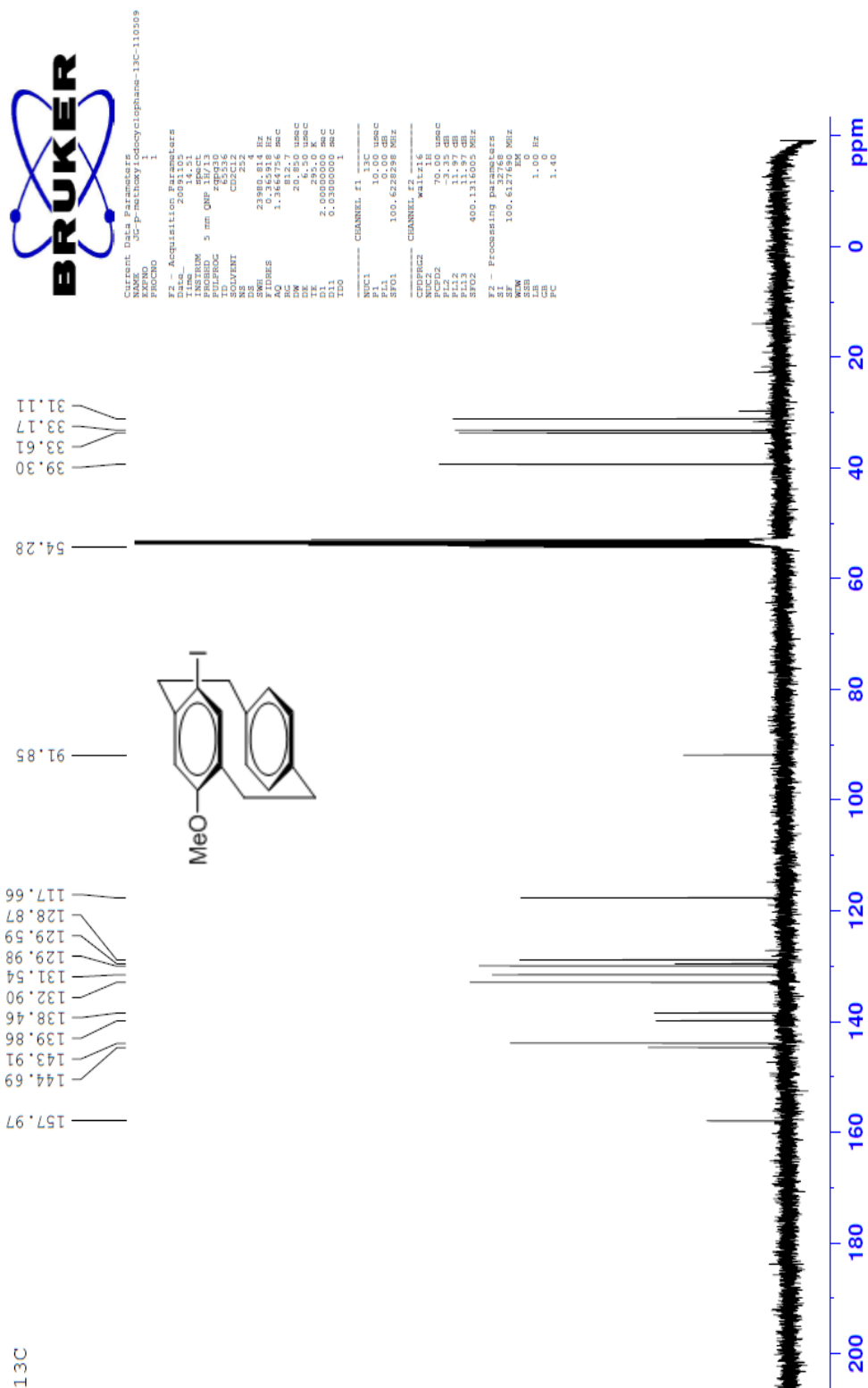
TD0 1

CHANNEL f1
 NUC1 13C
 P1 10.00 usec
 PL1 0.50 dB
 SF01 100.6228298 MHz

CHANNEL f2
 WALTZ16
 NUC2 1H
 P2 70.00 usec
 PL2 -3.35 dB
 PL12 11.97 dB
 PL13 11.97 dB
 SF02 400.1316005 MHz
 SI 32768
 SF 100.6127554 MHz
 KIM EM
 SEB 0
 LB 1.00 Hz
 GB 0
 PC 1.40

200 180 160 140 120 100 80 60 40 20 0 ppm





1D Proton NMR



Current Data Parameters
NAME 32-PCMO6-conc-011310-1H
EXPNO 1
PROCNO 1

F2 - Acquisition Parameters
Date_ 201013
Time 10.02

PROBHD 5 mm QNP 1H/13
PULPROG zgpg30

TD 65536
SOLVENT CDCl3

MS 16
DS 2

QMR 9379.146 Hz
FIDRES 0.126314 Hz

AQ 3.2594243 sec
RG 191

WE 60.400 usec
DE 6.50 usec

TE 294.1 K
D1 1.00000000 sec

TD0 1

===== CHANNEL f1 =====
NUC1 1H

PL1 12.50 usec
PL2 1.30 dB

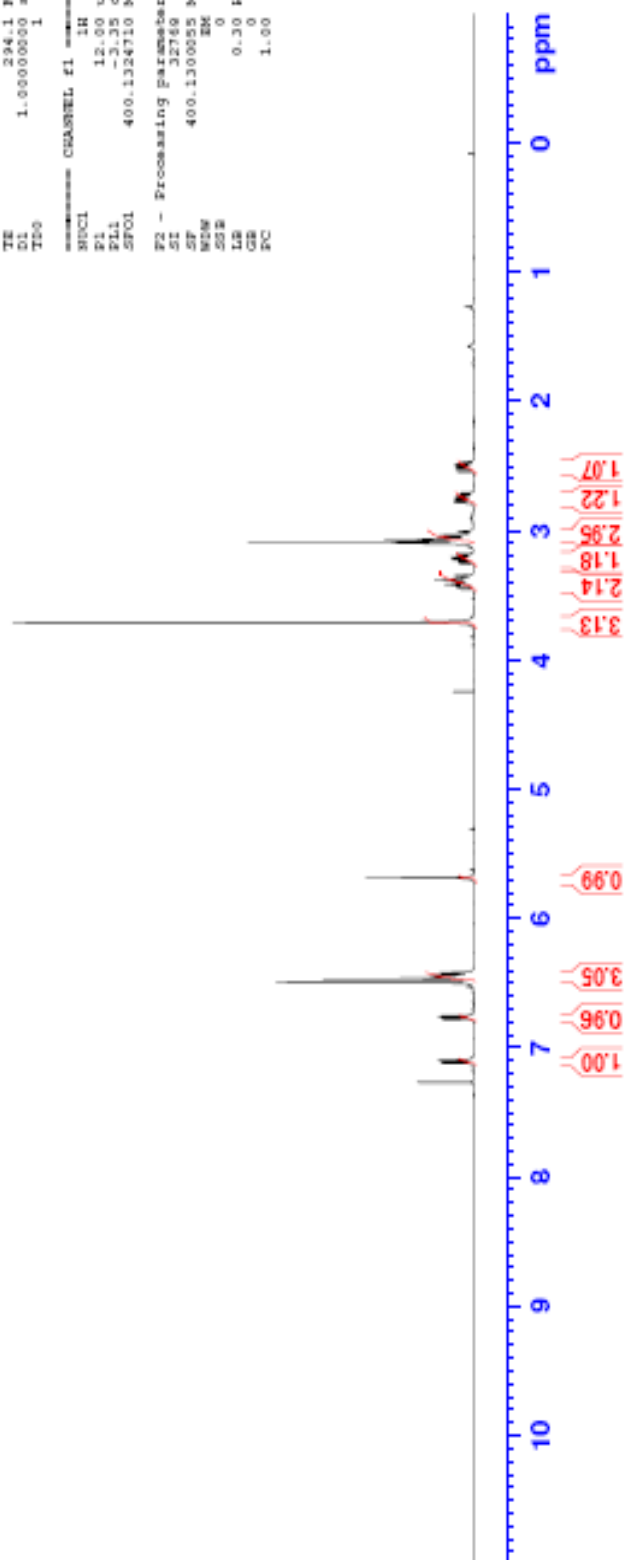
RF01 400.1324710 MHz
=====

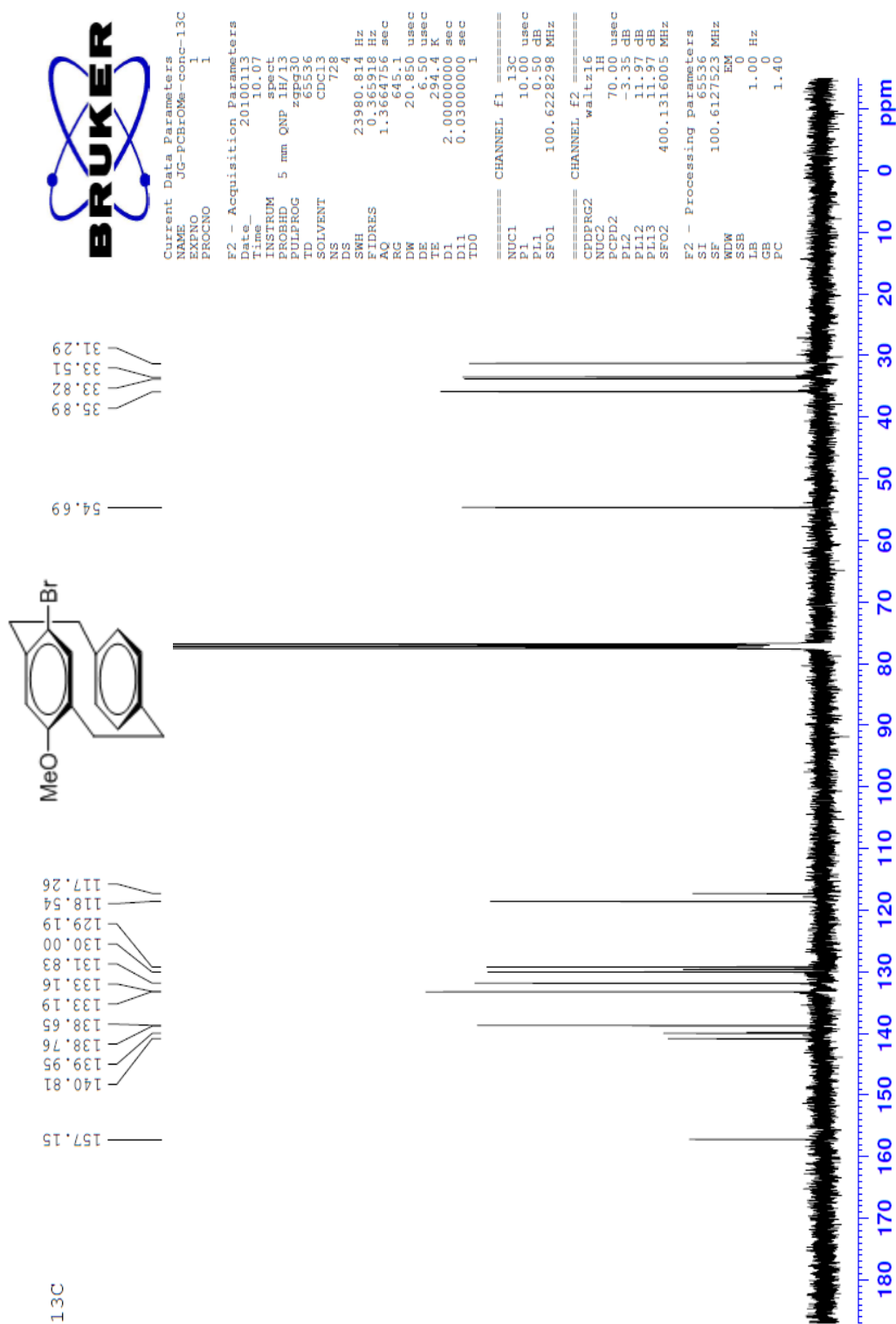
F2 - Processing parameters
SI 32768

SF 400.130055 MHz
WDW EM

SSB 0
LB 0.30 Hz

GB 0
PC 1.00





E2-HSQC



NAME 30-PCR06a-0000-130

INSTRUM spect

PROCNO 1

Date 201008113

Time 11.02

PROBHD 5 mm QNP 1H/13

PULPROG zgpg30

TD 3274

SOLVENT CDCl3

NS 4

DS 16

SWH 3296.16 Hz

FIDRES 0.1201128 Hz

AQ 0.1257428 sec

RG 1024

GB 1024

DN 147.208 sec

DE 6.58 sec

TE 299.2 K

CH2 145.000 MHz

C1 0.8003008 sec

C2 1.5003008 sec

C3 0.80172414 sec

C4 0.8003008 sec

C5 0.8003008 sec

C6 0.8003008 sec

C7 0.8003008 sec

C8 0.8003008 sec

C9 0.8003008 sec

C10 0.8003008 sec

C11 0.8003008 sec

C12 0.8003008 sec

C13 0.8003008 sec

C14 0.8003008 sec

C15 0.8003008 sec

C16 0.8003008 sec

C17 0.8003008 sec

C18 0.8003008 sec

C19 0.8003008 sec

C20 0.8003008 sec

C21 0.8003008 sec

C22 0.8003008 sec

C23 0.8003008 sec

C24 0.8003008 sec

C25 0.8003008 sec

C26 0.8003008 sec

C27 0.8003008 sec

C28 0.8003008 sec

C29 0.8003008 sec

C30 0.8003008 sec

C31 0.8003008 sec

C32 0.8003008 sec

C33 0.8003008 sec

C34 0.8003008 sec

C35 0.8003008 sec

C36 0.8003008 sec

C37 0.8003008 sec

C38 0.8003008 sec

C39 0.8003008 sec

C40 0.8003008 sec

C41 0.8003008 sec

C42 0.8003008 sec

C43 0.8003008 sec

C44 0.8003008 sec

C45 0.8003008 sec

C46 0.8003008 sec

C47 0.8003008 sec

C48 0.8003008 sec

C49 0.8003008 sec

C50 0.8003008 sec

C51 0.8003008 sec

C52 0.8003008 sec

C53 0.8003008 sec

C54 0.8003008 sec

C55 0.8003008 sec

C56 0.8003008 sec

C57 0.8003008 sec

C58 0.8003008 sec

C59 0.8003008 sec

C60 0.8003008 sec

C61 0.8003008 sec

C62 0.8003008 sec

C63 0.8003008 sec

C64 0.8003008 sec

C65 0.8003008 sec

C66 0.8003008 sec

C67 0.8003008 sec

C68 0.8003008 sec

C69 0.8003008 sec

C70 0.8003008 sec

C71 0.8003008 sec

C72 0.8003008 sec

C73 0.8003008 sec

C74 0.8003008 sec

C75 0.8003008 sec

C76 0.8003008 sec

C77 0.8003008 sec

C78 0.8003008 sec

C79 0.8003008 sec

C80 0.8003008 sec

C81 0.8003008 sec

C82 0.8003008 sec

C83 0.8003008 sec

C84 0.8003008 sec

C85 0.8003008 sec

C86 0.8003008 sec

C87 0.8003008 sec

C88 0.8003008 sec

C89 0.8003008 sec

C90 0.8003008 sec

C91 0.8003008 sec

C92 0.8003008 sec

C93 0.8003008 sec

C94 0.8003008 sec

C95 0.8003008 sec

C96 0.8003008 sec

C97 0.8003008 sec

C98 0.8003008 sec

C99 0.8003008 sec

C100 0.8003008 sec

C101 0.8003008 sec

C102 0.8003008 sec

C103 0.8003008 sec

C104 0.8003008 sec

C105 0.8003008 sec

C106 0.8003008 sec

C107 0.8003008 sec

C108 0.8003008 sec

C109 0.8003008 sec

C110 0.8003008 sec

C111 0.8003008 sec

C112 0.8003008 sec

C113 0.8003008 sec

C114 0.8003008 sec

C115 0.8003008 sec

C116 0.8003008 sec

C117 0.8003008 sec

C118 0.8003008 sec

C119 0.8003008 sec

C120 0.8003008 sec

C121 0.8003008 sec

C122 0.8003008 sec

C123 0.8003008 sec

C124 0.8003008 sec

C125 0.8003008 sec

C126 0.8003008 sec

C127 0.8003008 sec

C128 0.8003008 sec

C129 0.8003008 sec

C130 0.8003008 sec

C131 0.8003008 sec

C132 0.8003008 sec

C133 0.8003008 sec

C134 0.8003008 sec

C135 0.8003008 sec

C136 0.8003008 sec

C137 0.8003008 sec

C138 0.8003008 sec

C139 0.8003008 sec

C140 0.8003008 sec

C141 0.8003008 sec

C142 0.8003008 sec

C143 0.8003008 sec

C144 0.8003008 sec

C145 0.8003008 sec

C146 0.8003008 sec

C147 0.8003008 sec

C148 0.8003008 sec

C149 0.8003008 sec

C150 0.8003008 sec

C151 0.8003008 sec

C152 0.8003008 sec

C153 0.8003008 sec

C154 0.8003008 sec

C155 0.8003008 sec

C156 0.8003008 sec

C157 0.8003008 sec

C158 0.8003008 sec

C159 0.8003008 sec

C160 0.8003008 sec

C161 0.8003008 sec

C162 0.8003008 sec

C163 0.8003008 sec

C164 0.8003008 sec

C165 0.8003008 sec

C166 0.8003008 sec

C167 0.8003008 sec

C168 0.8003008 sec

C169 0.8003008 sec

C170 0.8003008 sec

C171 0.8003008 sec

C172 0.8003008 sec

C173 0.8003008 sec

C174 0.8003008 sec

C175 0.8003008 sec

C176 0.8003008 sec

C177 0.8003008 sec

C178 0.8003008 sec

C179 0.8003008 sec

C180 0.8003008 sec

C181 0.8003008 sec

C182 0.8003008 sec

C183 0.8003008 sec

C184 0.8003008 sec

C185 0.8003008 sec

C186 0.8003008 sec

C187 0.8003008 sec

C188 0.8003008 sec

C189 0.8003008 sec

C190 0.8003008 sec

C191 0.8003008 sec

C192 0.8003008 sec

C193 0.8003008 sec

C194 0.8003008 sec

C195 0.8003008 sec

C196 0.8003008 sec

C197 0.8003008 sec

C198 0.8003008 sec

C199 0.8003008 sec

C200 0.8003008 sec

C201 0.8003008 sec

C202 0.8003008 sec

C203 0.8003008 sec

C204 0.8003008 sec

C205 0.8003008 sec

C206 0.8003008 sec

C207 0.8003008 sec

C208 0.8003008 sec

C209 0.8003008 sec

C210 0.8003008 sec

C211 0.8003008 sec

C212 0.8003008 sec

C213 0.8003008 sec

C214 0.8003008 sec

C215 0.8003008 sec

C216 0.8003008 sec

C217 0.8003008 sec

C218 0.8003008 sec

C219 0.8003008 sec

C220 0.8003008 sec

C221 0.8003008 sec

C222 0.8003008 sec

C223 0.8003008 sec

C224 0.8003008 sec

C225 0.8003008 sec

C226 0.8003008 sec

C227 0.8003008 sec

C228 0.8003008 sec

C229 0.8003008 sec

C230 0.8003008 sec

C231 0.8003008 sec

C232 0.8003008 sec

C233 0.8003008 sec

C234 0.8003008 sec

C235 0.8003008 sec

C236 0.8003008 sec

C237 0.8003008 sec

C238 0.8003008 sec

C239 0.8003008 sec

C240 0.8003008 sec

C241 0.8003008 sec

C242 0.8003008 sec

C243 0.8003008 sec

C244 0.8003008 sec

C245 0.8003008 sec

C246 0.8003008 sec

C247 0.8003008 sec

C248 0.8003008 sec

C249 0.8003008 sec

C250 0.8003008 sec

C251 0.8003008 sec

C252 0.8003008 sec

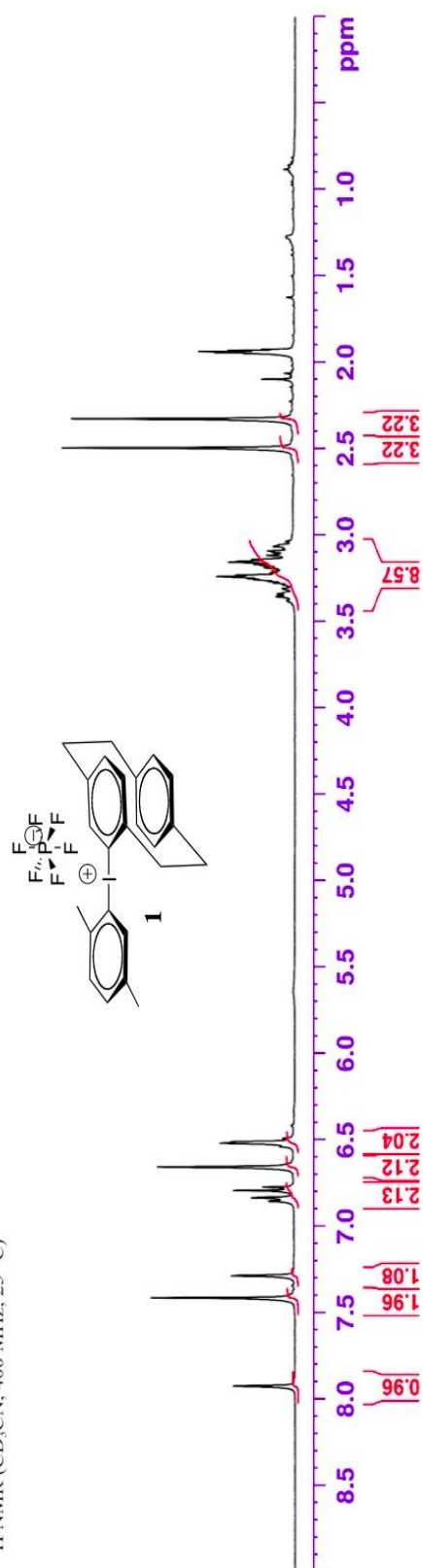
C253 0.8003008 sec

C254 0.8003008 sec

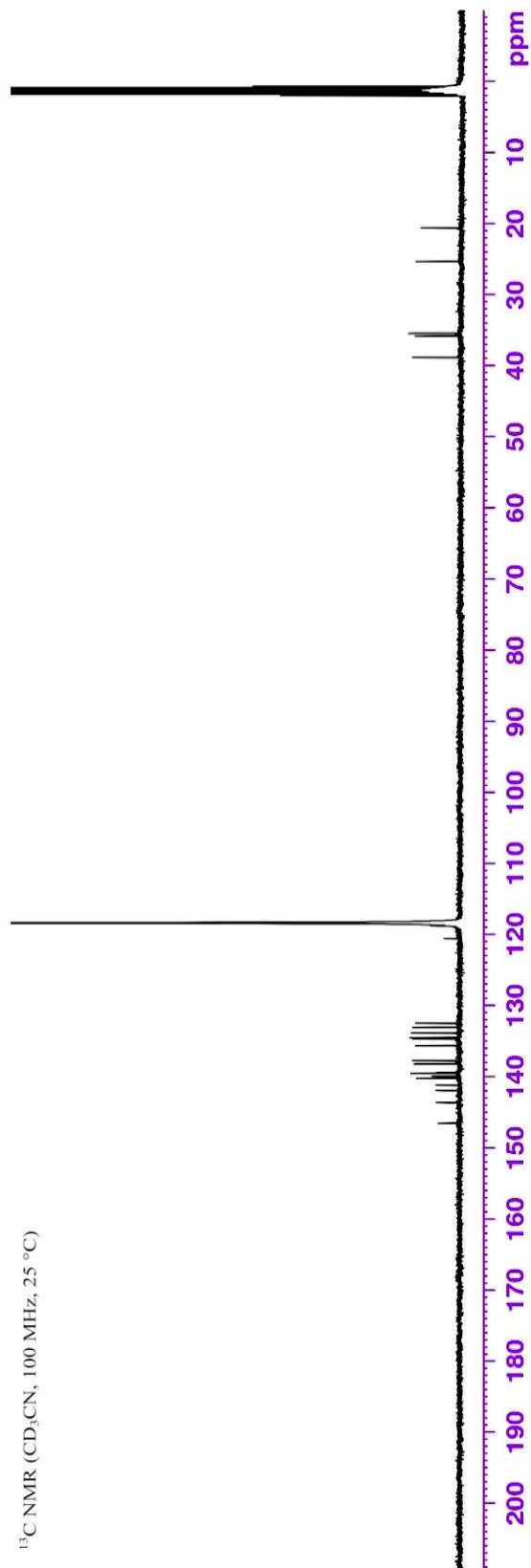
C255 0.8003008 sec

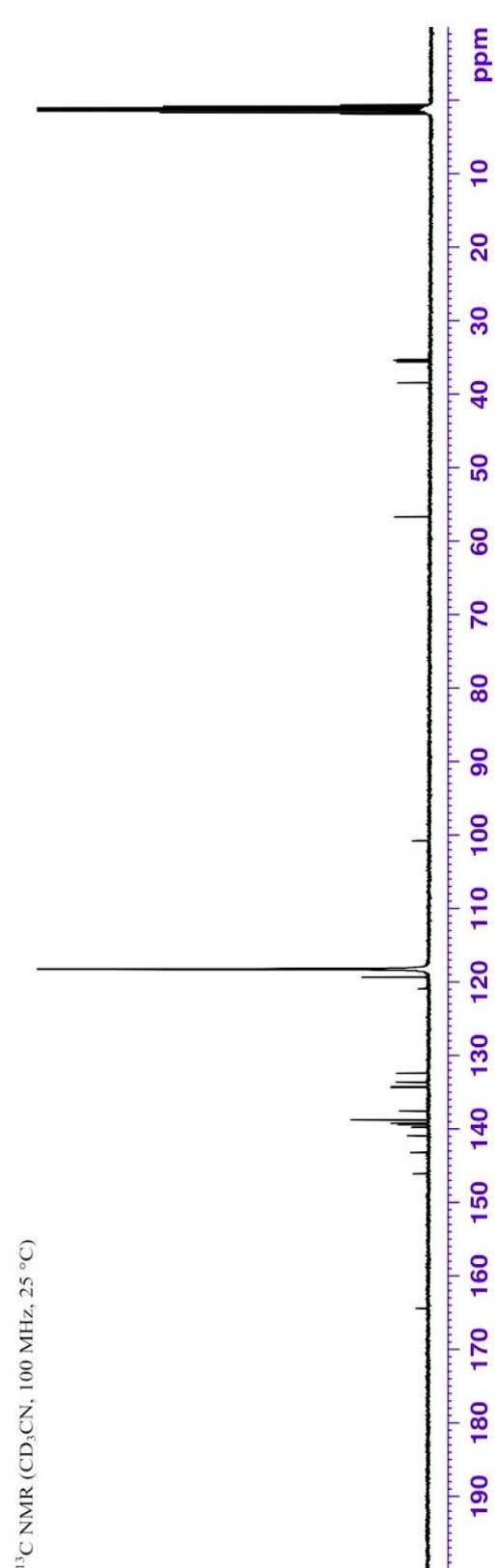
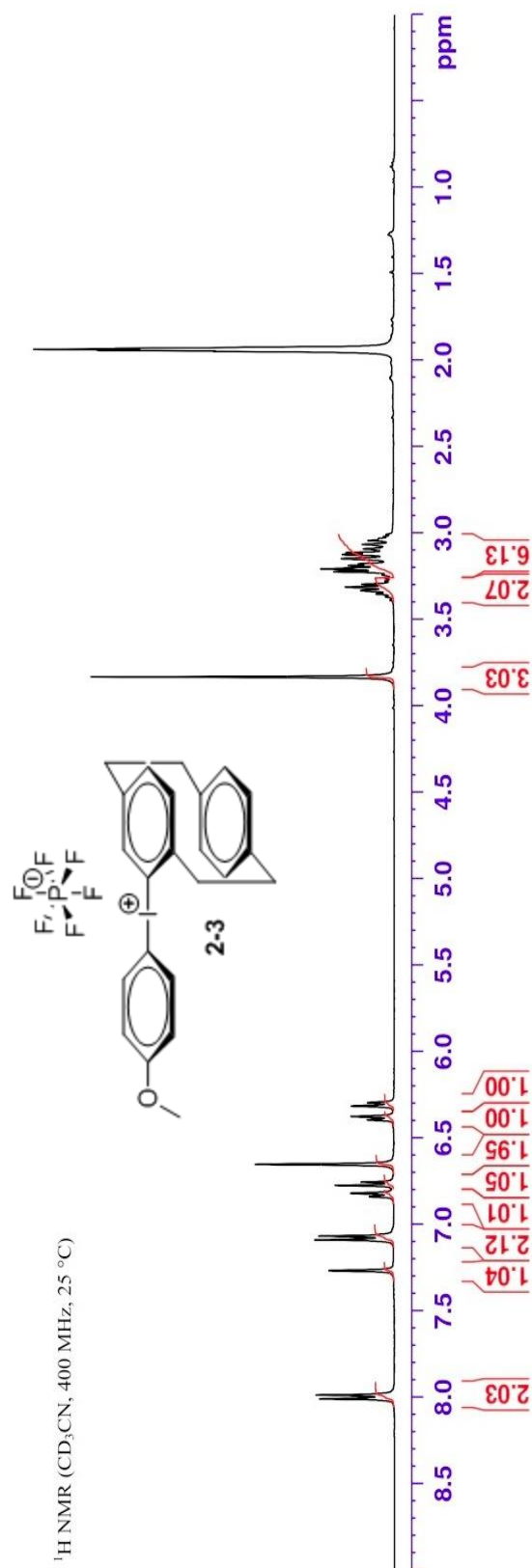
C256 0.800

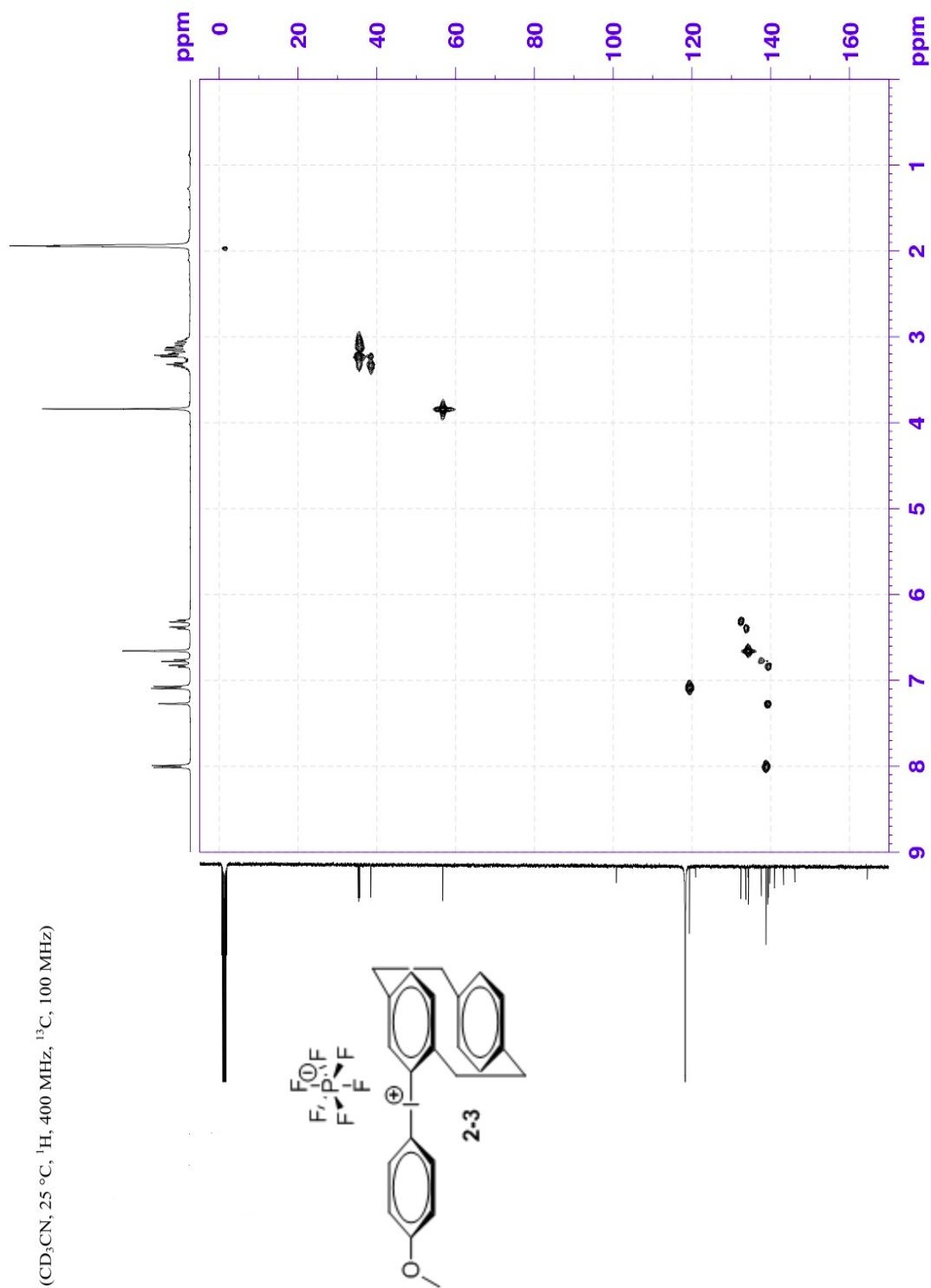
^1H NMR (CD_3CN , 400 MHz, 25 °C)

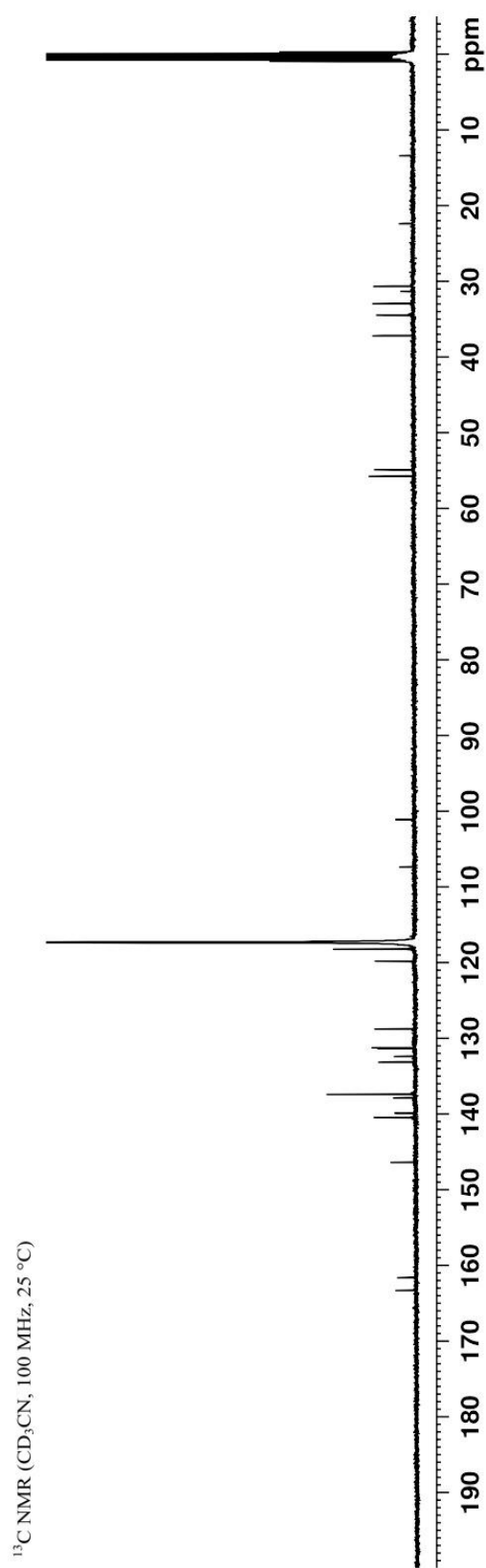
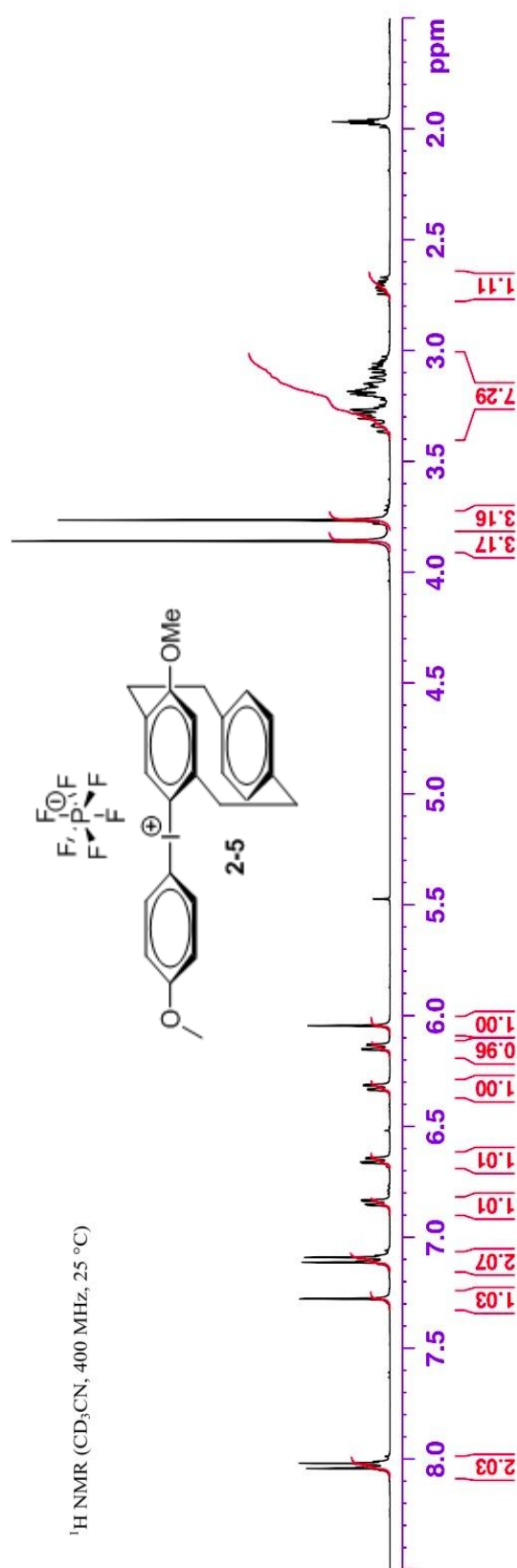


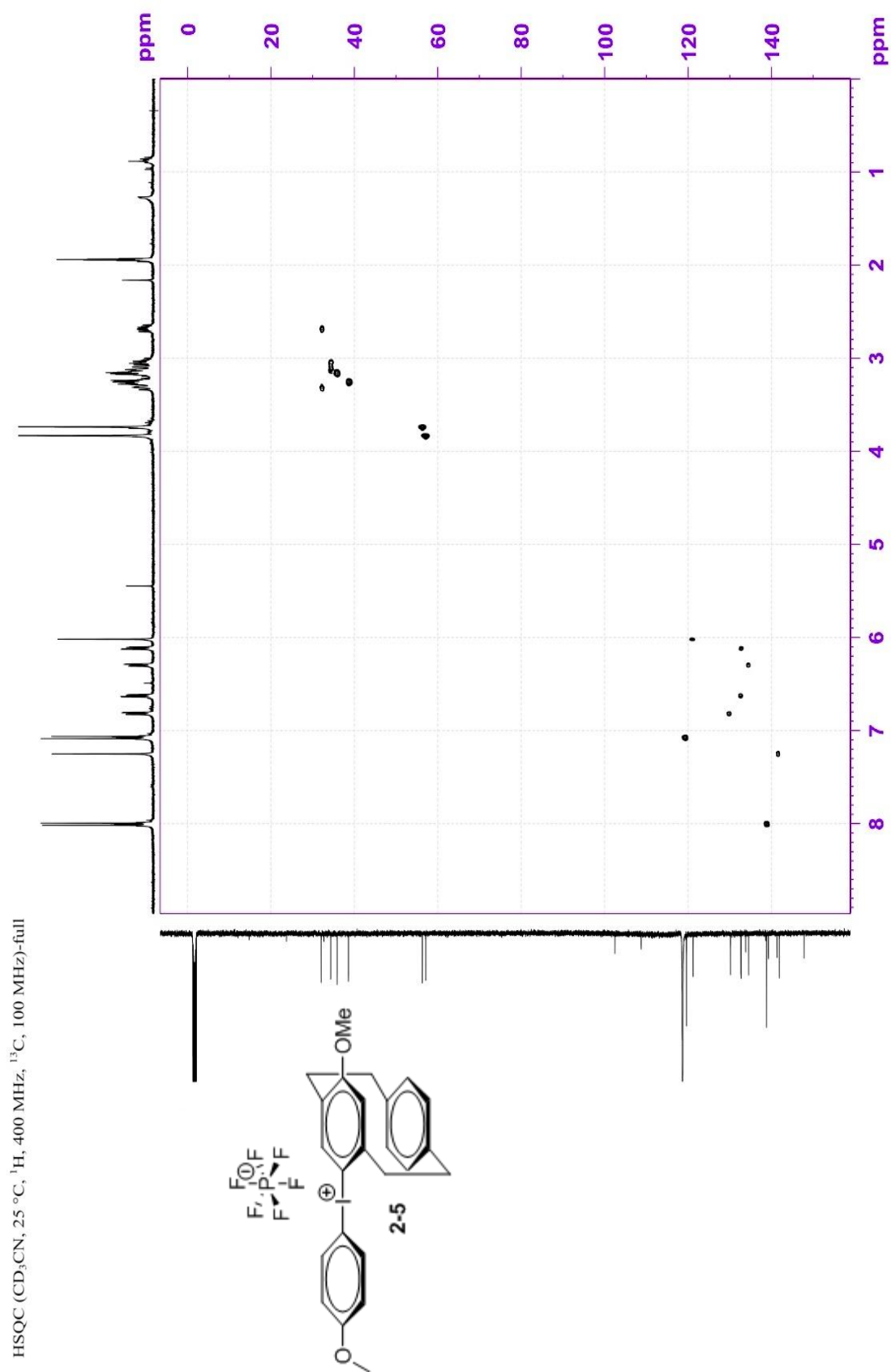
^{13}C NMR (CD_3CN , 100 MHz, 25 °C)

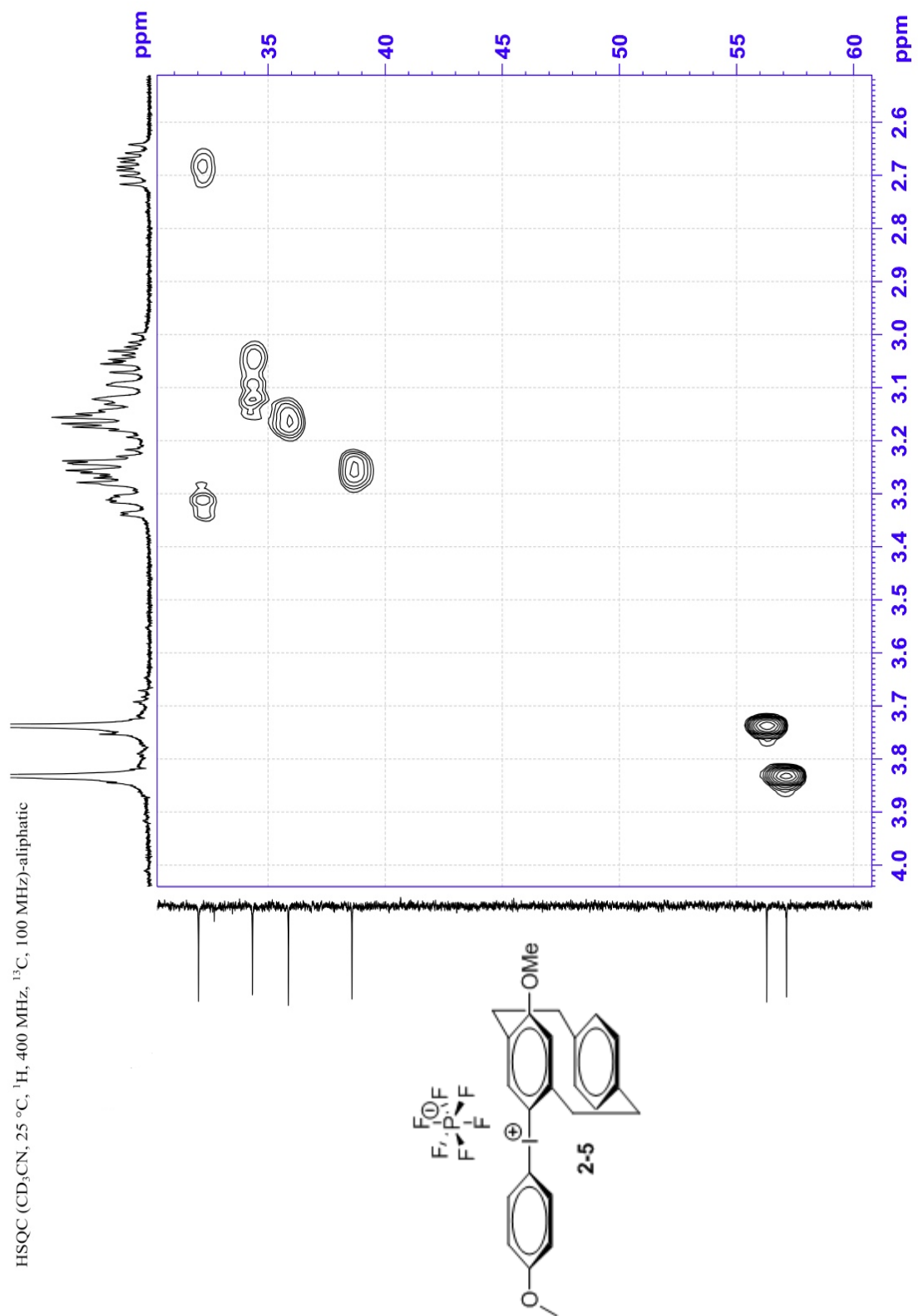




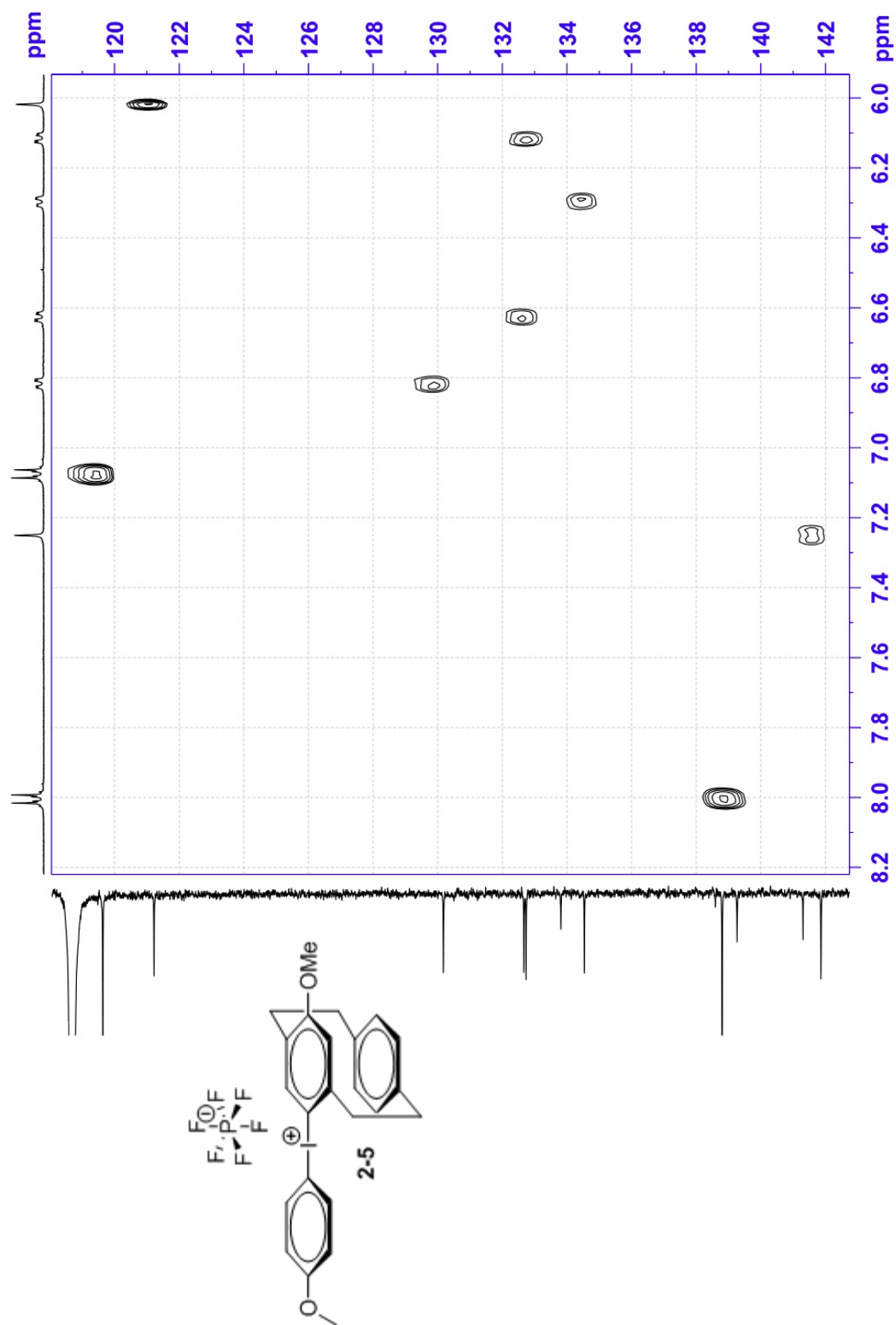


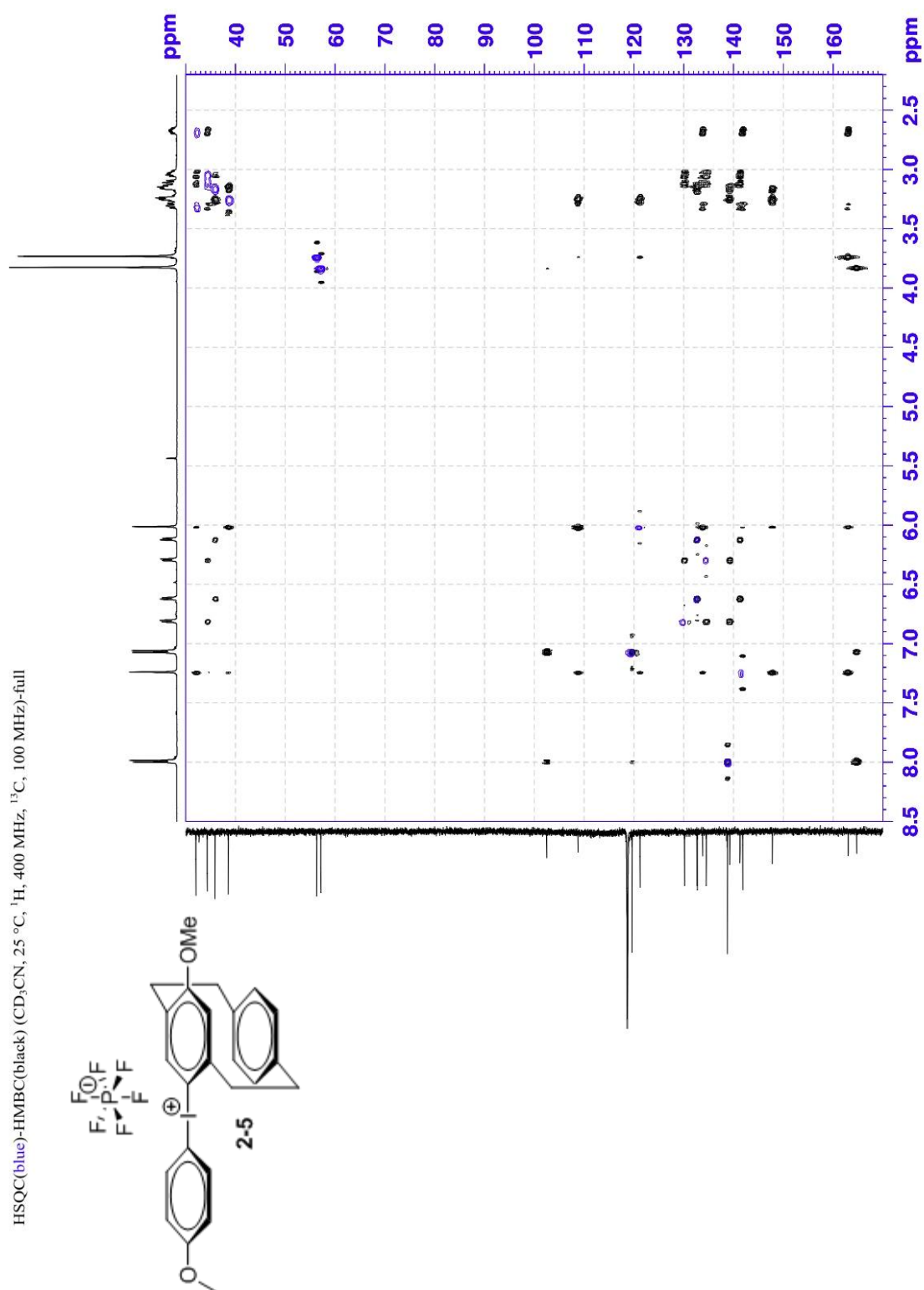




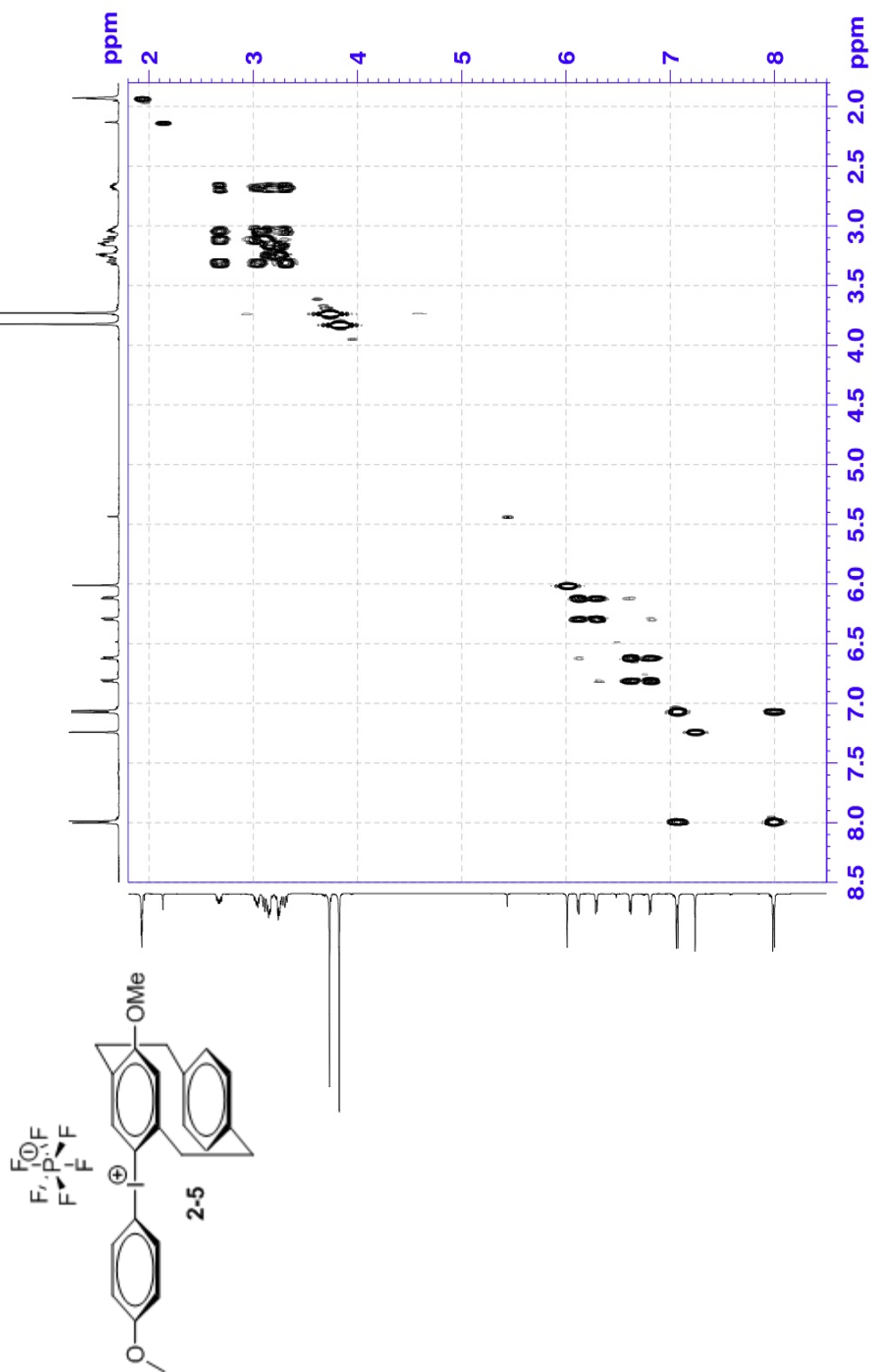


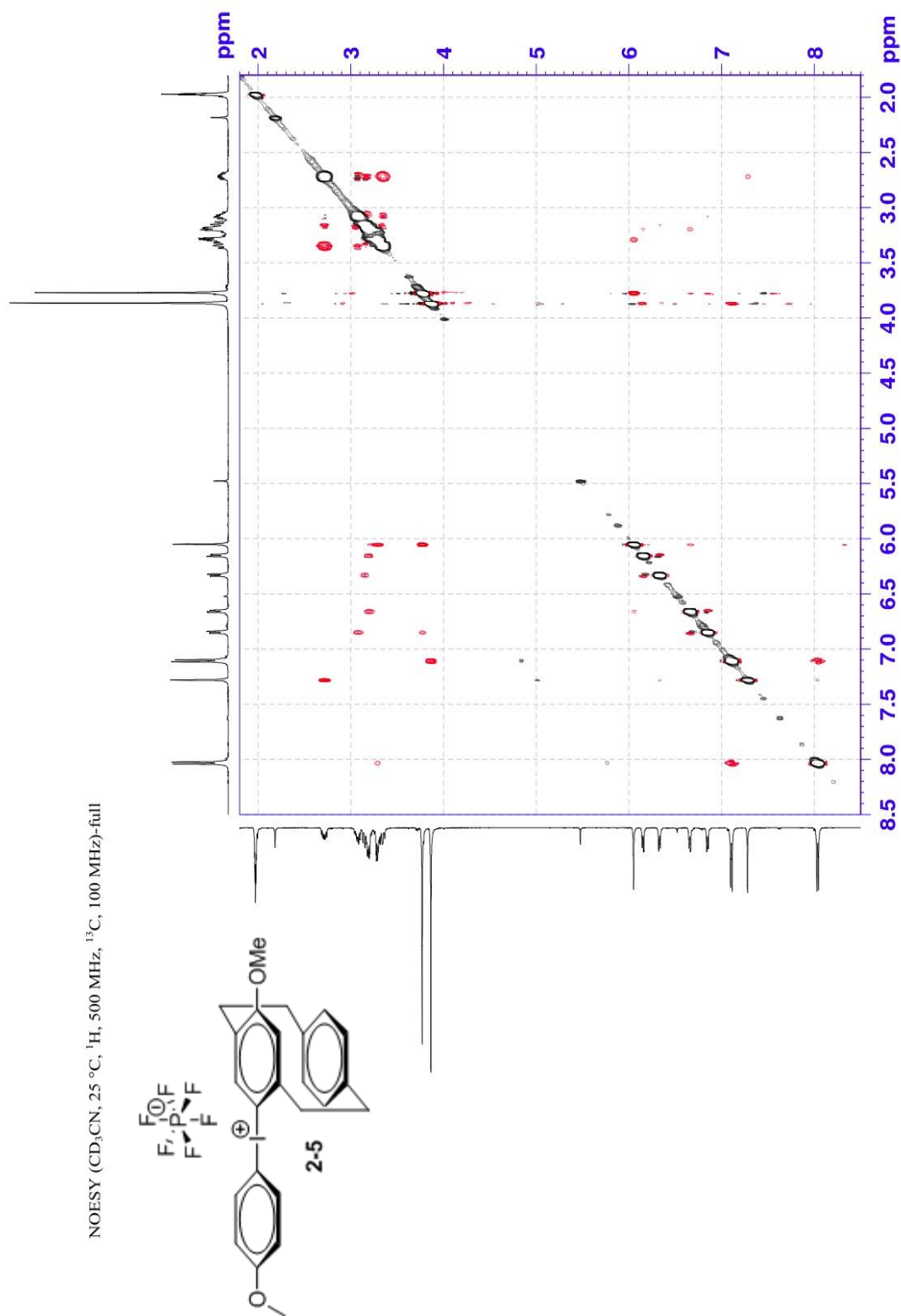
HSQC (CD₃CN, 25 °C, ¹H, 400 MHz, ¹³C, 100 MHz)-aromatic

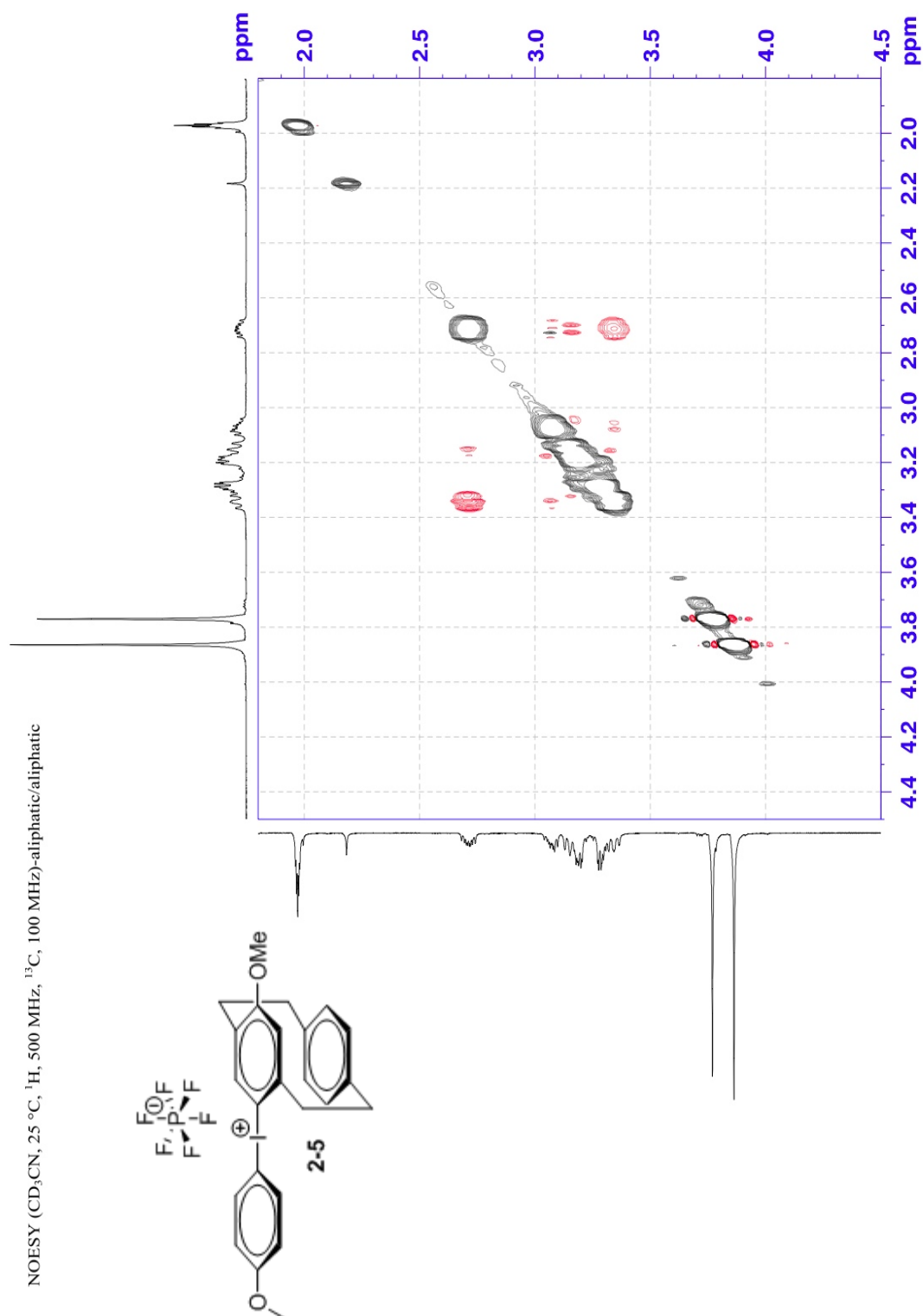


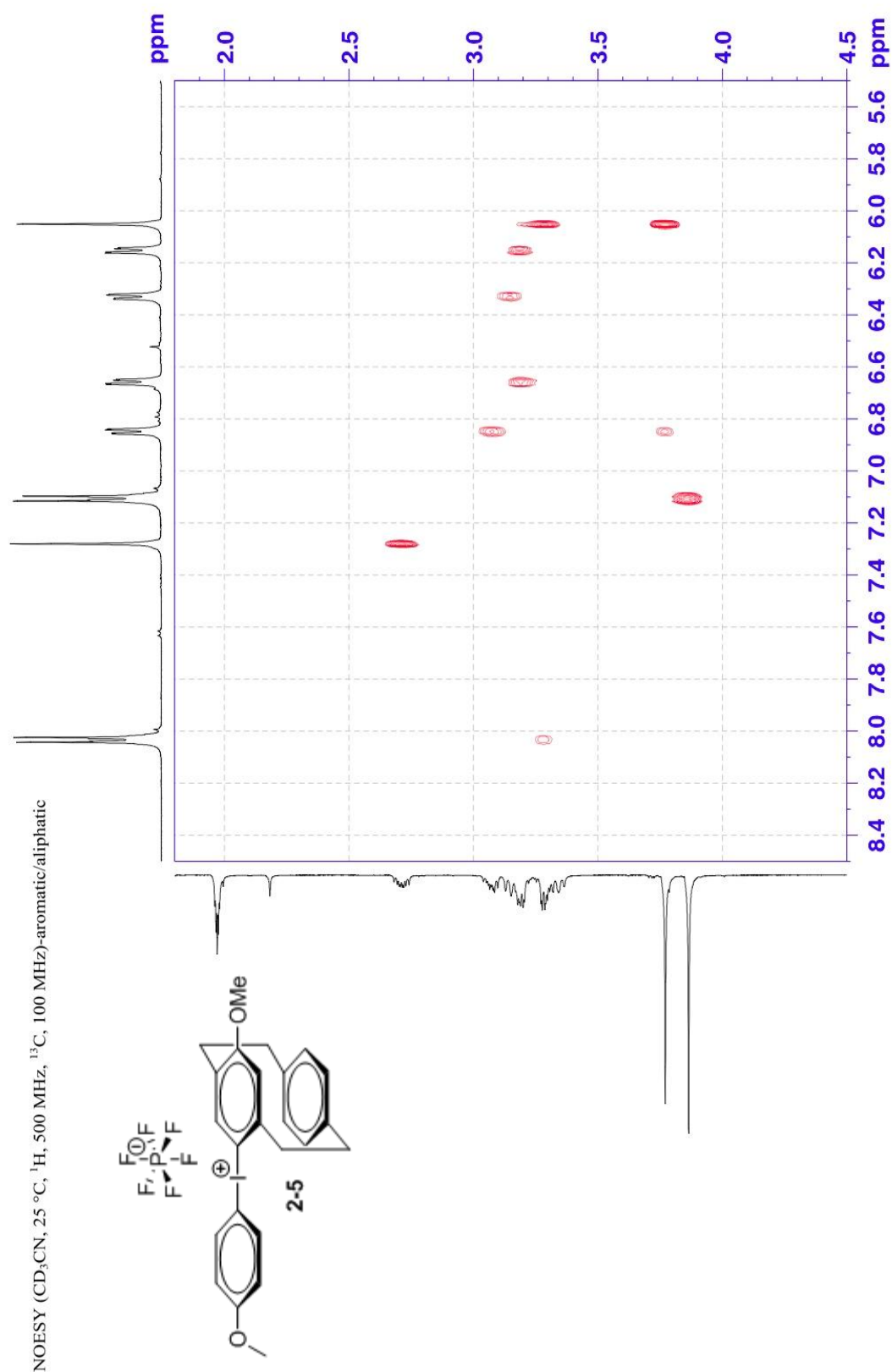


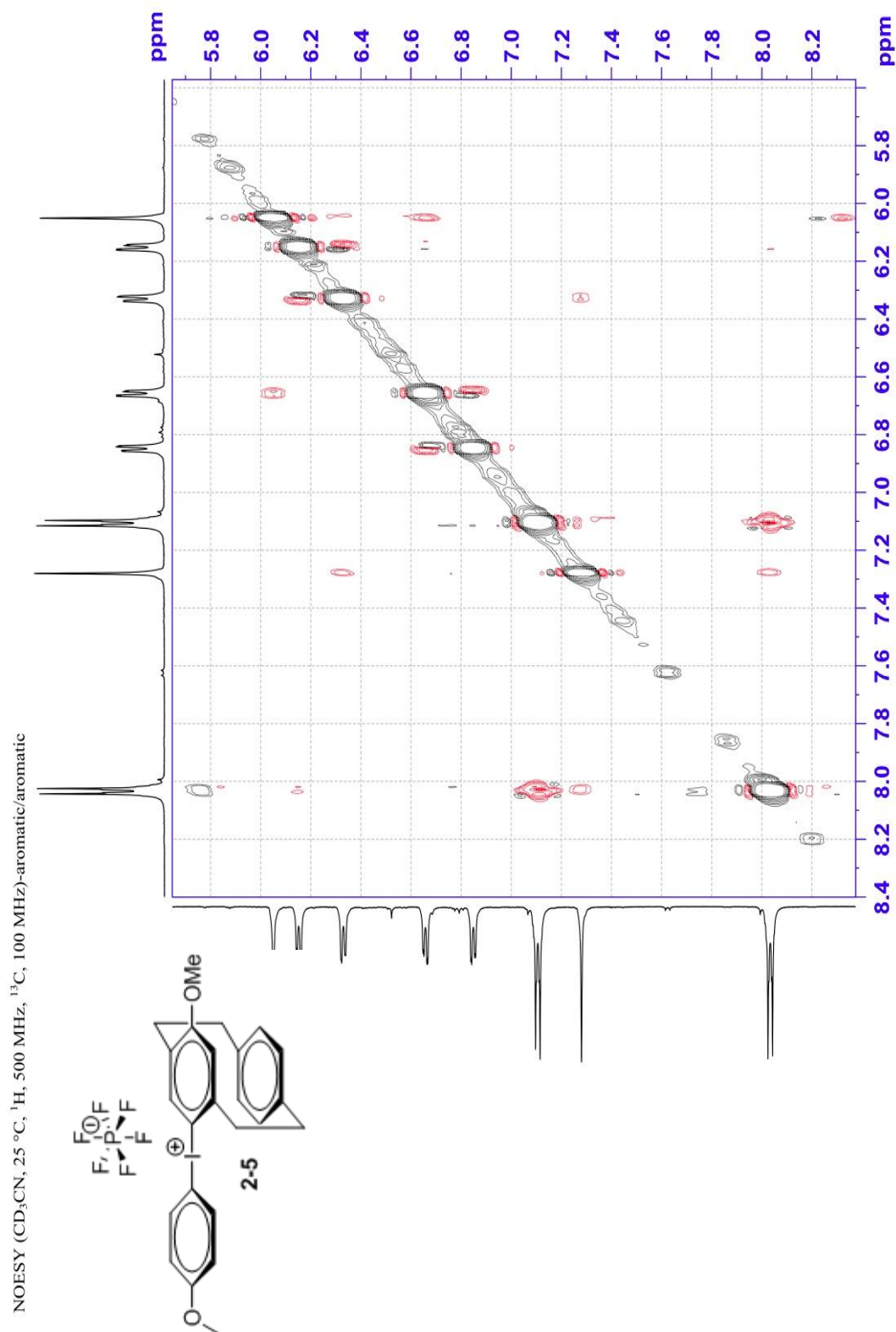
COSY (CD₃CN, 25 °C, ¹H, 400 MHz, ¹³C, 100 MHz)-full



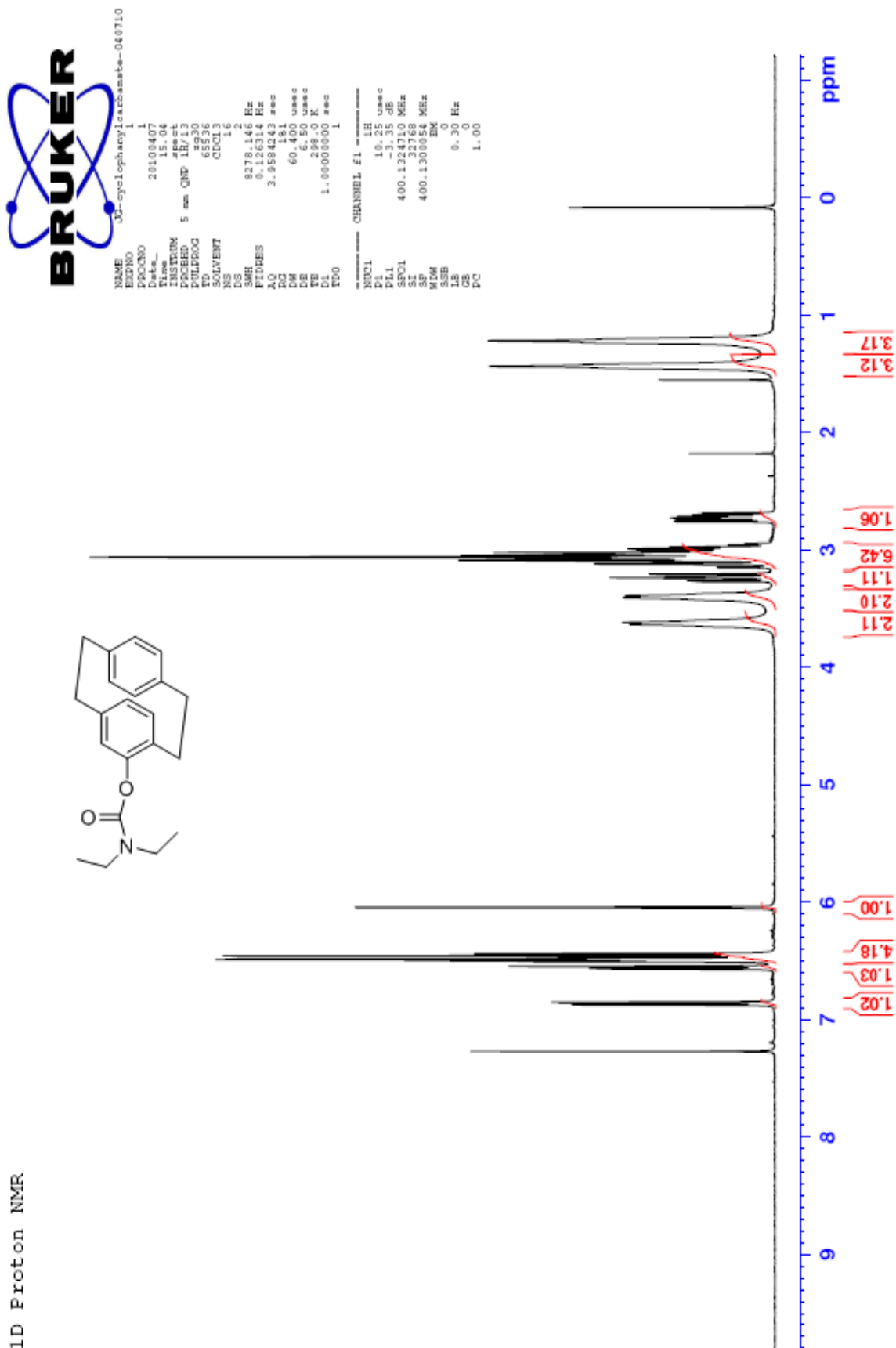


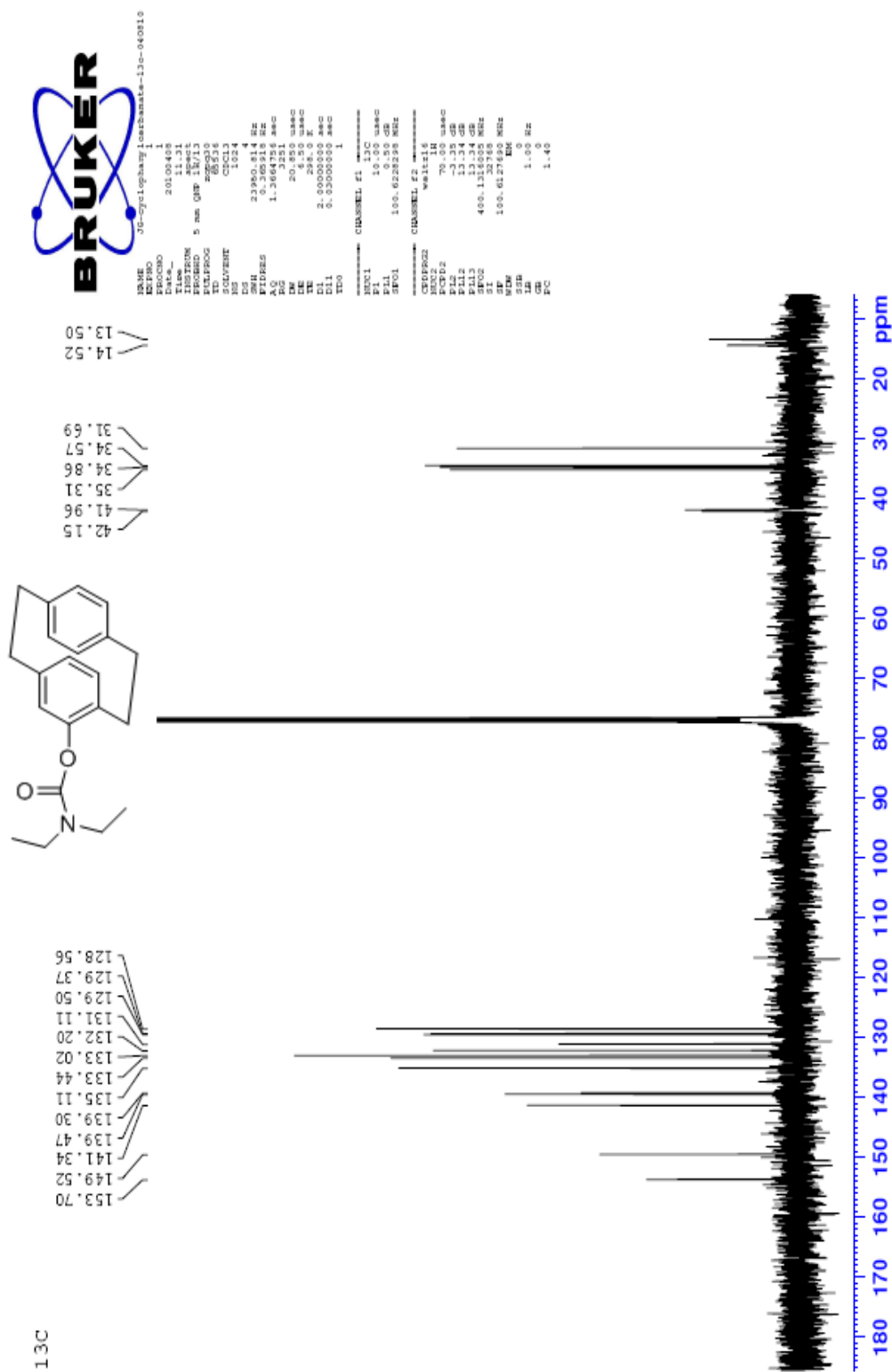


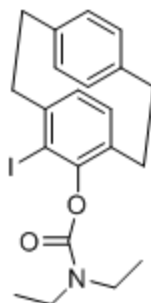




1D Proton NMR







Current Data Parameters
NAME JC-o-iodocharinate-041410-1H

EXPNO 1
PROCNO 1

F2 - Acquisition Parameters

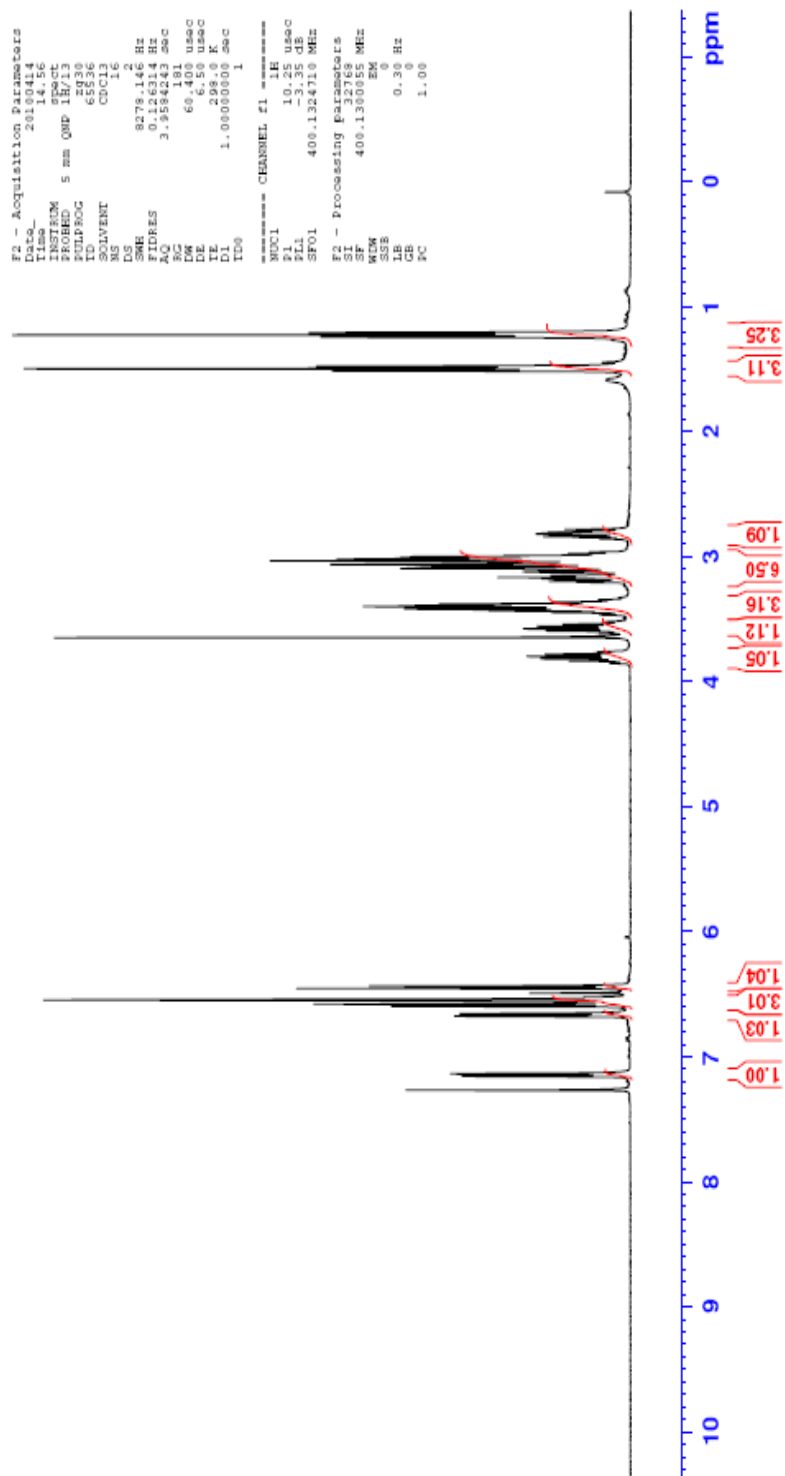
Date_ 20100414
Time 14.56
PROBHD 5 mm QNP 1H/13
PULPROG zgpg30
ID0 65836
SOLVENT CDCl3
NS 16
DS 2
SWH 8278.146 Hz
FIDRES 0.152654 Hz
AQ 3.155811 sec
RG 181
EQ 1.81
LW 60.400 usec
LE 3.50 usec
TE 300.2 K
D1 1.0000000 sec
D11 0.0500000 sec
D12 0.0500000 sec
D13 0.0500000 sec
D14 0.0500000 sec
D15 0.0500000 sec
D16 0.0500000 sec
D17 0.0500000 sec
D18 0.0500000 sec
D19 0.0500000 sec
D20 0.0500000 sec
D21 0.0500000 sec
D22 0.0500000 sec
D23 0.0500000 sec
D24 0.0500000 sec
D25 0.0500000 sec
D26 0.0500000 sec
D27 0.0500000 sec
D28 0.0500000 sec
D29 0.0500000 sec
D30 0.0500000 sec
D31 0.0500000 sec
D32 0.0500000 sec
D33 0.0500000 sec
D34 0.0500000 sec
D35 0.0500000 sec
D36 0.0500000 sec
D37 0.0500000 sec
D38 0.0500000 sec
D39 0.0500000 sec
D40 0.0500000 sec
D41 0.0500000 sec
D42 0.0500000 sec
D43 0.0500000 sec
D44 0.0500000 sec
D45 0.0500000 sec
D46 0.0500000 sec
D47 0.0500000 sec
D48 0.0500000 sec
D49 0.0500000 sec
D50 0.0500000 sec
D51 0.0500000 sec
D52 0.0500000 sec
D53 0.0500000 sec
D54 0.0500000 sec
D55 0.0500000 sec
D56 0.0500000 sec
D57 0.0500000 sec
D58 0.0500000 sec
D59 0.0500000 sec
D60 0.0500000 sec
D61 0.0500000 sec
D62 0.0500000 sec
D63 0.0500000 sec
D64 0.0500000 sec
D65 0.0500000 sec
D66 0.0500000 sec
D67 0.0500000 sec
D68 0.0500000 sec
D69 0.0500000 sec
D70 0.0500000 sec
D71 0.0500000 sec
D72 0.0500000 sec
D73 0.0500000 sec
D74 0.0500000 sec
D75 0.0500000 sec
D76 0.0500000 sec
D77 0.0500000 sec
D78 0.0500000 sec
D79 0.0500000 sec
D80 0.0500000 sec
D81 0.0500000 sec
D82 0.0500000 sec
D83 0.0500000 sec
D84 0.0500000 sec
D85 0.0500000 sec
D86 0.0500000 sec
D87 0.0500000 sec
D88 0.0500000 sec
D89 0.0500000 sec
D90 0.0500000 sec
D91 0.0500000 sec
D92 0.0500000 sec
D93 0.0500000 sec
D94 0.0500000 sec
D95 0.0500000 sec
D96 0.0500000 sec
D97 0.0500000 sec
D98 0.0500000 sec
D99 0.0500000 sec
D100 0.0500000 sec

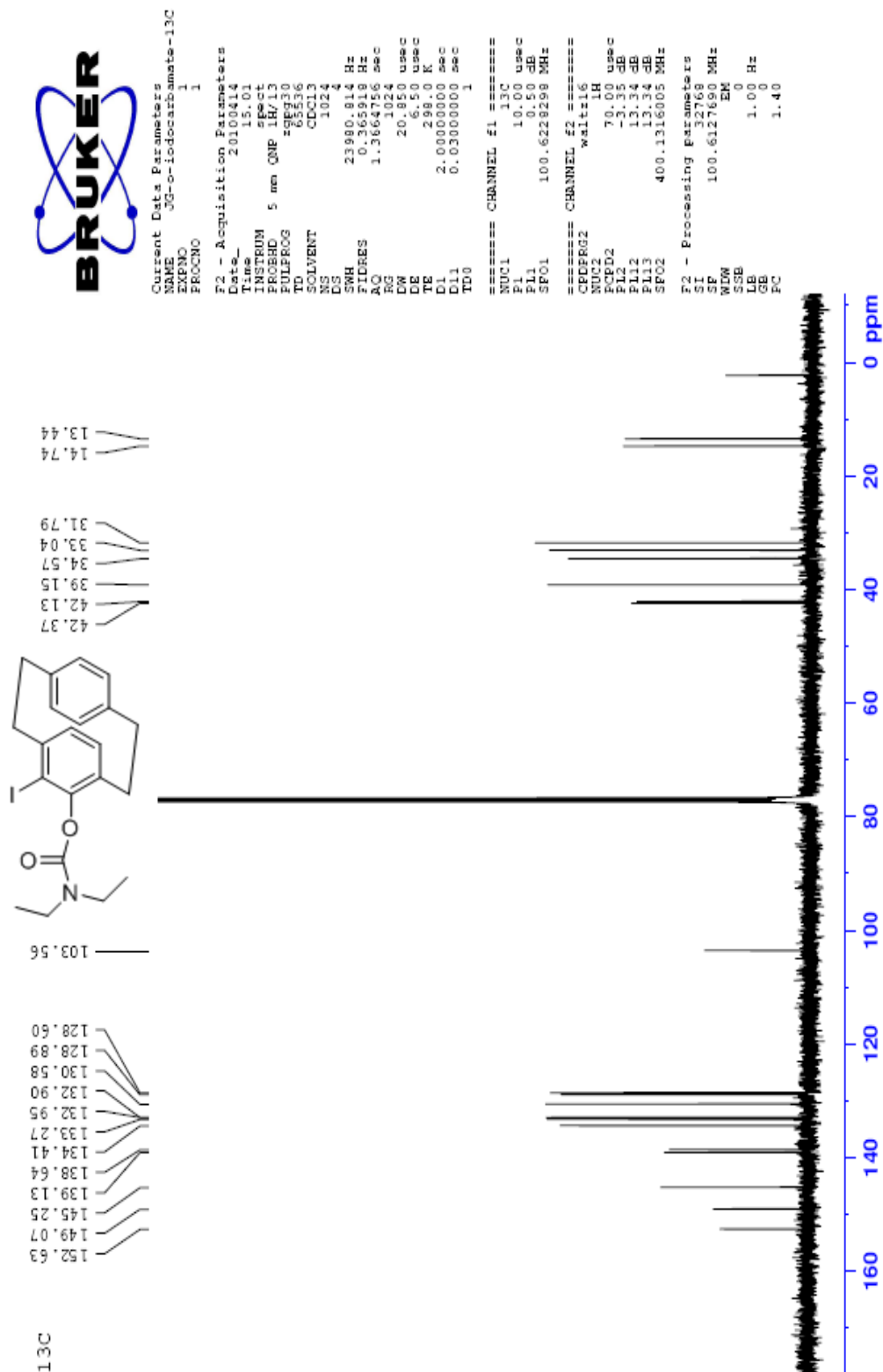
===== CHANNEL f1 =====

MUCL 1H
P1 10.25 usec
PL1 -3.35 dB
SFO1 400.132410 MHz

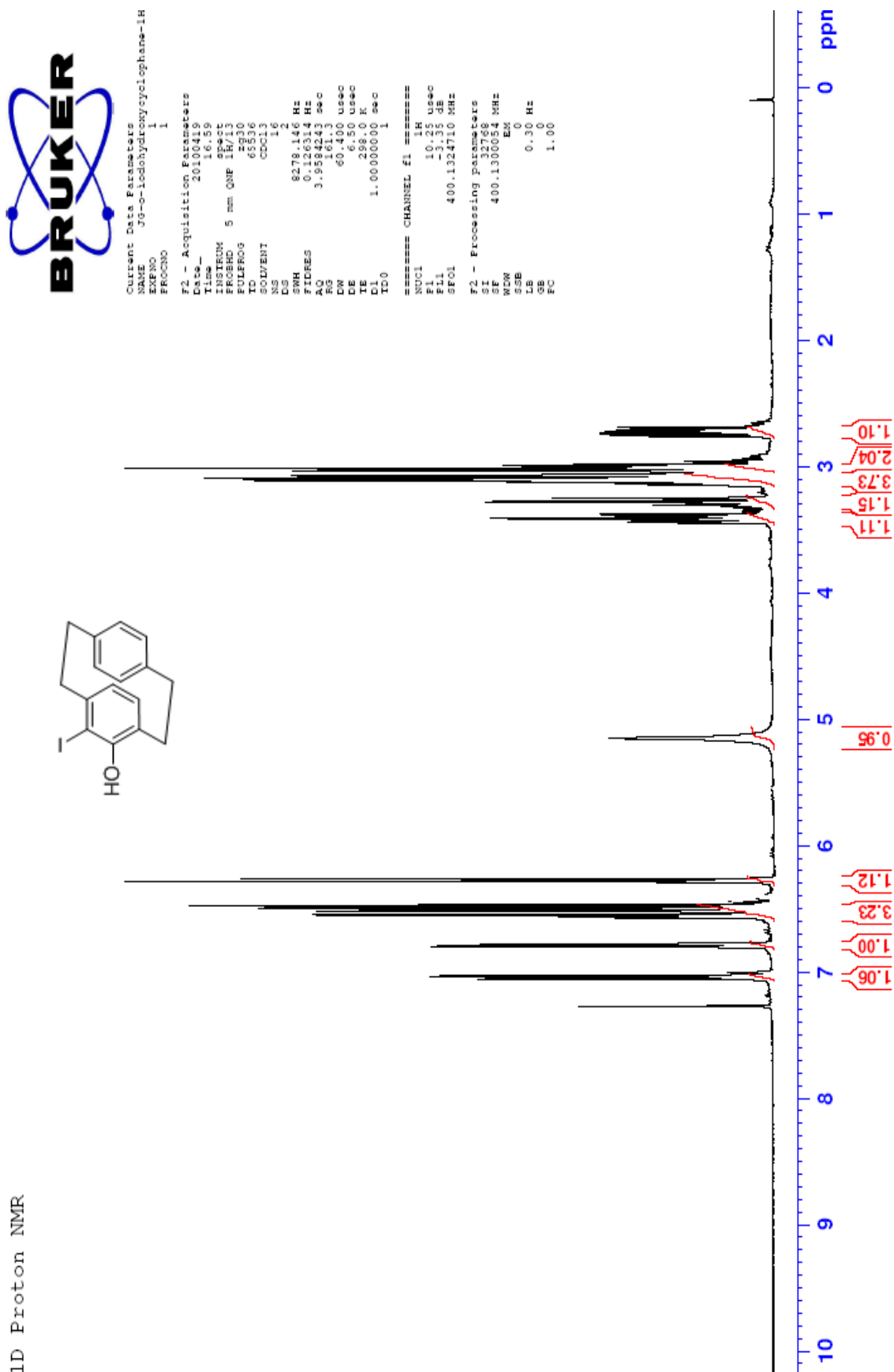
F2 - Processing Parameters

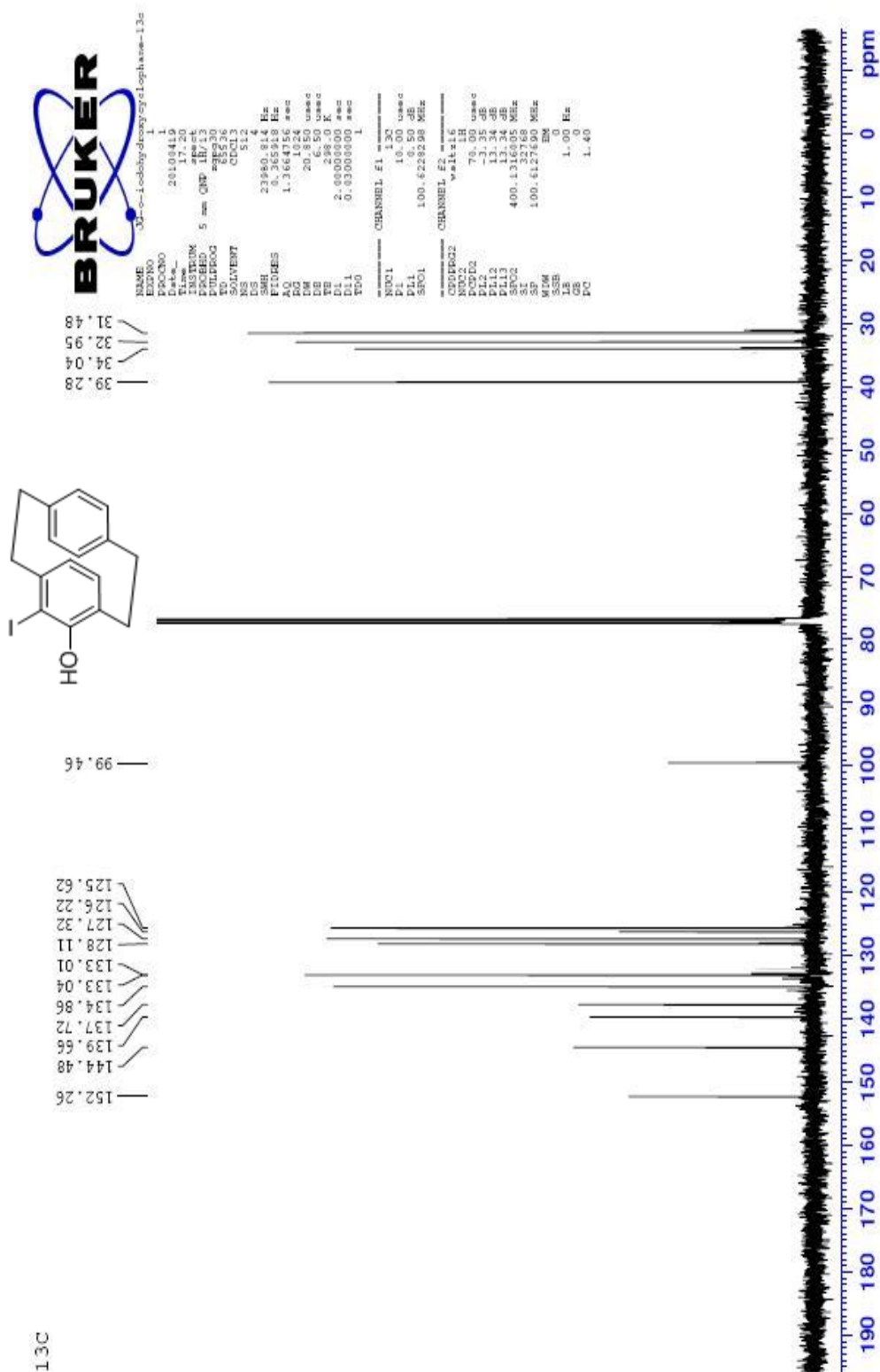
SI 32768
SF 400.130050 MHz
WDW EM
SSB 0
LB 0.30 Hz
GB 0
PC 1.00



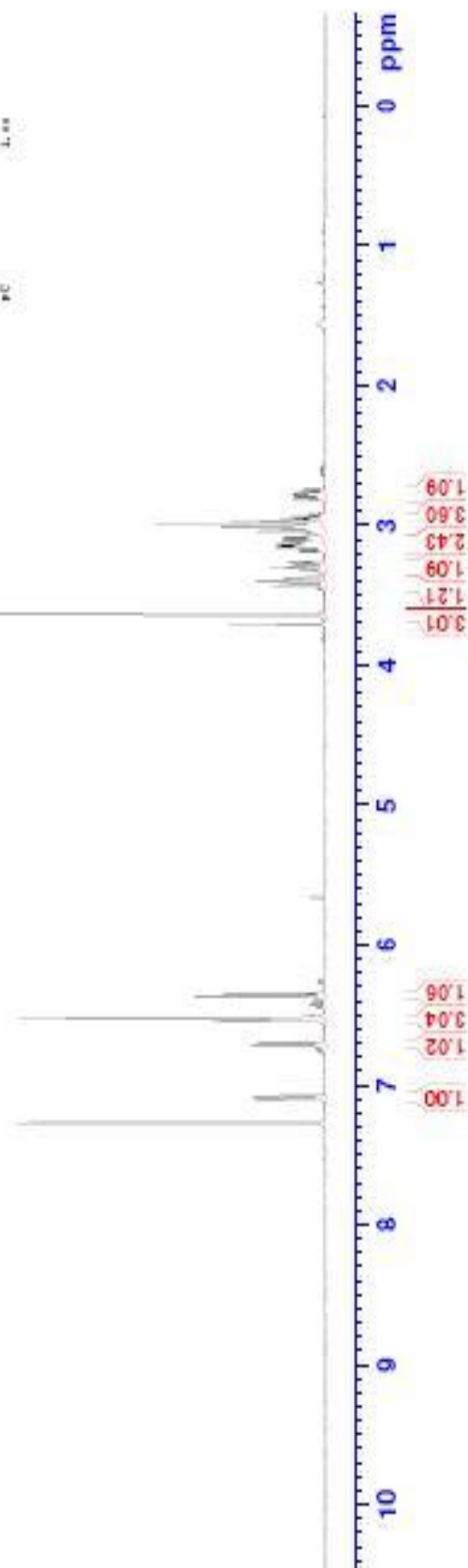
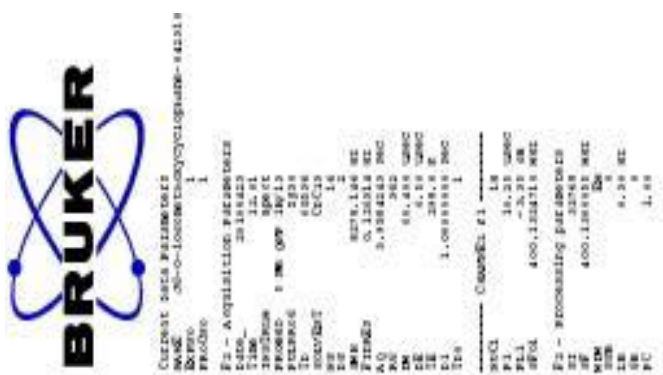
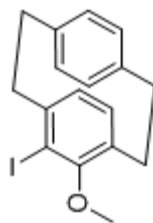


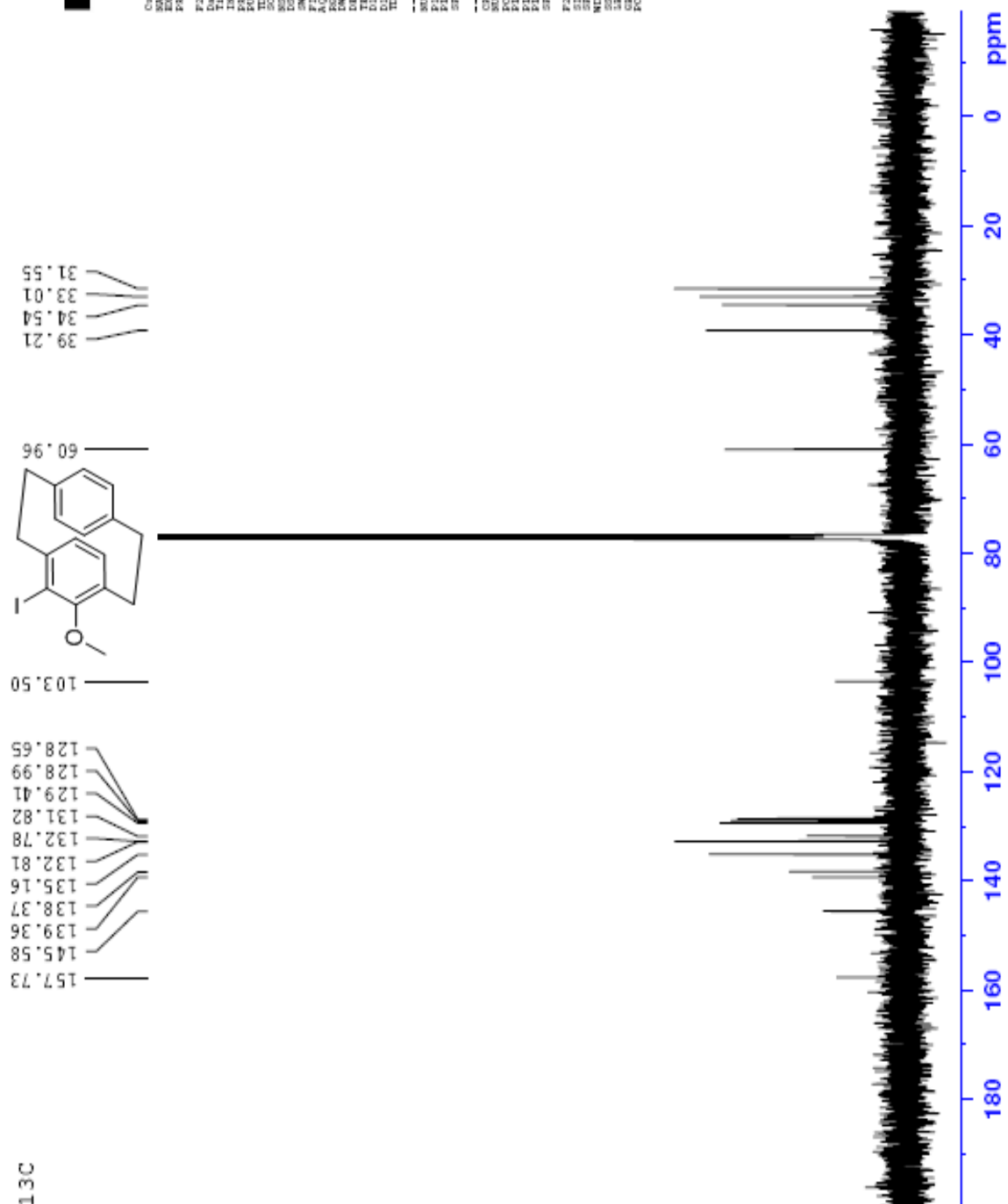
1D Proton NMR





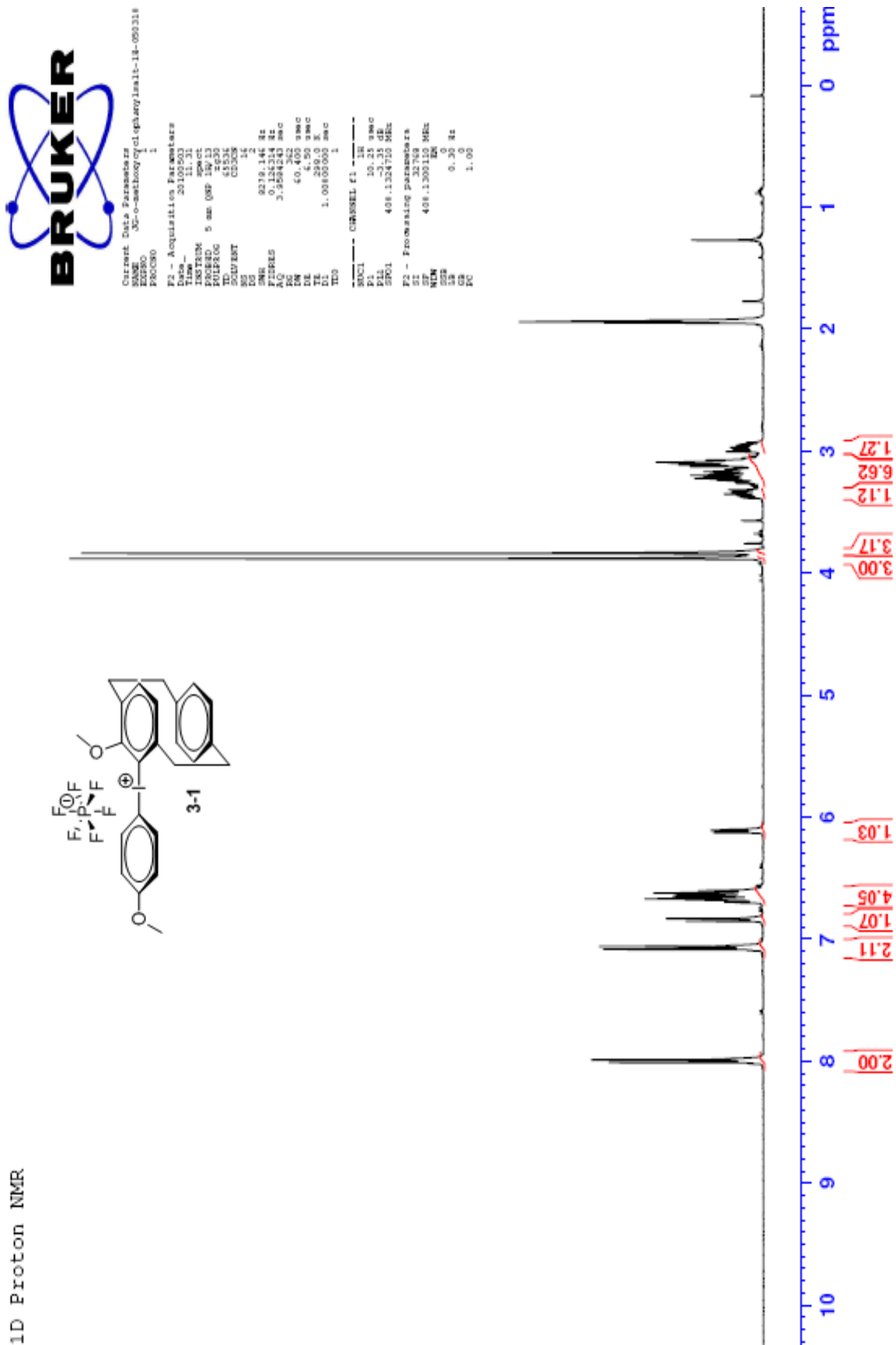
1D Proton NMR



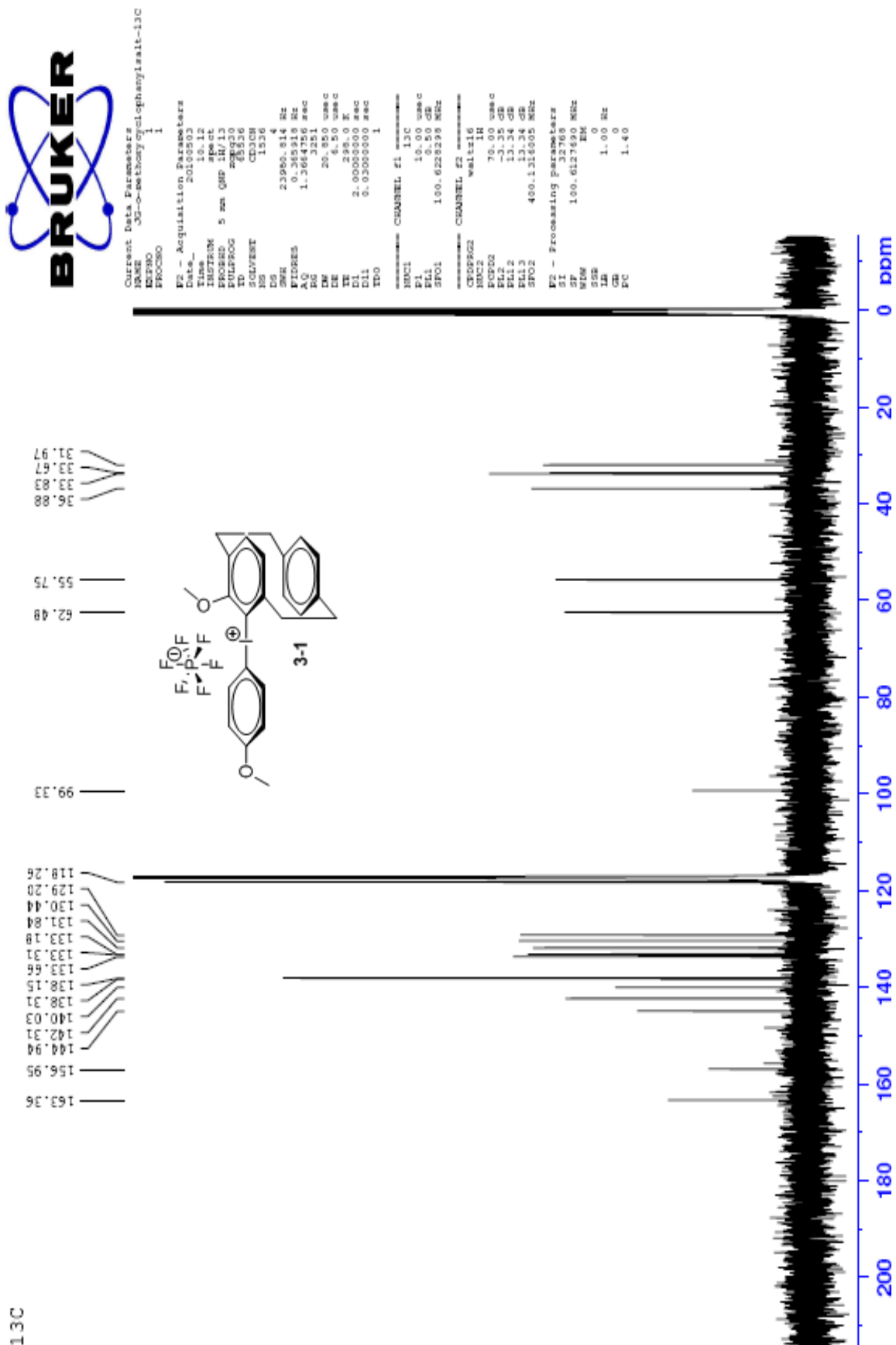
¹³C

Current Data Parameters
 EXPNO 3
 PROCNO 1
 F2 - Acquisition Parameters
 Date_ 20100423
 Time 13.04
 INSTRUM spect
 PULPROG zgpg30
 5 mm QNP 150 13
 TD 65536
 SFO 125.13
 AQ 1.024
 RG 1024
 DQ 204.8000000 sec
 DE 4.50
 TE 290.0 K
 D1 2.00000000 sec
 DELT 0.03000000 sec
 T2 1
 T20
 CHANNEL f1 13C
 MCH1 13C
 P1 10.00 sec
 PL 0.50 dB
 SFO1 100.6224298 MHz
 CHANNEL f2
 MCH2 waitlist
 P2 10.00 sec
 PL -3.35 dB
 SFO2 125.7600000 MHz
 P3 10.00 sec
 PL -3.35 dB
 SFO3 125.7600000 MHz
 F2 - Processing parameters
 SI 32768
 SF 100.6127620 MHz
 MD 1D
 AS 0
 GB 1.00 Hz
 PC 1.40

1D Proton NMR



13C



EZ-COSY



Current Data Parameters
NAME 3C-o-methoxyphenylmalt-2D-042918
EXPNO 1
PROCNO 1

F2 - Acquisition Parameters

Date_ 20100429
Time 14.12

PROBHD 5 mm QNP 1H/13

PULPROG zgpg30

TD 65536

SI 2

DS 4

SWH 1600 Hz

F2 101.254 MHz

AQ 8.197429 sec

RG 1024

DE 3.50 mmC

TE 298.0 K

TO 0.000000 sec

LO 0.000000 sec

DL3 0.000000 sec

DLS 0.000000 sec

195 0.000000 sec

CHANEL F1

NUC1 13C

F1 101.254 MHz

PL2 -3.35 dB

SFO1 408.1304057 MHz

GRAB1 100

GRAB2 100

GRAB3 100

GRAB4 100

GRAB5 100

GRAB6 100

GRAB7 100

GRAB8 100

GRAB9 100

GRAB10 100

GRAB11 100

GRAB12 100

GRAB13 100

GRAB14 100

GRAB15 100

GRAB16 100

GRAB17 100

GRAB18 100

GRAB19 100

GRAB20 100

GRAB21 100

GRAB22 100

GRAB23 100

GRAB24 100

GRAB25 100

